UNIVERSITÀ DELLA CALABRIA

UNIVERSITÀ DELLA CALABRIA

Dipartimento di
Economia, Statistica e Finanza "Giovanni Anania"

Dottorato di Ricerca in

Scienze Economiche e Aziendali

CICLO

XXXVII

Modelling Cryptocurrency Market Risk: Do Macroeconomic Indicators and Financial Data Explain the Risk within the Cryptocurrency Market?

Settore Scientifico Disciplinare: Economia Politica (SECS-P/01)

Coordinatore: Ch.mo Prof. Fabio Piluso

Firma: _____ FABIO PILUSO 20.01.2025 11:54:25 ~~GMT+01:00~~

Supervisore: Ch.mo Prof. Bernardina Algieri

Firma: _____ BERNARDINA ALGIERI 16.01.2025 17:05:21 GMT+01:00

Tutor: Ch.mo Prof. Arturo Leccadito

Firma: _ _____ ARTURO LECCADITO 15.01.2025 15:11:23 GMT+02:00

Dottorando: Dott. Kokulo Kpai Lawuobahsumo

Firma: Firma oscurata in base alle linee guida del Garante della privacy

Abstract

This dissertation explores the intricate relationship between cryptocurrency market risk and an array of macroeconomic indicators and financial data. The central inquiry revolves around whether traditional financial metrics and broader economic factors can elucidate the underlying risk dynamics within the cryptocurrency market. By integrating insights from financial economics, econometrics, and risk management, this study aims to provide a nuanced understanding of how external economic variables influence cryptocurrency return.

Chapter 2 aims to investigate calendar effects in the cryptocurrency market. We consider the day-of-the-week, the month-of-the-year, quarter-of-the-year, the US Holidays, and Weekend calendar anomalies for the leading cryptocurrencies: Bitcoin, Dash, Dogecoin, Litecoin, Ripple, and Stellar. Our study employs the Autoregressive Conditional Density model with dummy variables to scrutinize these calendar effects. We find anomalies in the mean, variance, skewness, and kurtosis for these cryptocurrencies' returns. Our result suggests that the cryptocurrency market in some periods tends to violate the Efficient Market Hypothesis.

Chapter 3 aims to jointly predict conditional quantiles and tail expectations for the returns of the most popular cryptocurrencies (Bitcoin, Ethereum, Ripple, Dogecoin and Litecoin) using financial and macroeconomic indicators as explanatory variables. We adopt a Monotone Composite Quantile Regression Neural Network (MCQRNN) model to make one- and five-steps-ahead predictions of Value-at-Risk (VaR) and Expected Shortfall (ES) based on a rolling window and compare the performance of our model against the Historical simulation and the standard ARMA(1,1)-GARCH(1,1) model used as benchmarks. The superior set of models is then chosen by backtesting VaR and ES using a Model Confidence Set procedure. Our results show that the MCQRNN performs better than both benchmark models for jointly predicting VaR and ES when considering daily data. Models with the implied volatility index, treasury yield spread and inflation expectations sharpen the extreme return predictions. The results are consistent for the two risk measures at the 1% and 5% level both, in the case of a long and short position and for all cryptocurrencies.

Chapter 4 use a robust measure of non-linear dependence, the Gerber cross-correlation statistic, to study the cross-dependence between the returns on Bitcoin and a set of

commodities, namely wheat, gold, platinum and crude oil WTI. The Gerber statistic enables us to obtain a more robust co-movement measure since it is neither affected by extremely large nor small movements that characterise financial time series; thus, it strips out noise from the data and allows us to capture effective co-movements between series when the movements are "substantial". Focusing on the period 2014–2022, we construct the bootstrapped confidence intervals for the Gerber statistic and test the null that all the Gerber cross-correlations up to lag $k_{\max}$ are zero. Our results indicate a low degree of dependence between Bitcoin and commodities prices, both when we consider contemporaneous correlation and when we employ correlations between current Bitcoin and lagged (one day, one week, or one month) commodities returns. Further, the cross-correlation between Bitcoin and commodities' returns, although scanty, shows an increasing trend during periods of economic, health and financial turbulence. This increased cross-correlation of returns during hectic market periods could be due to the contagion effect of some markets by others, which could also explain the strong dependence across volatilities we detected. Based on our results, Bitcoin cannot be considered the "new digital gold".

Chapter 5 proposes a novel framework leveraging an asymmetric Student-t distribution for asset returns enhanced with correlations governed by Generalized Autoregressive Score dynamics. We incorporate explanatory variables to examine their impact on correlations. Empirical analysis using cryptocurrency (Bitcoin and Ripple) and traditional financial market (S&P 500, NASDAQ, VIX, and WTI) data reveals that the asymmetric Student-t model consistently outperforms competing models, as it effectively captures asymmetry and heavy tails. Explanatory variables, especially gold and market yield on US treasury securities, significantly impact the correlations between cryptocurrencies and financial market data.

Keywords: Cryptocurrency, Gerber correlation, Cross-correlation, Time-varying correlation, Comovements, Asymmetric Student$-t$ Distribution, Generalized Autoregressive Score, Calendar effects, Higher Moments, Value-at-Risk, Expected Shortfall, Quantile Regression, Neural Networks.

To Meako Layweh-Lawuobahsum

and Jacob & Rebecca Lawuobahsumo

Co-Authorship Statement

This dissertation is presented as a collection of independent yet related research papers. Each chapter represents a standalone paper either published, under review, or in preparation for submission. The following statement outlines the contributions of each coauthor to the respective chapters of this dissertation:

The introductory chapter was solely authored by Kokulo Kpai Lawuobahsumo and provides an overview of the research context, objectives, and structure of the dissertation.

Chapter 2 is currently under review for publication. The research was conducted in collaboration with the following co-authors: Prof. Bernardina Algieri, Prof. Arturo Leccadito, and Iliess Zahid.

Chapter 3 has been published in Quantity and Quality Journal. The research was a collaborative effort with contributions from: Prof. Bernardina Algieri, Prof. Arturo Leccadito.

Chapter 4 has been published in MDPI Commodities Journal. The work was carried out with the assistance of: Prof. Bernardina Algieri, Prof. Leonardo Iania and Prof. Arturo Leccadito.

Chapter 5 is currently under review for publication. The research involved contributions from: Prof. Bernardina Algieri, Prof. Arturo Leccadito, Dr. Federico P. Cortese.

Acknowledgements

I would first acknowledge the grace of God Almighty for guiding me through this journey and extend my deepest gratitude to all who have supported me in completing this milestone. I am profoundly grateful to my advisor, Prof. Bernardina Algieri, and my tutor, Prof. Arturo Leccadito, for their unwavering support, insightful feedback, and continuous encouragement throughout the research process. Their expertise and patience have been invaluable in guiding me through the complexities of this project.

I acknowledge and extend my gratitude to Georgia State University, Maurice R. Greenberg School of Risk Science, for allowing me to spend time as a research scholar. The experience was valuable in facilitating my research and was instrumental in my academic growth. I am particularly grateful to Prof. Ajay Subramanian for agreeing to supervise me at Georgia State University. I acknowledge Prof. Liang Peng, Prof. Scott Murray, Prof. Pierre Nguimkeu, and Prof. Baozhong Yang for accepting me to sit in their lectures, enriching my research and broadening my perspectives. I am thankful for the warm hospitality and the intellectual generosity of my fellow Ph.D colleagues and the entire team at Georgia State University for making my period with them rewarding.

I express my profound gratitude and appreciation to my co-authors, Prof. Bernardina Algieri, Prof. Arturo Leccadito, Prof. Leonardo Iania, Dr. Federico P. Cortese, and Iliess Zahid, for their collaborations. The collaborative discussions, shared knowledge, and rigorous analyses provided by Prof. Bernardina Algieri, Prof. Arturo Leccadito, Prof. Leonardo Iania, Dr. Federico P. Cortese, and Iliess Zahid significantly improved the quality of this research. Our shared commitment to academic excellence and dedication to advancing our field of study have made this dissertation a collective endeavor. I acknowledged all referees for their constructive criticism and valuable suggestions, which significantly contributed to the depth and quality of this dissertation.

Lastly, I am deeply grateful to my family, especially my wife, Meako Layweh-Lawuobahsumo, for their unending support and encouragement. Their belief in me has been my anchor through the highs and lows of this academic journey. Without you by my side, I would not have achieved this honor. My heartfelt thanks go to my fellow graduate students and friends for their moral support and camaraderie. To all who have contributed to this work, directly or indirectly, I extend my sincerest thanks.

Contents

List of Figures

List of Tables

Chapter 1

Introduction

1.1 Background and overview of cryptocurrency

In recent years, the cryptocurrency market has emerged as a dynamic and highly volatile domain, attracting significant attention from investors, regulators, and researchers alike. The rapid growth and diversification of cryptocurrencies have not only fostered innovation in financial technology but have also presented unprecedented challenges in understanding and managing market risks.

Studying financial market linkages is essential for understanding and managing risk during market uncertainty. Market participants need to assess the benefits of portfolio diversification while regulators focus regulation on stabilizing the financial system. Within a highly interconnected financial system, a crisis in one country usually spills over to other countries, resulting in the so-called contagion effect. As a result of the inter-connectedness, market linkages strengthen, thus diminishing the diversification benefits of investors and increasing policymakers' concerns about financial stability. Following the 2008 financial crisis, many lost trust in banks as trusted third parties. Some have questioned whether banks are efficient custodians of the global financial system. Major institutions' poor investment decisions led to devastating consequences.

Bitcoin was introduced as an alternative to the banking system to address these concerns. The introduction of Bitcoin gave birth to the world of cryptocurrencies. As a Decentralized Autonomous Organization (DAO), Bitcoin operates as an open-source, peer-to-peer digital network governed by its foundational rules. The integrity of the network eliminates the need for human participants because, in a DAO setting, rules based on an algorithm define the cryptocurrency supply. The Bitcoin whitepa-

per, Nakamoto (2009), describes Bitcoin as an online payment system that transfers directly between parties without the need for financial institutions. Bitcoin enabled digital transactions without a trusted intermediary. Cryptography enables world-scale verification of transactions and asset integrity, similar to the role of commercial banks, financial regulators, and central banks.

Since Nakamoto (2009) introduced and documented Bitcoin as an electronic payment system based on cryptographic proof, cryptocurrencies have gained popularity among retail and institutional investors as a new and attractive asset class. Since 2009, the total crypto-assets market capitalization has experienced exponential growth, from about EUR 20 billion in January 2017 to more than EUR 3 trillion by the end of 2021 and decelerating in the second quarter of 2022[1]. The dynamics of cryptocurrencies have not only attracted the attention of market participants but also from academicians[2] as well (Ahmad et al., 2023; Ante, 2023; Rudkin et al., 2023; Geuder et al., 2019; Vasek, 2015). As suggested by Fry and Cheah (2016) and Zhang et al. (2023), Bitcoin properties have drawn divergent opinions economically. For instance, Baek and Elbeck (2015) classifies Bitcoin as a speculative asset, not a genuine currency. In contrast, Selgin (2015) claims that Bitcoin has functioned as a monetary instrument that investors have utilized for investment and demonetization purposes. According to the Bank for International Settlements (BIS),[3] cryptocurrencies are assets similar in concept to commodities with value determined by supply and demand, but they have zero intrinsic value. BIS further noted that cryptocurrency values are speculative since they rely on the belief that these coins might be exchanged at a higher value for other goods or services or a certain amount of sovereign currency in the future.

1.1.1 Characteristics of Cryptocurrencies

Cryptocurrencies are decentralized, public ledgers with no trusted third party controlling the ledgers. Anyone owning a cryptocurrency can participate in the network, send and receive cryptocurrency, and even hold a copy of this ledger. Distributed ledgers[4], as shown in Figure 1.1, are shared databases across a network, scattered over multiple

[1] sources: https://coinmarketcap.com/

[2] See Corbet et al. (2019) for a systematic review of the empirical literature on the main topics related to the market for cryptocurrencies.

[3] BIS (2015), Digital currencies. Retrieved from https://www.bis.org/cpmi/publ/d137.htm

[4] https://fintechlatvia.eu/crypto-asset/technology-and-regulation-of-the-distributed-ledger-technology/

locations. A ledger is a collection of financial accounts that are distributed and regulated internationally. As a result, distributed ledgers are maintained and rearranged by several people in various locations and institutions.

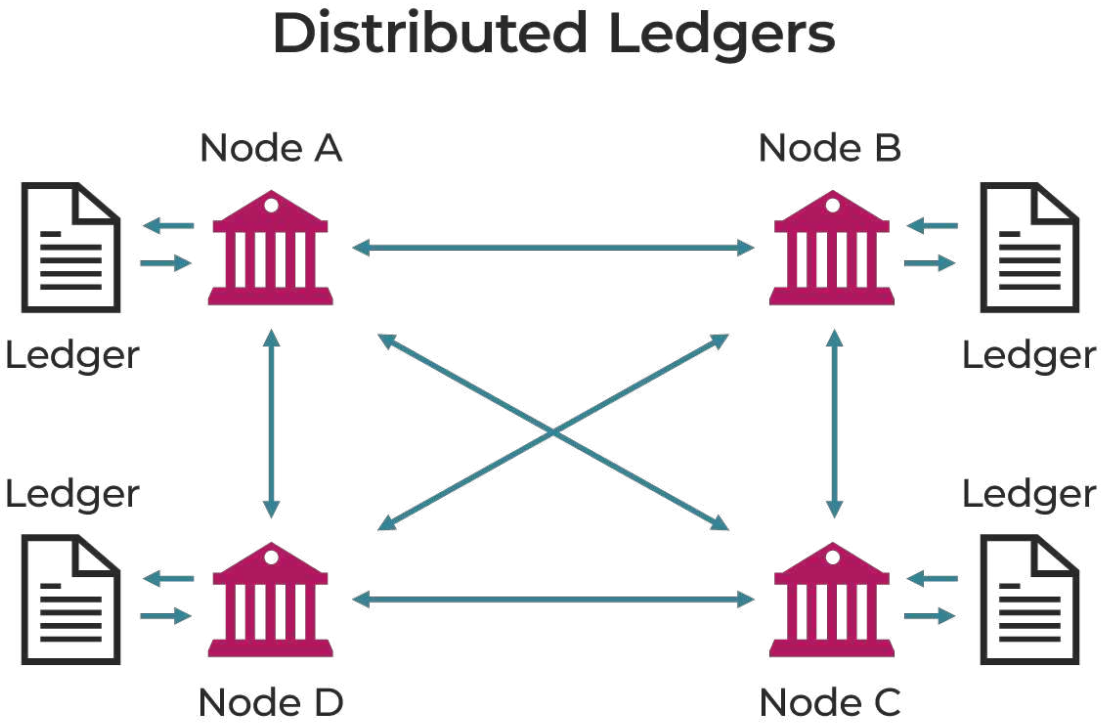

Figure 1.1: Distributed Ledger
Source: This figure was adapted from Fintech Latvia

Distributed Ledgers are highly transparent, secure, tamper-proof, and immutable, eliminating the need for a third party. Distributed Ledgers enable records in a networked database to be simultaneously accessed, validated, and updated. A network of nodes maintains a distributed ledger, letting users see all changes, identify responsible parties, eliminate the need for data auditing, ensure data dependability, and limit access to authorized individuals.

This ledger is known as a blockchain and is not controlled by a trusted third party (Bech and Garratt, 2017). Instead, anyone can read it, write on it, and keep a copy. For example, Bitcoin's blockchain tracks Bitcoin coin and requires all participants to agree to the rules before using it. Blockchains and distributed ledgers typically include five components: cryptography, peer-to-peer networks, consensus mechanisms, ledgers, and validity rules[5]. Key characteristics are common to all cryptocurrencies: Anonymity, Decentralized and Immutable.

[5]Morris et al. (2018)

- **Anonymity**

  There are no requirements for cryptocurrency users to identify themselves when transacting because there is no central authority. Whenever a transaction request is received, the decentralized network checks and verifies the transaction before recording it on the blockchain. Cryptocurrencies, for example, Bitcoin or Ethereum use a private key and public key scheme to authenticate transactions. When transacting on the decentralized system, the current owner transfers the coin to the new owner by digitally signing a hash of the previous transaction securely authenticating their transactions (See Figure 1.2). Transactions are associated with a random sequence of characters rather than the owner's identity, including personal or company information. It is virtually impossible to associate contracts with individuals or businesses.

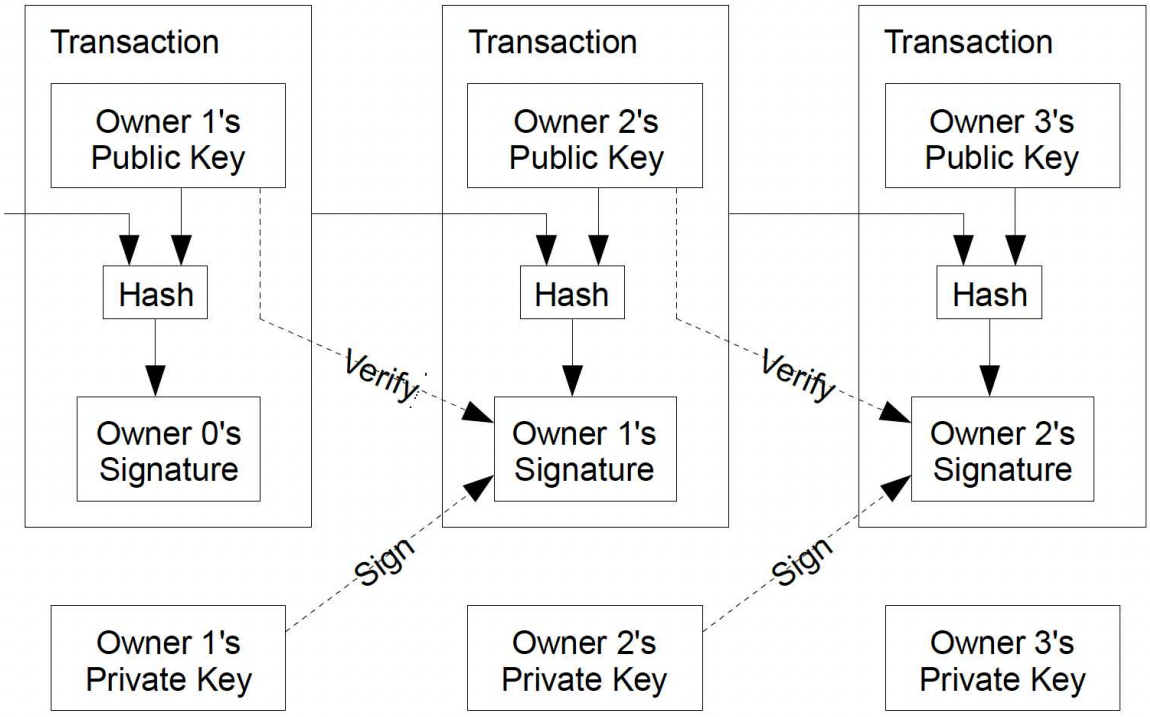

Figure 1.2: Blockchain Transaction
Source: Adopted from Bitcoin White paper (Nakamoto, 2009)

- **Decentralized (intermediaries, or supervisory bodies)**

  The flow of Bitcoin transactions is not regulated by authorities or financial institutions. There are no authorities regulating cryptocurrencies flow or quotations. Virtual currency trading takes place in multiple locations. Transaction data spreads throughout the network because it is stored directly by cryptocurrency

holders. Network nodes use cryptography to verify transactions, which are then recorded to the blockchain. The transaction is broadcast to the entire network and copied by each node, reaching a large number of nodes in a matter of seconds.

- **Immutable**

  Because there is no institutional oversight of the virtual currency market, commissioned transactions cannot be reversed. If an error occurs, such as wrong recipient information, no organization can assist with the correction. The irreversible and unchangeable nature of cryptocurrencies means that no one other than the owner of the relevant private key may move their digital assets, and transactions recorded on the blockchain cannot be reversed. As a result, transaction records become public and immutable. Although it is possible to modify the transaction ledger, cryptographic security makes it extremely challenging. It requires you to compromise the entire cryptocurrency network.

1.2 Motivation and Objective

The cryptocurrency market, characterized by its rapid growth and extreme volatility, has emerged as a focal point in the financial world over the past decade. Its introduction has added to the complexity of market volatility, deregulation, and globalization concerns. It has enhanced sensitivity to market members of economic and financial risk variables. Deregulation limits government authority, giving rise to rapid growth innovation. These assets are prone to extraordinary price swings, sometimes within short periods. These fluctuations can result in substantial gains or significant losses, underscoring the importance of comprehensively understanding the risk factors. At the heart of this discourse lies the issue of market risk—particularly how traditional financial data and macroeconomic indicators interact with the volatile nature of cryptocurrencies. The nascent state of the market, coupled with its speculative nature, makes it distinct from traditional financial markets. Thus, conventional risk assessment models may not fully capture the complexities inherent in the cryptocurrency market. The growing attractiveness of cryptocurrencies has sparked critical questions for market participants and researchers alike: **What drives the risk within the cryptocurrency market? Are traditional financial theories and empirical evidence applicable in assessing cryptocurrency market risks?** Understand-

ing their dynamics is crucial for developing effective risk management strategies and fostering the market's stability and maturity.

This dissertation addresses these questions by investigating the intricate relationship between macroeconomic indicators, financial data, and cryptocurrency market risk. By synthesizing existing literature and employing rigorous empirical analysis, this study seeks to uncover patterns, correlations, and causal relationships that highlight drivers of cryptocurrency risk. The primary objective of this study is to explore whether macroeconomic indicators and financial data can provide explanatory power for the risk observed within the cryptocurrency market. By leveraging machine learning and advanced modeling techniques, this research aims to:

- Assess the impact of macroeconomic factors such as interest rates, inflation, and economic growth on cryptocurrency return volatility.
- Investigate the impact of financial variables such as market indexes and commodities on cryptocurrency return volatility.
- Explore potential interactions and dependencies between traditional financial markets and the cryptocurrency ecosystem.

1.3 Structure of the dissertation

This dissertation comprised four research papers focused on deepening our understanding of the dynamics of cryptocurrency data and its interactions with other market variables, paving the way for informed decision-making and strategic interventions in an increasingly digital financial landscape.

Chapter 2 considers calendar effects in the cryptocurrency market, investigating if cryptocurrency returns behave contrary to the market efficiency hypothesis. We study six cryptocurrencies, namely Bitcoin, Dash, Dogecoin, Litecoin, Ripple, and Stellar, for day-of-the-week (DOW), the month-of-the-year (MOY), Quarter-of-the-Year (QOY), the U.S. Holidays, and Weekend calendar effects. We employ the Autoregressive Conditional Density (ACD) model with dummy variables and broaden the investigation of these calendar anomalies to include higher moments, namely skewness and kurtosis, beyond mean and variance. Our study holds significance for cryptocurrency market participants because:

- It assesses the state of cryptocurrencies markets in terms of calendar anomalies to inform decision-making
- It aids investors in developing trading strategies to capitalize on abnormal returns
- It suggests constructing diversified portfolios of various cryptocurrencies by leveraging seasonal statistics, thereby formulating strategies based on the seasonal patterns observed in the cryptocurrency market
- Our results guide their choice of distribution and model specifications when analyzing cryptocurrency returns

Chapter 3 aims to jointly predict conditional quantiles and tail expectations for the returns of cryptocurrencies. We fit the Monotone Composite quantile regression neural network model (MCQRNN) of Cannon (2018) based on a number of macroeconomic and financial variables, to derive one-step-ahead and five-step-ahead VaR and Expected Shortfall predictions for Bitcoin, Dogecoin, Ethereum, Ripple, and Litecoin. The main advantage of the MCQRNN model is that it ensures non-crossing quantile, Allows multiple quantile functions to be estimated simultaneously, and estimates are more approximate to the actual conditional quantile function. The main contributions of this work are the following:

- We provide the forecasts of negative and positive returns (i.e., located on the left and right tails of the distributions) for the leading digital currencies
- We introduce explanatory variables to check whether their inclusion improves the volatility forecasting.
- We provide out-of-sample forecasts for joint conditional quantile and Expected Shortfall imposing monotonicity constraints, thus solving the quantile crossing problem

In Chapter 4, we employ the Gerber cross-correlation statistic to study the cross-dependence between the returns on Bitcoin and a set of commodities, namely wheat, gold, platinum, and crude oil WTI. This non-linear dependence method strips noise from the data and allows us to capture effective co-movements between series when the movements are "substantial." We construct the bootstrapped confidence intervals for the Gerber statistic and test the null that all the Gerber Cross-Correlations up

to lag $k_{\max}$ are zero. The Gerber statistic enables us to obtain a more robust co-movement measure since it is neither affected by extremely large nor small movements that characterize cryptocurrency data.

Chapter 5 proposes a novel framework based on an asymmetric Student-t distribution (Azzalini, 2005), with correlations governed by a Generalized Autoregressive Score (GAS, Creal et al., 2013) dynamics. Traditional correlation often fails to capture the dynamic and non-linear relationships between financial assets, ignoring factors like volatility clustering and tail dependence. This advanced approach overcomes the limitations of traditional models by offering a more flexible and accurate representation of financial returns. This method incorporates exogenous macroeconomic indicators into correlation models to enhance prediction accuracy. Our proposed technique effectively captures the asymmetry and heavy tails in the data.

We contribute to the existing literature as follows:

- Develop an asymmetric Student-t framework for modeling time-varying correlation based on the GAS framework.
- Our approach offers a more flexible and accurate representation of financial series by capturing asymmetries and heavy tails in returns.
- We also introduce explanatory variables in the model to examine their impact on the time-varying correlation.

1.4 Contribution to Knowledge

This research contributes to the existing body of knowledge in several ways. Firstly, it offers empirical evidence on the relationship between macroeconomic indicators, financial data, and cryptocurrency market risk, addressing a significant gap in current research. Secondly, this study provides a nuanced understanding of the underlying mechanisms driving cryptocurrency volatility. Finally, the findings contribute to informed decision-making among investors, policymakers, and regulators navigating the evolving landscape of digital assets, equipping market participants with the tools and knowledge to navigate and harness the potential of this evolving asset class amidst the challenges posed by market volatility and macroeconomic fluctuations.

1.5 Data Descriptions

In this section, we present the data used in Chapters 3, 4 and 5. The data used in Chapter 2 is analyzed separately because it includes weekends and holidays, reflecting the continuous trading nature of cryptocurrencies, unlike traditional assets. However, in Chapters 3, 4 and 5, cryptocurrency data from non-conventional trading days was excluded to ensure alignment with the conventional economic and financial data incorporated into our models. We gather data for cryptocurrencies, financial markets and economic indicators, see Table 1.1 for details. The data range from September 18, 2014, to December 7, 2023. Figures 1.3, 1.4, 1.5, and 1.6, present the plots of cryptocurrencies log-return, economic, and financial data used as predictor variables, respectively.

Table 1.1: List of variables used in Chapters 3, 4 and 5

Abbreviations	Description	Source
	Cryptocurrencies	
BTC	Bitcoin	Yahoo Finance
ETH	Ethereum	
XRP	Ripple	
LTC	Litecoin	
DOGE	Dogecoin	
	Financial Market Data	
S&P500	Standard and Poor's 500 Index	Yahoo Finance
NASDAQ	NASDAQ Composite Index	
VIX	CBOE Volatility Index	
DXY	U.S. Dollar Index	
WTI	West Texas Intermediate crude oil	Bloomberg
GOLD	Gold first generic futures	
Platinum	Platinum first generic futures	
Wheat	Wheat first generic futures	
	Economic Indicator Variables	
T10Y3M	10-year Treasury constant maturity minus 3-month Treasury constant maturity	FRED
T10YIE	10-year breakeven inflation rate	
T5YIFR	5-Year Forward Inflation Expectation Rate	
DGS10	Market Yield on U.S. Treasury Securities at 10-Year Constant Maturity	

Table 1.2 displays the descriptive statistics for the data. Descriptive statistics provides an initial understanding of the dataset. We observe in Table 1.2 that the average returns are higher for ETH, BTC, DOGE, and XRP. The DOGE and VIX series have the highest positive skewness (suggesting frequent small losses and a few extreme gains) compared to the other variables. Of the cryptocurrencies, BTC returns are negatively

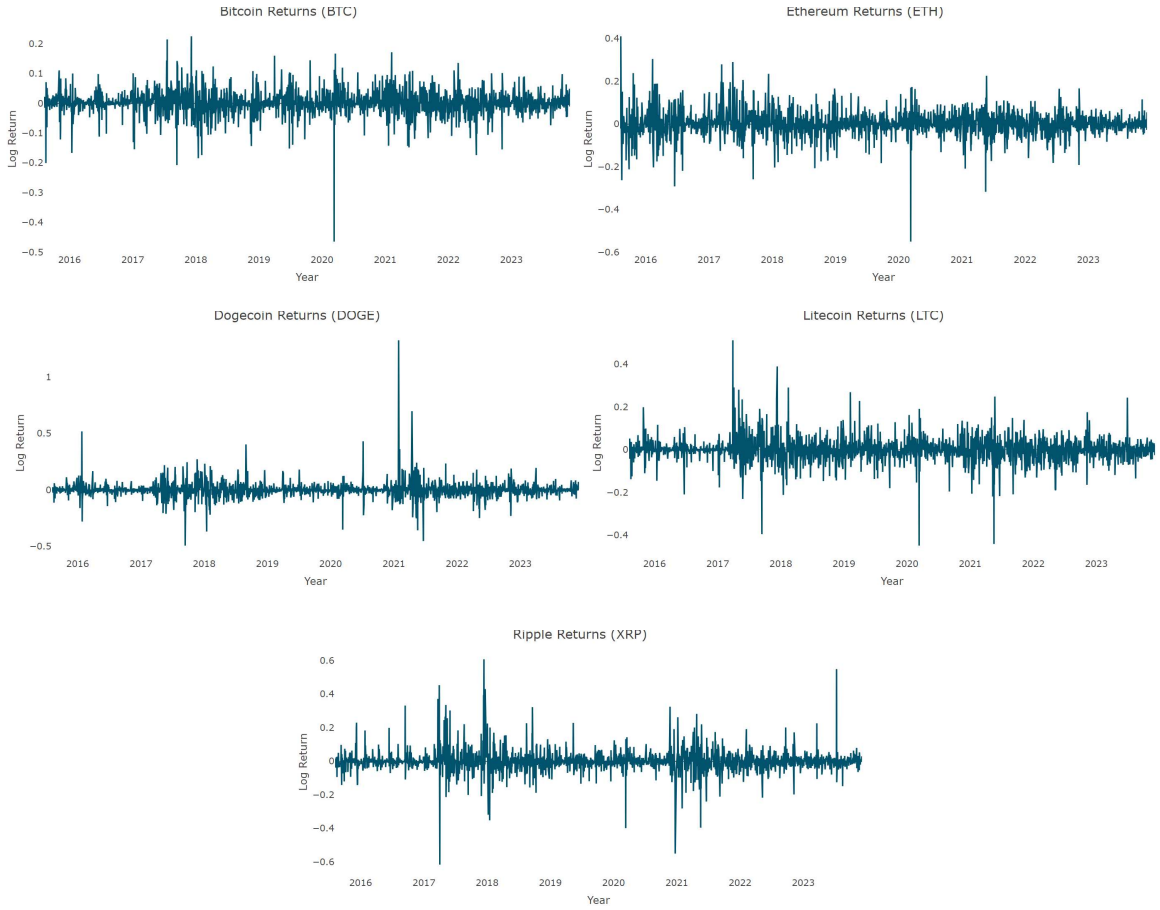

Figure 1.3: Plot of Cryptocurrencies Log Returns

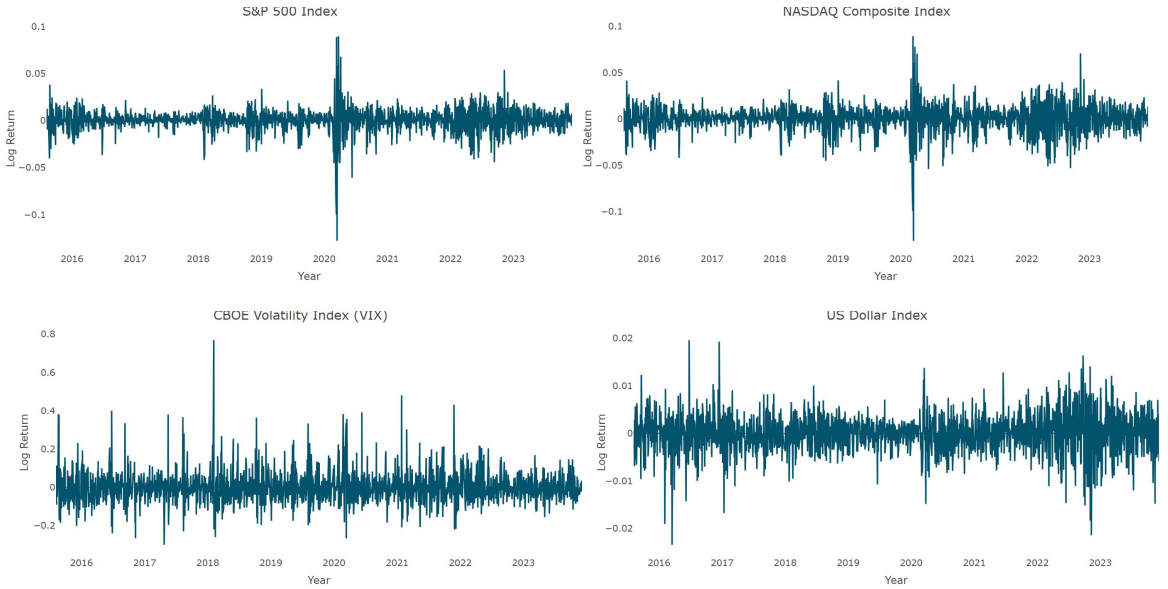

Figure 1.4: Plot of Financial (Stock Market) Data Log Returns

skewed, indicating frequent small gains and a few extreme losses see Algieri and Leccadito (2019). The standard deviations across the returns of the five cryptocurrencies

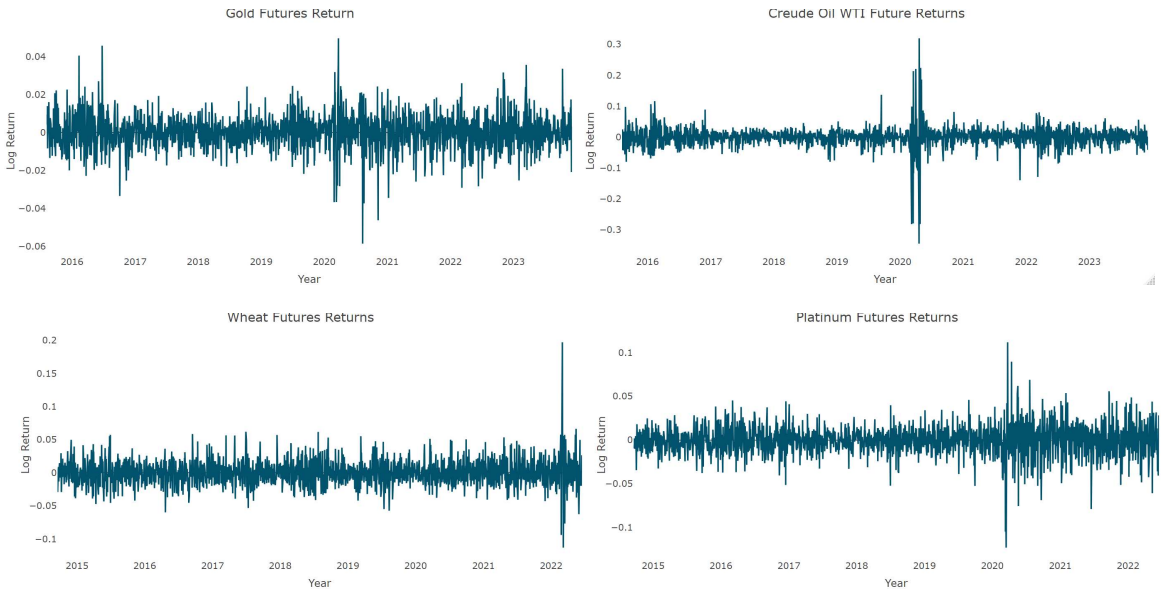

Figure 1.5: Plot of Financial (Commodities) Data Log Returns

Figure 1.6: Plot of Economic indicators Data Log Returns

are high while the expected values are low – implying that cryptocurrencies provide high risk and small return. Indeed, all series show excess kurtosis, with DOGE and WTI have the highest values. These results confirm that stylized facts of financial returns that return are not normally distributed, leptokurtic, and negatively skewed. High volatility makes all average returns not statistically different from zero, evident by the median.

Table 1.3 shows the Pearson correlation coefficient among the variables. Figure 1.7 shows that among cryptocurrencies, there exists a high positive correlation. The

Table 1.2: Descriptive Statistics

	μ	σ	Median	Min	Max	SE	Skew	Kurt
BTC	0.0018	0.0408	0.0018	-0.4647	0.2251	0.0009	-0.8294	14.5706
ETH	0.0023	0.0600	-0.0004	-0.5507	0.4103	0.0013	0.0105	11.2870
XRP	0.0013	0.0666	-0.0017	-0.6163	0.6069	0.0015	0.6440	21.0628
LTC	0.0000	0.0570	-0.0003	-0.4491	0.5114	0.0013	0.2318	14.8729
DOGE	0.0015	0.0722	-0.0004	-0.4929	1.3235	0.0016	3.7935	68.8549
S&P500	0.0003	0.0119	0.0006	-0.1277	0.0897	0.0003	-0.8445	18.4368
VIX	-0.0003	0.0803	-0.0075	-0.2998	0.7682	0.0018	1.3762	10.7570
WTI	0.0002	0.0318	0.0022	-0.3454	0.3196	0.0007	-0.7703	30.4150
DXY	0.0000	0.0040	0.0002	-0.0234	0.0196	0.0001	-0.2569	5.7261
T10Y3M	-0.0009	0.0542	0.0000	-0.3200	0.3400	0.0012	-0.3232	7.2802
T10YIE	0.0003	0.0325	0.0000	-0.3200	0.2500	0.0007	-0.5021	11.4963
T5YIFR	0.0001	0.0379	0.0000	-0.3000	0.3300	0.0008	-0.0418	9.6714
DGS10	0.0012	0.0529	0.0000	-0.3000	0.2900	0.0012	-0.1071	5.5010
GOLD	0.0003	0.0087	0.0004	-0.0586	0.0497	0.0002	-0.1147	6.4821
NASDAQ	0.0004	0.0141	0.0009	-0.1315	0.0893	0.0003	-0.6628	11.0180
Platinum	-0.0001	0.0174	0.0005	-0.1232	0.1118	0.0004	-0.2265	7.0478
Wheat	0.0002	0.0203	-0.0006	-0.1130	0.1970	0.0004	0.5244	9.0646

Note: Descriptive statistics for Bitcoin (BTC), Ethereum (ETH), Ripple (XRP), Litecoin (LTC), Dogecoin (DOGE), S&P 500 Index (S&P 500), CBOE Volatility Index (VIX), West Texas Intermediate (WTI) crude oil, U.S. Dollar Index (DXY), 10-year Treasury constant maturity minus 3-month Treasury constant maturity (T10Y3M), 10-year breakeven inflation rate (T10YIE), 5-Year Forward Inflation Expectation Rate (T5YIFR), Market Yield on U.S. Treasury Securities at 10-Year Constant Maturity (DGS10), Gold first generic futures (GOLD), NASDAQ Composite Index (NASDAQ), Generic 1st Platinum futures (Platinum) and Generic 1st Wheat futures (Wheat). In particular, the statistics include the mean (μ), standard deviation (σ), median, minimum (Min), maximum (Max), standard error (SE), skewness (Skew), kurtosis (Kurt).

high positive correlation implies that cryptocurrencies are exposed to the same extreme factors and are rapidly contagious to each other during extreme events. This means that there exist systematic risks in the cryptocurrency market. Moreover, Bitcoin and Litecoin have the highest dependence. There is also a strong positive correlation between S&P 500 and NASDAQ, T10YIE and DGS10 and T5YIFR, Gold and Platinum. We also observe a positive but weak correlation between the selected cryptocurrencies and the NASDAQ Composite Index and gold, and a negative but weak correlation with the VIX and US Dollar Index. The correlation in figure 1.7 also confirms the high negative dependence between VIX and NASDAQ index and S&P 500 index. Our results further show a weak positive correlation between BTC and the S&P 500, BTC and NASDAQ, and a weak negative correlation between BTC and VIX. Furthermore, we observe a weak correlation between XRP and S&P 500, NASDAQ, VIX, and WTI. We also notice low correlations between BTC and XRP and DGS10, T10Y3M, and T10YIE.

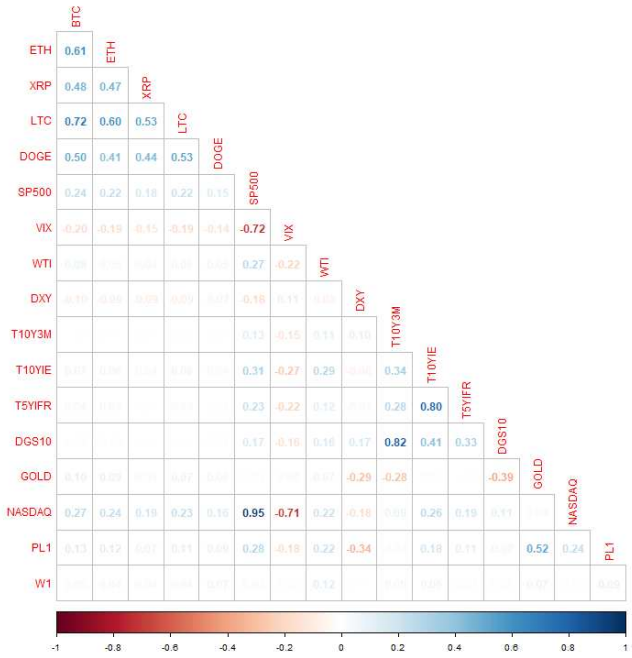

Figure 1.7: Correlation Plot of Variables

Note: Bitcoin (BTC), Ethereum (ETH), Ripple (XRP), Litecoin (LTC), Dogecoin (DOGE), S&P 500 Index (S&P 500), CBOE Volatility Index (VIX), West Texas Intermediate (WTI) crude oil, U.S. Dollar Index (DXY), 10-year Treasury constant maturity minus 3-month Treasury constant maturity (T10Y3M), 10-year breakeven inflation rate (T10YIE), 5-Year Forward Inflation Expectation Rate (T5YIFR), Market Yield on U.S. Treasury Securities at 10-Year Constant Maturity (DGS10), Gold first generic futures (Gold), NASDAQ Composite Index (NASDAQ), Generic 1st Platinum futures (PL1) and Generic 1st Wheat futures (W1)Table.

Table 1.3: Pearson correlation between variables

	BTC	ETH	XRP	LTC	DOGE	SP500	VIX	WTI	DXY	T10Y3M	T10YIE	T5YIFR	DGS10	GOLD	NASDAQ	Platinum
ETH	0.6058															
XRP	0.4767	0.4674														
LTC	0.7189	0.6018	0.5325													
DOGE	0.5049	0.4143	0.4433	0.5253												
S&P 500	0.2430	0.2243	0.1768	0.2192	0.1493											
VIX	-0.1958	-0.1862	-0.1473	-0.1921	-0.1446	-0.7188										
WTI	0.0756	0.0491	0.0403	0.0575	0.0503	0.2735	-0.2180									
DXY	-0.0978	-0.0888	-0.0940	-0.0909	-0.0685	-0.1834	0.1097	-0.0793								
T10Y3M	-0.0059	-0.0092	0.0090	0.0039	-0.0083	0.1309	-0.1478	0.1094	0.0992							
T10YIE	0.0667	0.0552	0.0438	0.0613	0.0369	0.3139	-0.2695	0.2895	-0.0790	0.3382						
T5YIFR	0.0403	0.0438	0.0108	0.0349	0.0196	0.2340	-0.2160	0.1163	-0.0440	0.2802	0.8035					
DGS10	-0.0187	-0.0199	0.0040	-0.0086	-0.0233	0.1694	-0.1609	0.1552	0.1710	0.8166	0.4140	0.3333				
GOLD	0.1021	0.0897	0.0383	0.0748	0.0592	0.0296	0.0373	0.0749	-0.2939	-0.2842	0.0258	-0.0012	-0.3949			
NASDAQ	0.2663	0.2386	0.1884	0.2341	0.1578	0.9483	-0.7070	0.2191	-0.1778	0.0897	0.2604	0.1921	0.1130	0.0359		
Platinum	0.1320	0.1203	0.0724	0.1051	0.0874	0.2753	-0.1839	0.2157	-0.3439	-0.0392	0.1814	0.1062	-0.0667	0.5172	0.2430	
Wheat	0.0494	0.0423	0.0352	0.0409	0.0677	0.0302	-0.0266	0.1217	-0.0065	0.0504	0.0621	0.0251	0.0222	0.0723	0.0148	0.0877

Note: Bitcoin (BTC), Ethereum (ETH), Ripple (XRP), Litecoin (LTC), Dogecoin (DOGE), S&P 500 Index (S&P 500), CBOE Volatility Index (VIX), West Texas Intermediate (WTI) crude oil, U.S. Dollar Index (DXY), 10-year Treasury constant maturity minus 3-month Treasury constant maturity (T10Y3M), 10-year breakeven inflation rate (T10YIE), 5-Year Forward Inflation Expectation Rate (T5YIFR), Market Yield on U.S. Treasury Securities at 10-Year Constant Maturity (DGS10), Gold first generic futures (Gold), NASDAQ Composite Index (NASDAQ), Generic 1st Platinum futures (Platinum) and Generic 1st Wheat futures (Wheat).

Since time series variables are usually assumed to be independent and identically distributed (iid) following the normal distribution, we conclude this section by performing some time series diagnostic tests. We begin by plotting the autocorrelation of the series to visually inspect for autocorrelation. We plot the ACF of the series in Figure 1.8, 1.9, 1.10, and 1.11. The ACF measures the correlation between the time series data points separated by different time lags. Peaks observed outside the confidence interval bands indicate significant autocorrelation at those lags.

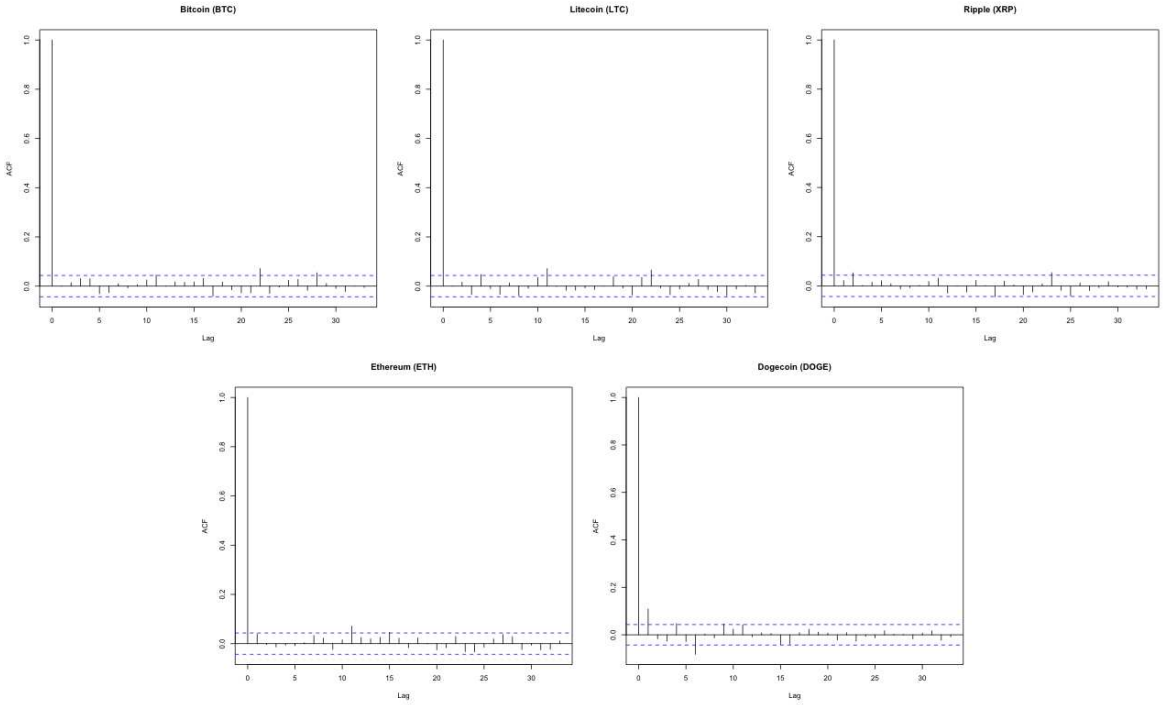

Figure 1.8: ACF Plot of Cryptocurrency

We performed the Ljung and Box (1978) test to check whether our series are independently distributed. Essentially, we test under the null hypothesis that the autocorrelations of our series are all zero up to a specified lag (8). We show the test result in Table 1.4. We fail to reject the null for BTC, ETH, XRP, LTC, DXY, T10Y3M, DGS10, GOLD, and Wheat, meaning there is no autocorrelation. We reject the null for DOGE, S&P500, VIX, T10YIE, T5YIFR, NASDAQ, and Platinum. The presence of autocorrelation in these series indicates that past values influence current and future values, which can lead to biased estimates of model parameters if not accounted for and also lead to underestimation or overestimation.

We considered the Jarque and Bera (1987) and the Shapiro and Wilk (1965) tests to test for normality for our data. The Jarque-Bera test (JB) checks whether a given data series follows a normal distribution. JB test is a Lagrange multiplier test for normality

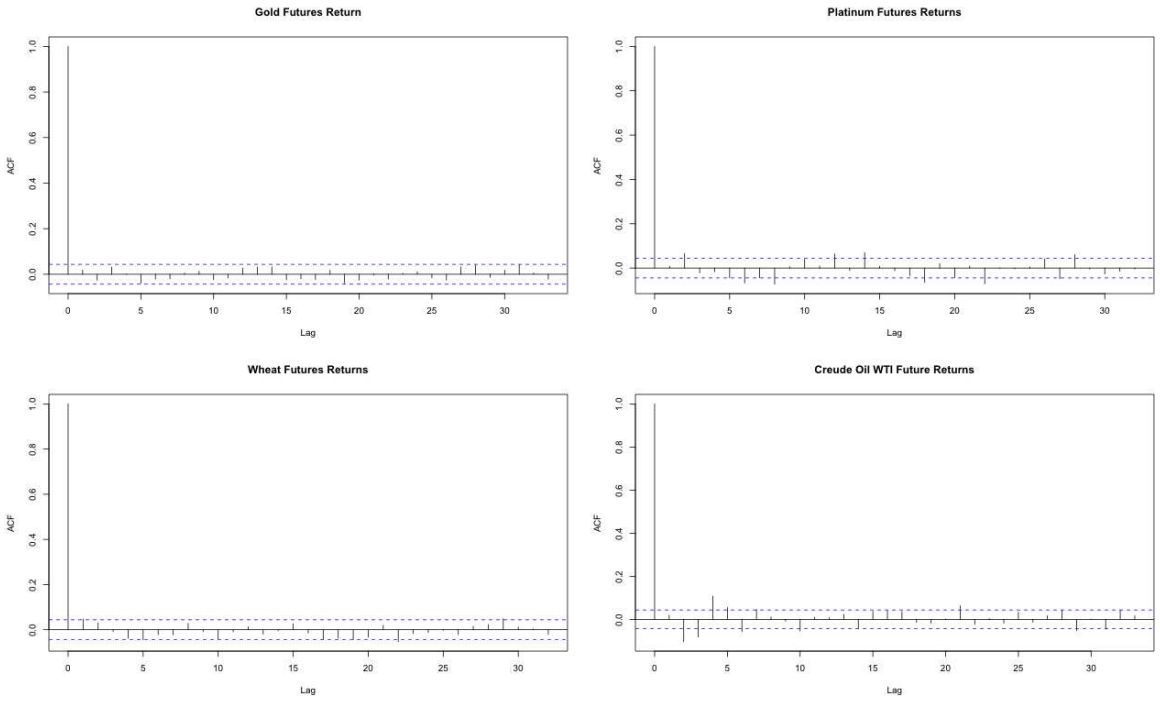

Figure 1.9: ACF Plot of Commodities Market Data

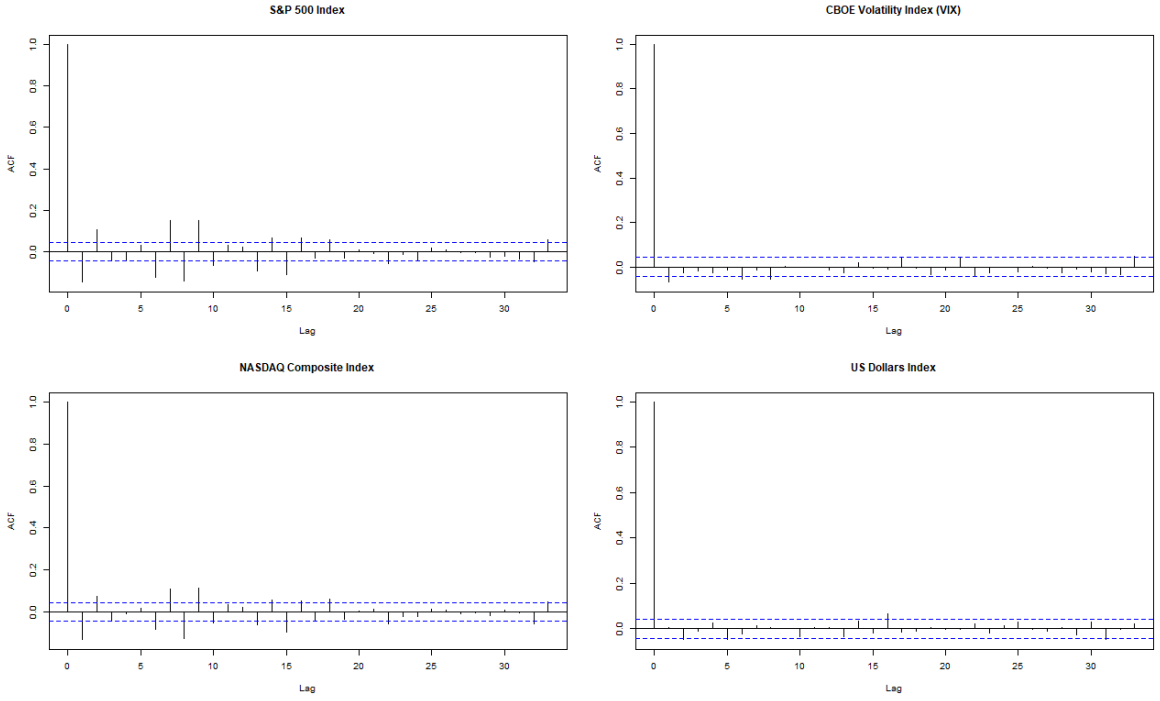

Figure 1.10: ACF Plot of Stock Market Data

under the null that the data is normally distributed. A normally distributed series has a zero skewness – perfectly symmetrical around the mean and kurtosis of three. The kurtosis tells us how is the tail of the data and informs us about the distribution "peaked." The test statistic of the JB test is computed as follows:

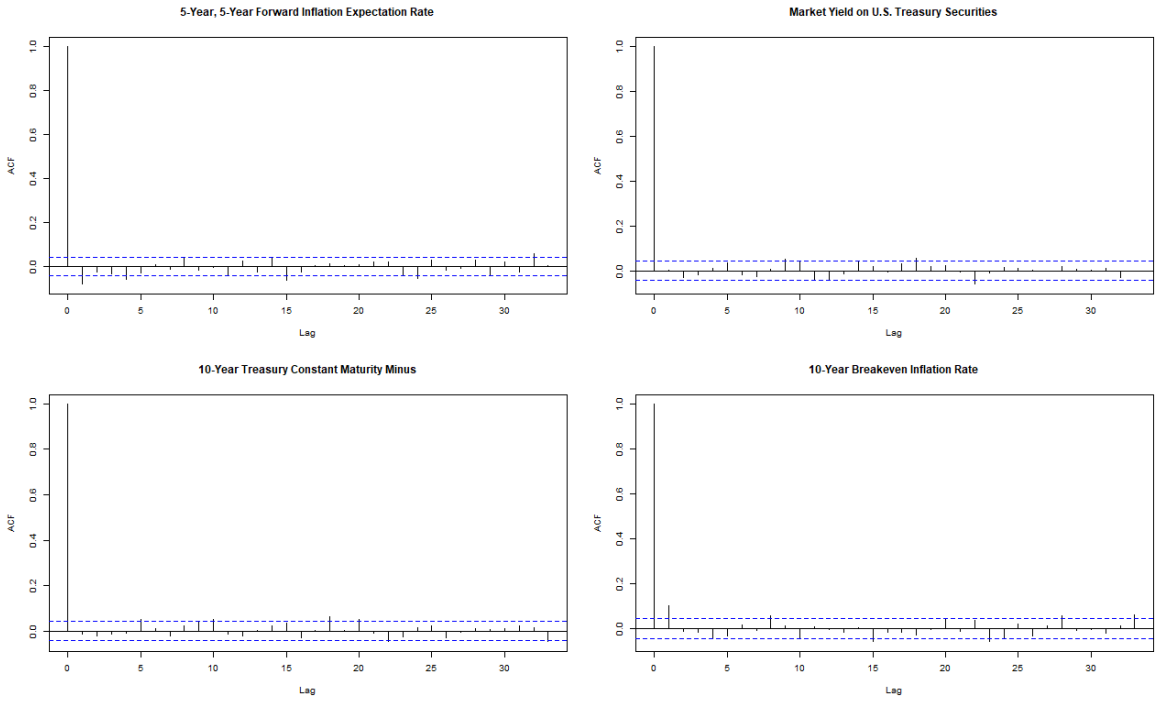

Figure 1.11: ACF Plot of Economic Indicators

Table 1.4: Box-Pierce Test for Autocorrelation

	t-Stat	P.Val	lag
BTC^2	7.6843	0.4649	8
ETH^2	6.9803	0.5388	8
XRP^2	8.4683	0.3891	8
LTC^2	13.3700	0.0997	8
$DOGE^2$	46.7130	0.0000	8
$S\&P500^2$	194.2792	0.0000	8
VIX^2	25.4633	0.0013	8
WTI^2	77.2249	0.0000	8
DXY^2	11.8514	0.1580	8
$T10Y3M^2$	9.0366	0.3392	8
$T10YIE^2$	34.6750	0.0000	8
$T5YIFR^2$	29.4532	0.0003	8
$DGS10^2$	7.0084	0.5357	8
$GOLD^2$	9.0716	0.3363	8
$NASDAQ^2$	121.0817	0.0000	8
$Platinum^2$	28.0922	0.0005	8
$Wheat^2$	14.3954	0.0720	8

Note: Autocorrelation test for Squared Bitcoin (BTC), Squared Ethereum (ETH), Squared Ripple (XRP), Squared Litecoin (LTC), Squared Dogecoin (DOGE), Squared S&P 500 Index (S&P 500), Squared CBOE Volatility Index (VIX), Squared West Texas Intermediate (WTI) crude oil, Squared U.S. Dollar Index (DXY), Squared 10-year Treasury constant maturity minus 3-month Treasury constant maturity (T10Y3M), Squared 10-year breakeven inflation rate (T10YIE), Squared 5-Year Forward Inflation Expectation Rate (T5YIFR), Squared Market Yield on U.S. Treasury Securities at 10-Year Constant Maturity (DGS10), Squared Gold first generic futures (GOLD), Squared NASDAQ Composite Index (NASDAQ), Squared Generic 1st Platinum futures (Platinum) and Squared Generic 1st Wheat futures (Wheat).

$$JB = \frac{n}{6}\left(S^2 + \frac{(K-3)^2}{4}\right)$$

Under the null hypothesis of normality, the JB test statistic follows a chi-square distribution with two degrees of freedom (skewness and kurtosis).

The Shapiro-Wilk test tests the data for normality under the null hypothesis that

Table 1.5: Normality Test

	Jarque-Bera		Shapiro-Wilk	
	t-Stat	P.Val	t-Stat	P.Val
BTC	11670.4638	0.0000	0.9059	0.0000
ETH	5866.0154	0.0000	0.9122	0.0000
XRP	28010.1118	0.0000	0.7980	0.0000
LTC	12059.2038	0.0000	0.8804	0.0000
DOGE	375358.1029	0.0000	0.7288	0.0000
SP500	20598.0281	0.0000	0.8705	0.0000
VIX	5786.7220	0.0000	0.9187	0.0000
WTI	64400.2710	0.0000	0.7963	0.0000
DXY	657.3177	0.0000	0.9736	0.0000
T10Y3M	1600.5560	0.0000	0.9559	0.0000
T10YIE	6252.1732	0.0000	0.9271	0.0000
T5YIFR	3802.2933	0.0000	0.9467	0.0000
DGS10	538.1881	0.0000	0.9737	0.0000
GOLD	1040.1650	0.0000	0.9674	0.0000
NASDAQ	5641.4640	0.0000	0.9242	0.0000
Platinum	1417.0747	0.0000	0.9666	0.0000
Wheat	3235.5498	0.0000	0.9593	0.0000

Note: Normality test for Bitcoin (BTC), Ethereum (ETH), Ripple (XRP), Litecoin (LTC), Dogecoin (DOGE), S&P 500 Index (S&P 500), CBOE Volatility Index (VIX), West Texas Intermediate (WTI) crude oil, U.S. Dollar Index (DXY), 10-year Treasury constant maturity minus 3-month Treasury constant maturity (T10Y3M), 10-year breakeven inflation rate (T10YIE), 5-Year Forward Inflation Expectation Rate (T5YIFR), Market Yield on U.S. Treasury Securities at 10-Year Constant Maturity (DGS10), Gold first generic futures (GOLD), NASDAQ Composite Index (NASDAQ), Generic 1st Platinum futures (Platinum) and Generic 1st Wheat futures (Wheat).

the sample data was obtained from a normally distributed population. The Shapiro-Wilk test statistic is as follows:

$$W = \frac{\left(\sum_{i=1}^{n} a_i x_{(i)}\right)^2}{\sum_{i=1}^{n}(x_i - \bar{x})^2}$$

where: $x_{(i)}$ are the ordered sample values (from smallest to largest), $\bar{x}$ is the mean of the sample data, and a_i are constants from a standard normal distribution.

Table 1.5 shows our test result for normality. Basing our decision on the p-value, using a significance level α of 0.05, we reject the null hypothesis (H_0) that the data are normally distributed. All the series violate the Gaussian distributions assumptions – they are leptokurtic and skewed.

Finally, we test for stationarity to check if our series mean, variance and autocorrelation are constant over time. Wang (2006) suggested that if the data is stationary, it will have a fixed element for an intercept or the series will be stationary around a fixed level. A series is non-stationary if it contains a unit root implying that the time series follows a random walk and does not revert to a long-term mean, making it unpredictable and potentially problematic for certain types of statistical analysis and forecasting. We performed three well-established stationarity tests for time series data – the Augmented Dickey-Fuller (ADF) test (Dickey and Fuller, 1981), the Kwiatkowski–Phillips–Schmidt–Shin (KPSS) test (Kwiatkowski et al., 1992) and the

Phillips-Perron (PP) test (Phillips and Perron, 1988).

ADF test tests the series for the presence of a unit root. A time series with a unit root is characterized by the mean and variance increasing over time and does not converge to a constant value, rendering time series data non-stationary, resulting in unpredictability and non-mean reversion. The ADF test regresses the time series on its lagged values and under the null hypothesis that the series has a unit root.

Considering a time series x_t, the ADF test checks for a unit root in the series as follows:

$$\Delta x_t = \alpha + \beta t + \gamma y_{t-1} + \sum_{i=1}^{p} \delta_i \Delta x_{t-i} + \epsilon_t$$

where: Δx_t is the first difference of x_t, α is the intercept, βt is the time trend, γx_{t-1} is the lagged time series value, ϵ_t is the error term.

KPSS test tests if the series is stationary around a mean or linear trend, or is non-stationary due to a unit root. The test is performed under the null hypothesis that the data is stationary. The KPSS test regresses the series broken up into three parts: a deterministic trend (βt), a random walk (r_t), and a stationary error term (ϵ_t), with the regression equation:

$$x_t = r_t + \beta t + \epsilon_t$$

The KPSS test differs from the ADF tests in that the KPSS test tests for stationarity in the 'presence of a deterministic trend'. ADF test looks for a unit root in the time series, but KPSS looks for stationarity around a deterministic trend. The KPSS test tends to reject the null hypothesis too often – high Type I error rate.

PP test is a non-parametric method for determining whether a time series is stationary or contains a unit root. The PP test is performed under the null that the time series contains a unit root. The PP test adjusts the Dickey-Fuller test to account for serial correlation and heteroskedasticity in the error terms. The PP test is done by regressing as follows:

$$\Delta x_t = \alpha + \beta t + \gamma x_{t-1} + \epsilon_t$$

where Δx_t is the first difference of the series, t is a time trend, and ϵ_t is the error term.

Table 1.6 presents the stationarity tests for our series. Based on p-value, we reject

Table 1.6: Stationarity Test

	ADF		KPSS		Phillips-Perron	
	t-Stat	P.Val	t-Stat	P.Val	t-Stat	P.Val
BTC	-11.6640	0.0100	0.1881	0.1000	-2101.992	0.0100
ETH	-11.0290	0.0100	0.4506	0.0554	-1952.443	0.0100
XRP	-12.2520	0.0100	0.1315	0.1000	-2117.851	0.0100
LTC	-12.0665	0.0100	0.1377	0.1000	-2043.090	0.0100
DOGE	-12.0266	0.0100	0.0614	0.1000	-1735.370	0.0100
SP500	-13.1394	0.0100	0.0257	0.1000	-2393.661	0.0100
VIX	-15.3624	0.0100	0.0238	0.1000	-1996.516	0.0100
WTI	-12.3544	0.0100	0.0422	0.1000	-1894.436	0.0100
DXY	-13.6662	0.0100	0.1558	0.1000	-1924.393	0.0100
T10Y3M	-11.6781	0.0100	0.2241	0.1000	-2056.875	0.0100
T10YIE	-12.5996	0.0100	0.0495	0.1000	-1749.003	0.0100
T5YIFR	-13.8379	0.0100	0.0350	0.1000	-2002.698	0.0100
DGS10	-12.7414	0.0100	0.2376	0.1000	-1990.228	0.0100
GOLD	-12.4443	0.0100	0.0428	0.1000	-1957.011	0.0100
NASDAQ	-12.9712	0.0100	0.0565	0.1000	-2334.031	0.0100
Platinum	-12.6349	0.0100	0.0164	0.1000	-1939.463	0.0100
Wheat	-13.3324	0.0100	0.0625	0.1000	-1877.339	0.0100

Note: Normality test for Bitcoin (BTC), Ethereum (ETH), Ripple (XRP), Litecoin (LTC), Dogecoin (DOGE), S&P 500 Index (S&P 500), CBOE Volatility Index (VIX), West Texas Intermediate (WTI) crude oil, U.S. Dollar Index (DXY), 10-year Treasury constant maturity minus 3-month Treasury constant maturity (T10Y3M), 10-year breakeven inflation rate (T10YIE), 5-Year Forward Inflation Expectation Rate (T5YIFR), Market Yield on U.S. Treasury Securities at 10-Year Constant Maturity (DGS10), Gold first generic futures (GOLD), NASDAQ Composite Index (NASDAQ), Generic 1st Platinum futures (Platinum) and Generic 1st Wheat futures (Wheat).

the null hypothesis, the data does not contain a unit root – it is stationary for both ADF and PP tests, and for the KPSS test, we fail to reject the null hypothesis, the data is stationary. We conclude that all our series are stationary.

There are several well-documented "stylized facts" about financial time-series returns that researchers have observed across various markets and over time. We observe from our data the following stylized facts of financial returns:

- **Fat Tails and Non-Normality**: more extreme outcomes (both gains and losses),
- **Absence of Autocorrelation**: squared returns tend to be highly autocorrelated,
- **Asymmetry in Returns**: exhibit skewness
- **Mean Reversion and Momentum**,
- **Leptokurtosis:** higher peaks and fatter tails
- **Volatility Clustering**: volatility is serially correlated.

In summary, our findings highlight critical characteristics of the data that influence the methodologies employed in subsequent analyses. The stationarity of the series, confirmed by various statistical tests, ensures the reliability of our model estimation and avoids the pitfalls associated with non-stationary data, such as biased parameter estimates, underestimation, or overestimation. Furthermore, rejecting normality

assumptions and the observed stylized facts, including fat tails, skewness, volatility clustering, and mean reversion, underscores the complexities inherent in financial time series requiring advanced modelling techniques. Recognizing these features allows for adopting robust econometric techniques tailored to capture these dynamics, thereby improving the accuracy and interpretability of results.

Chapter 2

Calendar Effects on Returns, Volatility and Higher Moments: Evidence from Crypto Markets

2.1 Introduction

Technological development and digital change are upending the financial system. Over the last few years, cryptocurrencies have become very popular for their unique properties that differentiate them from traditional financial assets such as commodities, stocks, and bonds. Cryptocurrencies exhibit complex risk dynamics such as high volatility, pronounced asymmetries, and high tail risk, with extreme fluctuations in the returns. The characteristics of these assets make it challenging to model their risk and manage portfolios containing digital assets.

Even though cryptocurrencies are high-risk assets, they are becoming attractive to an increasing number of new retail and institutional investors, with cryptocurrency exchange-traded notes (ETNs) and derivatives, including futures and options, now traded in the market. With the growing interest in these digital assets, studies such as Lawuobahsumo et al. (2024); Basher and Sadorsky (2022); Bakas et al. (2022); Wang et al. (2022); Borri (2019) have focused on the determinants of cryptocurrency returns. Due to the high volatility behavior of cryptocurrencies, Lawuobahsumo et al. (2024) show that the VIX index, the Treasury Yield Spread, the 5-year Forward Inflation Expectation Rate, and the 10-year Breakeven Inflation Rate are significant determinants of cryptocurrency tail risks. Basher and Sadorsky (2022) report that technical

indicators, such as MA50, WAD, MACDSignal, and macroeconomic variables, like the oil volatility index and ten-year bond yields, can predict Bitcoin price direction. Wang et al. (2022) show that technical indicators are more accurate in forecasting Bitcoin volatility during low volatility phases. Bakas et al. (2022) show that Google trends can positively impact Bitcoin volatility, while total circulation of Bitcoins, the US consumer confidence, and the S&P500 index have a negative effect on Bitcoin volatility. Conversely, Borri (2019) finds no exposure of cryptocurrency tail risks arising from assets such as equities or gold. Cryptocurrencies not only lack any intrinsic value but also do not pay dividends. Furthermore, they are not accepted as legal tender or an official medium of exchange. With Bitcoin having a limited supply, investors can believe that buying it will enable them to sell it at a higher price later, which can result in speculative bubbles. Bitcoin has seen its price rise to around $20,000 per coin between August and December 2017 and a similar fall (around $22,700) between May and June 2021. These patterns may be due to the "fear of missing out" of many private investors.

Starting from this background, the present study aims to explore calendar effects in the cryptocurrency market. Calendar effects are anomalies in financial returns related to the calendar, such as the day-of-the-week, the month-of-the-year, the quarter-of-the-year, or holidays. Equities, for instance, would trade the least amount on Mondays and register high returns on Fridays (e.g. Birru, 2018; Kiymaz and Berument, 2003; Tang, 1997). Bouman and Jacobsen (2002) show that stock returns are lower in the summer months (from May to October) and higher in the winter months (from November to April); this is the so-called "sell-in-May-and-go-away" effect and the Halloween effect (leaving the market in May and coming back after Halloween, 31 October). The presence of calendar effects gives rise to predictable patterns in returns exploitable by market participants. Calendar effects imply, indeed, that in a particular period, financial returns behave contrary to the Efficient Market Hypothesis[1] (EMH) proposed by Fama (1965), and the existence of a systematic pattern creates an opportunity to earn abnormal returns through the existing information. Thus, taking advantage of calendar effects or seasonal anomalies may be beneficial in terms of investment timing.

From this backdrop, we endeavor to study the calendar anomalies of six cryptocurrencies, namely Bitcoin, Dash, Dogecoin, Litecoin, Ripple, and Stellar. Similar to Kinateder and Papavassiliou (2021), we explore several calendar anomalies, such as the

[1] A market is efficient if market prices fully reflect all available information (MacDonald and Taylor, 1988).

day-of-the-week (DOW), the month-of-the-year (MOY) Quarter-of-the-Year (QOY), the US Holidays and Weekend calendar effects, for the selected cryptocurrencies. Contrary to Kinateder and Papavassiliou (2021), we employ the Autoregressive Conditional Density (ACD) model with dummy variables and hence broaden the investigation of these calendar anomalies to include higher moments, namely skewness and kurtosis, in addition to mean and variance. The ACD model is an extension of the GARCH model, allowing for time variation in higher moments, thus providing a deeper understanding of the sources of seasonalities at different moment levels.

Studying anomalies in higher moments is relevant since they give insights into the shape and behavior of a probability distribution beyond what is captured by the mean and the variance.Chung et al. (2006) suggest that in the absence of normality, investors should be very concerned with the shape of the tails of the distribution of portfolio returns, captured by higher-order moments. Skewness captures the distributional asymmetry, with positive skewness indicating a distribution with a tail on the right side that is longer than the left side and vice-versa. It is essential to study skewness anomalies because they would indicate return asymmetries and possible severe losses or gains. In addition, ignoring such anomalies may lead to a misinterpretation of the underlying distribution's shape. Since kurtosis measures the tail heaviness of a distribution, it shows that outliers exist in the tails, indicating more extreme returns than a normal distribution, a typical feature of several financial series (Brooks and Henry, 2002; Dufour et al., 2003). Furthermore, ignoring these higher moments' anomalies may lead to inaccurate characterizations of the distribution, which can affect the robustness of the models and the accuracy of return predictions.

Our results show anomalies in the mean, variance, skewness, and kurtosis of these cryptocurrencies' returns, which signifies that the cryptocurrency market tends to violate the Efficient Market Hypothesis. Our findings are relevant to the various stakeholders in the cryptocurrency market. Crypto market participants can also consider the state of crypto markets with respect to calendar anomalies for their decision-making. Institutional and retail traders can build diversified portfolios of different cryptocurrencies using seasonal statistics and devise strategies based on seasonal patterns of a given cryptocurrency. Analysts can use our results to inform the choice of distribution and model specification when analyzing cryptocurrency returns. As mentioned, higher-order moments are significant in cryptocurrency markets and should be given

consideration when modeling cryptocurrency returns.

The remainder of this paper is organized as follow: Section 2.2 reviews the existing literature on calendar anomalies. Section 2.3 discusses our methodology, while Section 2.4 presents the results of the empirical analysis. Section 2.5 concludes the paper.

2.2 Literature review

Calendar anomalies studies aim at describing the tendency of financial assets to behave dissimilarly during different periods of the week, the month or the year. For instance, researchers have documented that returns tend to be higher in January in contrast to other months and observe different patterns across days of the week, within the day, beginning-of-quarter, end-of-quarter, beginning-of-year, and end-of-year, among others. Most of these studies analyze volume and volatility as well as returns. We focus our review of the literature on calendar anomalies involving stock, commodity, and cryptocurrency markets.

Wachtel (1942) was the first to report calendar effects as a form of seasonality. He studied the monthly effect in the US stock market, which other researchers later elaborated on. Rozeff and Kinney Jr (1976) scrutinized the New York Stock Exchange from 1904 to 1974 and found seasonality in monthly rates of return with a distinct January effect on the equity market.

French (1980) in another study detected consistent negative returns on Mondays for S&P 500 returns from 1953 through 1977. He highlighted that the weekend effect was responsible for the negative Monday returns, not a general 'closed-market' effect. Gibbons and Hess (1981) showed that the daily seasonality is most evident on Mondays when there are consistently negative mean returns for stocks and below-average returns for T-bills. They further noted that market-adjusted returns exhibited a day-of-the-week effect.

Kohli and Kohers (1992) identified a week-of-the-month return effect in the S&P 500 index as a seasonal anomaly due to a previously unidentifiable and ongoing pattern. These results imply significant differences in weekly return patterns across the weeks of a month. Kim and Park (1994) reported abnormally high returns in three of the major stock markets in the US (NYSE, AMEX, and NASDAQ) on the trading days

before the holidays. They also observed relevant holiday effects in the US and Japanese stock markets, given each country's difference in holidays and institutions. Boudreaux (1995) investigated Denmark, France, Germany, Norway, Singapore/Malaysia, Spain, and Switzerland stock markets for monthly effects. They detected the monthly effects in almost all of these countries. They also confirmed the existence of a January effect and a monthly effect in the US stock market. Shum and Tang (2005) found no evidence of January effect in the Hong Kong equity market but they detected a January effect in the book-to-market equity ratio premium in Singapore.

Haug and Hirschey (2006) investigated the presence of the January effect in value-weighted returns for the years 1802-2004 and in equal-weighted returns for the years 1927-2004. Their results showed a persistent January effect for small-cap stocks. Similarly, Rompotis (2009) found that Greek equity funds experienced a highly depressive January effect on returns. Marrett and Worthington (2009) showed that the Australian market exhibited a pre-holiday effect common to small-cap stocks. Chia and Liew (2012) detected that from January 2000 to June 2009, the Japanese stock market experienced the November effect.

Fabozzi et al. (1994) found evidence of a holiday effect in futures commodities market. They observed significantly higher preholiday returns in futures contracts compared to nonholiday returns. Kohli (2014) singled out a DOW effect and January effect in crude oil returns in the period from 1983 through 2012. The research further indicated that there might be a daily seasonality in the variance of oil returns. Arendas (2017) showed that the Halloween effect was evident in the agricultural commodities markets. Qadan et al. (2019), in another study, observed within the commodity the presence of the Halloween effect, seasonal affective disorder (SAD)[2] effect, January effect, during-the-month effect, and start-of-the-month effect. Chhabra and Gupta (2022) investigated the calendar anomalies for the Indian commodity market and found that the calendar anomalies have been more prevalent in energy-based commodities than metals. Meek and Hoelscher (2023) investigated the DOW effect for petroleum and related products. They observed that the DOW effect varies across energy commodities. For instance, oil future return showed a negative Monday but a positive Wednesday return. They noted that when oil prices close higher on Friday, equity prices for energy companies the following Monday may be higher.

[2]SAD refers to the seasonal variation in stock returns, which is linked to the depression caused by shorter days in the fall and winter.

Studying the market efficiency of Bitcoin, Urquhart (2016) showed that the Bitcoin market was not inefficient during the entire sample period (August 2010 - July 2016). Nadarajah and Chu (2017) used the simple power transformation of the Bitcoin returns to study the efficiency of crypto markets. They concluded that Bitcoin returns do not support the efficient market hypothesis. In further studies, Aharon and Qadan (2019) used OLS and GARCH models to analyze anomalies in Bitcoin returns. They reported evidence of the DOW effect on Bitcoin at the mean and variance levels for data from 2010–2017.

According to Baur et al. (2019), there existed time-specific anomalies in Bitcoin returns but they were not persistent for DOW and MOY, suggesting that investors could exploit these anomalies, reducing or eliminating them. According to Ma and Tanizaki (2019), the Bitcoin return and volatility were affected by the DOW effect. Kaiser (2019) tests for seasonality patterns in cryptocurrency returns, volatility, trading volume, and a spread estimator. The author observed that cryptocurrency returns do not have consistent and robust calendar effects and concluded that cryptocurrencies experience weak-form market efficiency. Caporale and Plastun (2019) investigated the day-of-the-week effect in the cryptocurrency market and detected no anomalies except for Bitcoin, for which returns on Mondays were significantly higher than those on the other days of the week. Kinateder and Papavassiliou (2021) examined Bitcoin returns for Halloween effects, DOW effect and MOY effects for the period between 2013-2019. They did not find a Halloween effect or DOW effect in Bitcoin return, but they identified the January effect. In a recent study, Naz et al. (2023) examined the day-of-the-week and January effects on cryptocurrencies with the highest capitalization. The results indicated that the Monday effect in the daily analysis generated a positive and significant coefficient for the considered currencies.

Similar to Urquhart (2016); Nadarajah and Chu (2017); Aharon and Qadan (2019); Baur et al. (2019); Caporale and Plastun (2019); Ma and Tanizaki (2019); Kaiser (2019); Kinateder and Papavassiliou (2021); Naz et al. (2023), we study calendar effects in crypocurrency market. A novelty of the present study is that calendar anomalies are investigated not just for Bitcoin but for several cryptocurrencies. We have only found the study by Caporale and Plastun (2019) that considers Bitcoin, Litecoin, Ripple and Dash. However, while these authors focus only on the day-of-the-week anomalies, we broaden the perspective to include the month-of-the-year, the quarter-of-the-year, the

US Holidays and Weekend calendar effects. Additionally and foremost, we are the first to study anomalies in higher moments (skewness and kurtosis) for the returns of the considered cryptocurrencies. The inclusion of higher moments is crucial since they offer insights into the shape and behavior of a probability distribution beyond what is seized by mean and variance; this means that in addition to average returns and volatility anomalies, also the asymmetries in return gains and losses and the occurrence of extreme returns are taken into account.

2.3 Methodology

We compute returns at time t, x_t, as the logarithmic change in daily closing prices (P) of a given cryptocurrency:

$$x_t = \log(P_t) - \log(P_{t-1}) \tag{2.1}$$

and consider the following Autoregressive Conditional Density (ACD) model:

$$x_t = \mu_t + \varepsilon_t = \mu_t + \sigma_t z_t \tag{2.2}$$

with $z_t \sim JSU\,(0, 1, \xi_t, \eta_t)$, where JSU denotes the reparameterized Johnson's SU distribution presented in Appendix A.1. The skew parameter ξ_t controls the asymmetry of the distribution, whereas η_t controls the thickness of the tail. We present in equations (2.3a)–(2.3d) the dynamics for the (transformed) parameters determining the mean (μ_t), variance (σ_t^2), skewness (ξ_t), and kurtosis (λ_t):

$$\mu_t = \mu + \sum_{i=1}^{P} \phi_i x_{t-i} + \sum_{j=1}^{Q} \delta_j \varepsilon_{t-j} \tag{2.3a}$$

$$\sigma_t^2 = q_t + \sum_{j=1}^{q} \alpha_j (\varepsilon_{t-j}^2 - q_{t-j}) + \sum_{j=1}^{p} \beta_j (\sigma_{t-j}^2 - q_{t-j}) \tag{2.3b}$$

$$\xi_t = c_1 + a_1 \left|z_{t-1}\right| I_{z_{t-1}<0} + g_1 \left|z_{t-1}\right| I_{z_{t-1}\geq 0} + b_1 \xi_{t-1} \tag{2.3c}$$

$$\lambda_t = \log(\eta_t) = c_2 + a_2 z_{t-1} + g_2 z_{t-1}^2 + b_2 \lambda_{t-1}. \tag{2.3d}$$

For the mean equation, we adopt an ARMA(P,Q), with the order of the model establish using the Bayesian Information Criteria (BIC). For the variance equation, we consider the component GARCH model of Lee and Engle (1999). In the Lee and Engle

(1999) model, the conditional variance is decomposed into a permanent and transitory component capturing the long- and short-run movements in volatility, respectively. In equation (2.3b), the permanent component of the conditional variance is specified as:

$$q_t = \omega - \rho q_{t-1} + \phi(\varepsilon_{t-1}^2 - \sigma_{t-1}^2) \tag{2.4}$$

where σ_{t-j}^2 is the lagged conditional variance and q_{t-j} its trend. The difference $\sigma_{t-j}^2 - q_{t-j}$ is the transitory component of the conditional variance. For the stationarity conditions to hold, the sum of the (α, β) coefficients in equation (2.3b) should be less than 1 and that $\rho < 1$ in equation (2.4).

In the case of the equation for the law of motion of the parameter ξ that determines the skewness of the distribution, we use a piece-wise linear model (equation 2.3c) as in Jondeau and Rockinger (2003). In equation (2.3c) and in the rest of this study, I_A denotes the indicator function, taking on value 1 if A is true, 0 otherwise. Finally, for the parameter determining the kurtosis of the distribution, we model its logarithm, $\lambda = \log(\eta)$ so that the positivity constraint is satisied for all t and model λ using a quadratic specification (equation 2.3d) as in Hansen (1994).

Our strategy to assess whether there are calendar effects affecting one of the first four moments of each cryptocurrency distribution involves adding dummies to equations (2.3a)–(2.3d). Specifically, we estimate the ACD model of equations (2.3a)–(2.3d) and add a dummy variable only to a specific equation. As an example, when investigating calendar effects in the skewness, we keep (2.3a), (2.3b), and (2.3d) as above and only change (2.3c) as follows:

$$\xi_t = c_1 + a_1 \left|z_{t-1}\right| I_{z_{t-1}<0} + g_1 \left|z_{t-1}\right| I_{z_{t-1}\geq 0} + b_1 \xi_{t-1} + d' D_{t,c}$$

where $D_{t,c}$ represent the time-t value of the dummy variables capturing a given calendar effect. The calendar effects we consider are listed in Table 2.1.

Table 2.1: List of Calendar Effects.

Calendar Effect	Description
Day Of The Week (DOW)	Dummies for days Monday to Sunday
Month Of The Year (MOY)	Dummies for months January to December
Quarter Of The Year (QOY)	Dummies for Q1 to Q4
Weekend	Dummies "SaturdayOrSunday"
Holiday	Dummies "Holiday"

Note: In the case of the Holiday calendar effect, we consider holidays in the United States.

2.4 Empirical Analysis

2.4.1 Data Description

We use daily closing prices for six cryptocurrencies to calculate daily returns. Our analysis covers the period ranging from August 8, 2015, to September 30, 2023. We have collected data for Bitcoin, Dash, Dogecoin, Litecoin, Ripple, and Stellar from coinMarketCap.com. Since cryptocurrencies trade seven days a week, we analyze $T = 2,976$ returns for each cryptocurrency. We present descriptive statistics in Table 2.2 for the selected cryptocurrencies[3]. Figure 2.1 and Figure 2.2 sketch the return dynamics of each cryptocurrency and density plots, respectively. In detail, Table 2.2 indicates that cryptocurrency returns have positive mean values, higher for Ripple, Bitcoin and Dogecoin than Stellar, Litecoin and Dash, and high standard deviations, suggesting dispersion in volatility across the six cryptocurrencies, with Ripple having the most considerable value. The data shows that Bitcoin returns are negatively skewed, denoting that this cryptocurrency experiences frequent modest gains and a few severe losses (Algieri and Leccadito, 2019). We also identify the presence of excess kurtosis in all cryptocurrencies, especially for Ripple and Dogecoin, and we can visually detect outliers in Figure 2.2. The zero p-values of the Jarque-Bera test show that returns do not conform to bell-shaped Gaussian distributions, i.e. cryptocurrency returns are not normally distributed and this is confirmed by the density plots reported in Figure 2.2.

Tables 2.3–2.7 present instead descriptive statistics for DOW, MOY, QOY, the US Holiday, and Weekend effects. In the case of the mean, reported in the first

[3]The cryptocurrencies data in this chapter includes the presence of weekend and U.S. holidays returns and accounts for the differences in descriptive statistics.

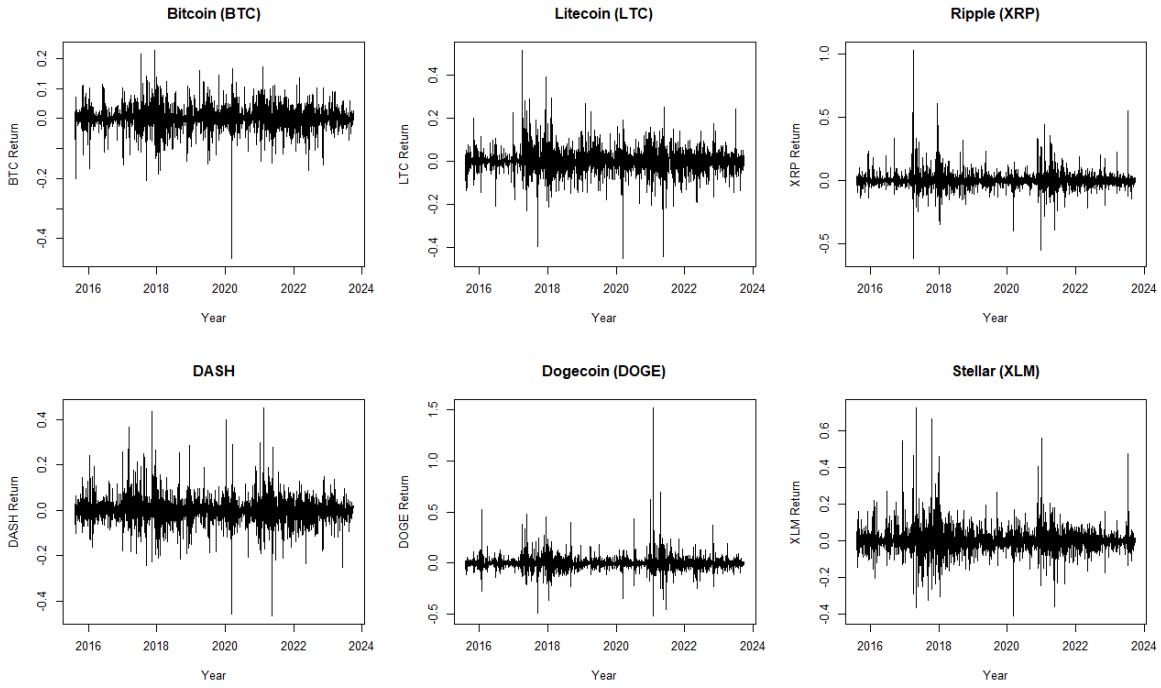

Figure 2.1: Plot of Cryptocurrencies Log Returns.
Note: Data spans from August 8, 2015, to September 30, 2023

panel of each table, we present $\hat{\mu}_{D_c} = \frac{1}{\sum_{t=1}^{T} I_{D_{t,c}=1}} \sum_{t=1}^{T} x_t I_{D_{t,c}=1}$, where $D_{t,c}$ is the dummy variable capturing a given calendar effect. The variance is calculated as $\hat{\sigma}^2_{D_c} = \frac{1}{\sum_{t=1}^{T} I_{D_{t,c}=1}} \sum_{t=1}^{T} (x_t - \hat{\mu}_{D_c})^2 I_{D_{t,c}=1}$ and skewness and kurtosis are calculated in a similar way. Table 2.3 shows that Bitcoin has a negative mean return on Thursday and Sunday. The table further reveals that the Bitcoin returns are negatively skewed except for Monday, meaning that there is a higher probability of significant negative returns and small gains during all the other days of the week. Considering the tail, the results show that Bitcoin returns have a fat tail implying extreme return risk.

Table 2.2: Descriptive Statistics for Daily Log-returns of Cryptocurrencies

	Bitcoin	Dash	Dogecoin	Litecoin	Ripple	Stellar
Mean	0.0015	0.0007	0.0014	0.0009	0.0020	0.0013
Standard Deviation	0.0377	0.0571	0.0648	0.0534	0.0711	0.0674
Median	0.0015	0.0002	-0.0017	-0.0002	-0.0008	-0.0016
Minimum	-0.4647	-0.4655	-0.6163	-0.4491	-0.5151	-0.4100
Maximum	0.2251	0.4513	1.0274	0.5114	1.5164	0.7231
Standard Error	0.0007	0.0010	0.0012	0.0010	0.0013	0.0012
Skewness	-0.7490	0.3599	2.1899	0.2898	4.2267	1.9492
Kurtosis	14.5331	12.3677	40.1637	14.5822	84.5862	22.9973
Jarque_Bera	16771.9173	10945.6337	173640.4181	16676.0117	834242.4603	51471.2115
p-value	0.0000	0.0000	0.0000	0.0000	0.0000	0.0000

Table 2.3: Descriptive Statistics, DOW Effect

	Bitcoin	Dash	Dogecoin	Litecoin	Ripple	Stellar
Mean $\hat{\mu}_{D_c}$						
Monday	0.0035	-0.0025	-0.0023	-0.0018	-0.0006	0.0020
Tuesday	0.0013	-0.0014	0.0000	0.0021	0.0011	0.0015
Wednesday	0.0021	0.0029	0.0013	-0.0008	-0.0014	-0.0002
Thursday	-0.0002	-0.0011	0.0026	-0.0035	0.0036	-0.0026
Friday	0.0017	0.0027	0.0043	0.0046	0.0055	0.0030
Saturday	0.0024	0.0037	0.0075	0.0063	0.0010	0.0048
Sunday	-0.0001	0.0007	0.0006	-0.0005	0.0006	0.0006
Variance $\hat{\sigma}^2_{D_c}$						
Monday	0.0016	0.0033	0.0039	0.0029	0.0048	0.0048
Tuesday	0.0014	0.0028	0.0041	0.0028	0.0038	0.0050
Wednesday	0.0015	0.0044	0.0043	0.0037	0.0042	0.0055
Thursday	0.0023	0.0038	0.0100	0.0039	0.0065	0.0052
Friday	0.0014	0.0025	0.0044	0.0031	0.0035	0.0040
Saturday	0.0009	0.0031	0.0051	0.0019	0.0024	0.0035
Sunday	0.0008	0.0030	0.0035	0.0016	0.0041	0.0038
Skewness $\hat{\tilde{\mu}}_{3,D_c}$						
Monday	0.0133	0.0369	-0.4775	0.5921	-0.9618	2.3037
Tuesday	-0.7867	0.0893	0.9832	0.9754	0.5654	1.1918
Wednesday	-0.1413	0.0477	0.6918	-0.3871	-1.6575	1.2780
Thursday	-1.9138	-0.7813	8.0543	-0.0710	2.6291	0.5069
Friday	-0.1357	-0.2308	3.2593	0.5856	2.3929	1.7158
Saturday	-0.1923	2.0295	1.9657	1.2680	2.7110	3.7711
Sunday	-0.2677	1.8522	2.3807	0.0038	9.9447	4.6476
Kurtosis $\hat{\tilde{\mu}}_{4,D_c}$						
Monday	6.1863	6.2081	11.6118	9.6903	22.5602	24.5955
Tuesday	7.8060	6.4168	16.9232	12.7437	11.5831	16.7589
Wednesday	6.1888	13.8149	11.6872	12.8703	18.8534	15.7204
Thursday	25.8294	12.1246	126.5007	22.3874	20.3143	11.5924
Friday	5.7936	4.9604	35.0872	7.2616	17.9070	14.6747
Saturday	7.4936	19.4319	28.6647	10.3004	26.8430	43.6662
Sunday	6.1495	16.0683	19.3824	5.9224	157.7111	53.3472

Note: This table reports, for each cryptocurrency, $\hat{\mu}_{D_c} = \frac{1}{T_{D_c}} \sum_{t=1}^{T} I_{D_{t,c}=1}$, $\hat{\sigma}^2_{D_c} = \frac{1}{T_{D_c}} \sum_{t=1}^{T} (x_t - \hat{\mu}_{D_c})^2 I_{D_{t,c}=1}$, $\hat{\tilde{\mu}}_{3,D_c} = \frac{1}{T_{D_c}} \sum_{t=1}^{T} \left(\frac{x_t - \hat{\mu}_{D_c}}{\hat{\sigma}_{D_c}} \right)^3 I_{D_{t,c}=1}$, and $\hat{\tilde{\mu}}_{4,D_c} = \frac{1}{T_{D_c}} \sum_{t=1}^{T} \left(\frac{x_t - \hat{\mu}_{D_c}}{\hat{\sigma}_{D_c}} \right)^4 I_{D_{t,c}=1}$, where $T_{D_c} = \sum_{t=1}^{T} I_{D_{t,c}=1}$ and $D_{t,c}$ is the dummy DOW at time t.

Table 2.4: Descriptive Statistics, MOY Effect

	Bitcoin	Dash	DOGE	Litecoin	Ripple	Stellar
Mean $\hat{\mu}_{D_m}$						
January	-3.17e-05	0.0045	0.0092	0.0002	0.0005	0.0048
February	0.0037	0.0056	-0.0006	0.0034	-0.0009	-0.0020
March	-0.0010	0.0036	-0.0017	0.0002	0.0045	0.0004
April	0.0040	0.0028	0.0154	0.0068	0.0086	0.0065
May	0.0015	-0.0018	0.0028	0.0009	0.0029	0.0054
June	-0.0003	-0.0046	-0.0033	-0.0015	-0.0043	-0.0046
July	0.0029	0.0006	-0.0013	0.0003	0.0005	0.0010
August	-0.0002	0.0013	0.0010	-0.0032	0.0000	-0.0014
September	-0.0013	-0.0034	-0.0037	-0.0026	0.0012	-0.0021
October	0.0061	-0.0019	0.0028	0.0022	-0.0009	0.0029
November	0.0007	0.0025	-0.0011	0.0027	0.0009	0.0027
December	0.0030	0.0002	0.0050	0.0029	0.0035	0.0020
Variance $\hat{\sigma}^2_{D_m}$						
January	0.0018	0.0053	0.0178	0.0027	0.0042	0.0060
February	0.0015	0.0044	0.0042	0.0031	0.0030	0.0029
March	0.0023	0.0051	0.0024	0.0036	0.0043	0.0031
April	0.0009	0.0028	0.0079	0.0028	0.0101	0.0040
May	0.0015	0.0045	0.0067	0.0048	0.0061	0.0101
June	0.0018	0.0023	0.0034	0.0032	0.0024	0.0031
July	0.0013	0.0019	0.0037	0.0018	0.0028	0.0042
August	0.0010	0.0027	0.0026	0.0016	0.0022	0.0020
September	0.0011	0.0023	0.0036	0.0029	0.0032	0.0035
October	0.0006	0.0010	0.0019	0.0011	0.0014	0.0050
November	0.0016	0.0039	0.0031	0.0028	0.0031	0.0046
December	0.0017	0.0032	0.0035	0.0040	0.0080	0.0063
Skewness $\hat{\tilde{\mu}}_{3,D_m}$						
January	-0.8818	0.9324	6.1209	-0.4973	0.7272	2.2486
February	0.1148	1.1560	1.4752	0.9097	-0.5539	-0.1065
March	-3.4955	0.0450	-1.0795	0.8459	1.4521	-1.2968
April	0.8756	0.1641	2.5677	1.0257	3.7471	1.3606
May	-0.2015	-1.2811	0.6604	-0.8565	0.2732	2.6382
June	-0.6245	-0.6679	-1.6992	0.4758	0.6539	0.2257
July	0.8352	0.2234	1.6578	0.4238	4.4437	1.4643
August	-0.9788	1.0924	2.5148	0.0822	1.1148	0.4756
September	-1.0327	-1.3424	-1.6353	-1.7748	1.2299	-0.3468
October	1.2063	0.1113	3.1064	1.4927	-0.1304	3.6986
November	-0.4504	1.3340	0.3530	-0.0450	1.4002	1.3602
December	0.8789	0.6399	2.0066	2.0976	1.7385	2.1475
Kurtosis $\hat{\tilde{\mu}}_{4,D_m}$						
January	6.3748	8.2984	69.7644	6.0694	18.2007	18.7897
February	6.8246	11.6866	10.3547	8.5924	7.2866	5.8667
March	37.0541	13.1870	13.7867	34.8098	21.5748	15.3220
April	7.9133	4.6426	19.5172	7.8770	51.4209	15.7956
May	4.9776	13.5475	10.4673	11.4335	9.0113	23.2215
June	4.9344	7.9620	18.0161	8.0862	11.8972	6.9478
July	9.0525	6.7293	14.2756	4.6741	48.6971	15.2006
August	9.4841	7.8278	18.8748	5.1324	8.4386	4.3103
September	12.1021	9.4592	23.3684	15.3721	12.5786	9.2234
October	8.4935	5.9045	24.7885	11.8093	6.8114	35.9730
November	5.3327	13.2577	7.8548	4.1082	14.0764	10.7267
December	8.0736	7.9804	17.6481	13.4828	21.4262	14.0087

Note: This table reports, for each cryptocurrency, $\hat{\mu}_{D_m} = \frac{1}{T_{D_m}} \sum_{t=1}^{T} I_{D_{t,m}=1}$, $\hat{\sigma}^2_{D_m} = \frac{1}{T_{D_m}} \sum_{t=1}^{T} (x_t - \hat{\mu}_{D_m})^2 I_{D_{t,m}=1}$, $\hat{\tilde{\mu}}_{3,D_m} = \frac{1}{T_{D_m}} \sum_{t=1}^{T} \left(\frac{x_t - \hat{\mu}_{D_m}}{\hat{\sigma}_{D_m}} \right)^3 I_{D_{t,m}=1}$, and $\hat{\tilde{\mu}}_{4,D_m} = \frac{1}{T_{D_m}} \sum_{t=1}^{T} \left(\frac{x_t - \hat{\mu}_{D_m}}{\hat{\sigma}_{D_m}} \right)^4 I_{D_{t,m}=1}$, where $T_{D_m} = \sum_{t=1}^{T} I_{D_{t,m}=1}$ and $D_{t,m}$ is the dummy MOY at time t.

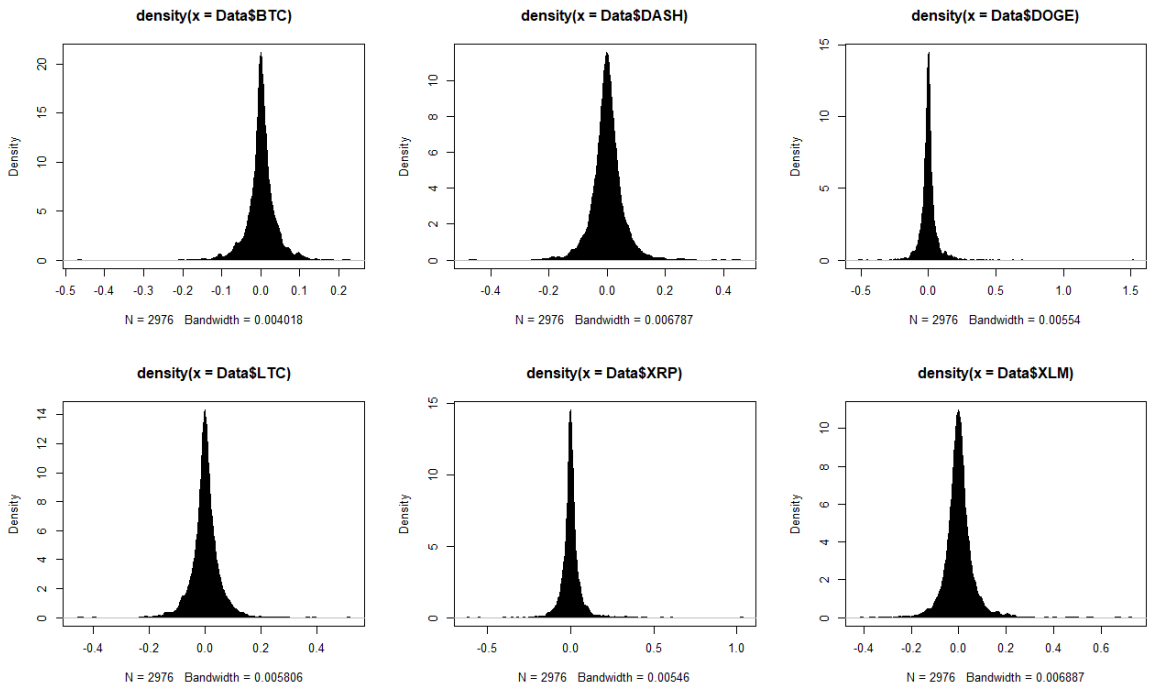

Figure 2.2: Density Plot of Cryptocurrencies Log Returns.
Note: Data spans from August 8, 2015, to September 30, 2023

Table 2.5: Descriptive Statistics, QOY Effect

	Bitcoin	Dash	DOGE	Litecoin	Ripple	Stellar
Mean $\hat{\mu}_{D_q}$						
Q1	0.0008	0.0045	0.0024	0.0012	0.0014	0.0012
Q2	0.0017	-0.0012	0.0049	0.0020	0.0024	0.0025
Q3	0.0004	-0.0005	-0.0014	-0.0019	0.0006	-0.0009
Q4	0.0033	0.0002	0.0022	0.0026	0.0012	0.0025
Variance $\hat{\sigma}^2_{D_q}$						
Q1	0.0019	0.0049	0.0083	0.0031	0.0038	0.0040
Q2	0.0014	0.0032	0.0060	0.0036	0.0062	0.0058
Q3	0.0011	0.0023	0.0033	0.0021	0.0027	0.0032
Q4	0.0013	0.0027	0.0028	0.0026	0.0041	0.0053
Skewness $\hat{\tilde{\mu}}_{3,D_q}$						
Q1	-1.8887	0.6757	6.9008	0.5002	0.7593	1.1446
Q2	-0.2610	-0.8129	1.3747	-0.1080	2.8183	2.4159
Q3	-0.2541	0.0713	0.5876	-0.8523	2.2652	0.6558
Q4	0.3322	1.0946	1.6498	1.4459	1.8959	2.4350
Kurtosis $\hat{\tilde{\mu}}_{4,D_q}$						
Q1	22.4599	11.0358	114.5941	20.0836	18.0947	18.8640
Q2	5.8140	11.6576	18.0262	10.6366	49.5222	27.6443
Q3	10.4371	8.4975	19.5626	12.0342	23.8907	12.7398
Q4	7.9494	13.3406	16.1541	12.7320	29.6279	20.0558

Note: This table reports, for each cryptocurrency, $\hat{\mu}_{D_q} = \frac{1}{T_{D_q}} \sum_{t=1}^{T} I_{D_{t,q}=1}$, $\hat{\sigma}^2_{D_q} = \frac{1}{T_{D_q}} \sum_{t=1}^{T} (x_t - \hat{\mu}_{D_q})^2 I_{D_{t,q}=1}$, $\hat{\tilde{\mu}}_{3,D_q} = \frac{1}{T_{D_q}} \sum_{t=1}^{T} \left(\frac{x_t - \hat{\mu}_{D_q}}{\hat{\sigma}_{D_q}} \right)^3 I_{D_{t,q}=1}$, and $\hat{\tilde{\mu}}_{4,D_q} = \frac{1}{T_{D_q}} \sum_{t=1}^{T} \left(\frac{x_t - \hat{\mu}_{D_q}}{\hat{\sigma}_{D_q}} \right)^4 I_{D_{t,q}=1}$, where $T_{D_q} = \sum_{t=1}^{T} I_{D_{t,q}=1}$ and $D_{t,q}$ is the dummy QOY at time t.

Table 2.6: Descriptive Statistics Holiday Effect

	Bitcoin	Dash	DOGE	Litecoin	Ripple	Stellar
Mean $\hat{\mu}_{D_h}$						
NoHoliday	0.0015	0.0007	0.0020	0.0009	0.0014	0.0013
Holiday	0.0162	-0.0088	0.0093	0.0194	0.0176	-0.0114
Variance $\hat{\sigma}^2_{D_h}$						
NoHoliday	0.0014	0.0033	0.0051	0.0028	0.0042	0.0045
Holiday	0.0044	0.0013	0.0007	0.0031	0.0016	0.0008
Skewness $\hat{\tilde{\mu}}_{3,D_h}$						
NoHoliday	-0.7588	0.3592	4.2224	0.2897	2.1900	1.9463
Holiday	0.0648	-0.1522	0.7341	0.3061	0.3785	0.3279
Kurtosis $\hat{\tilde{\mu}}_{4,D_h}$						
NoHoliday	14.6187	12.3512	84.4045	14.5984	40.1222	22.9496
Holiday	1.4657	0.8850	1.9387	1.2156	1.5662	1.2112

Note: This table reports, for each cryptocurrency, $\hat{\mu}_{D_h} = \frac{1}{T_{D_h}} \sum_{t=1}^{T} I_{D_{t,h}=1}$, $\hat{\sigma}^2_{D_h} = \frac{1}{T_{D_h}} \sum_{t=1}^{T} (x_t - \hat{\mu}_{D_h})^2 I_{D_{t,h}=1}$, $\hat{\tilde{\mu}}_{3,D_h} = \frac{1}{T_{D_h}} \sum_{t=1}^{T} \left(\frac{x_t - \hat{\mu}_{D_h}}{\hat{\sigma}_{D_h}}\right)^3 I_{D_{t,h}=1}$, and $\hat{\tilde{\mu}}_{4,D_h} = \frac{1}{T_{D_h}} \sum_{t=1}^{T} \left(\frac{x_t - \hat{\mu}_{D_h}}{\hat{\sigma}_{D_h}}\right)^4 I_{D_{t,h}=1}$, where $T_{D_h} = \sum_{t=1}^{T} I_{D_{t,h}=1}$ and $D_{t,h}$ is the dummy U.S. Holidays at time t.

Table 2.7: Descriptive Statistics Weekend Effect

	Bitcoin	Dash	DOGE	Litecoin	Ripple	Stellar
Mean $\hat{\mu}_{D_w}$						
MonToFriday	0.0017	0.0001	0.0012	0.0001	0.0016	0.0007
SatSun	0.0012	0.0022	0.0040	0.0029	0.0008	0.0027
Variance $\hat{\sigma}^2_{D_w}$						
MonToFriday	0.0017	0.0034	0.0053	0.0033	0.0046	0.0049
SatSun	0.0008	0.0030	0.0043	0.0018	0.0033	0.0036
Skewness $\hat{\tilde{\mu}}_{3,D_w}$						
MonToFriday	-0.8085	-0.1780	4.8074	0.2341	0.7898	1.3572
SatSun	-0.2276	1.9448	2.1675	0.7167	7.8773	4.2388
Kurtosis $\hat{\tilde{\mu}}_{4,D_w}$						
MonToFriday	14.3382	10.4788	98.7522	14.3743	20.4727	16.8096
SatSun	6.8447	17.8275	26.6089	8.6390	132.0155	48.9787

Note: This table reports, for each cryptocurrency, $\hat{\mu}_{D_w} = \frac{1}{T_{D_w}} \sum_{t=1}^{T} I_{D_{t,w}=1}$, $\hat{\sigma}^2_{D_w} = \frac{1}{T_{D_w}} \sum_{t=1}^{T} (x_t - \hat{\mu}_{D_w})^2 I_{D_{t,w}=1}$, $\hat{\tilde{\mu}}_{3,D_w} = \frac{1}{T_{D_w}} \sum_{t=1}^{T} \left(\frac{x_t - \hat{\mu}_{D_w}}{\hat{\sigma}_{D_w}}\right)^3 I_{D_{t,w}=1}$, and $\hat{\tilde{\mu}}_{4,D_w} = \frac{1}{T_{D_w}} \sum_{t=1}^{T} \left(\frac{x_t - \hat{\mu}_{D_w}}{\hat{\sigma}_{D_w}}\right)^4 I_{D_{t,w}=1}$, where $T_{D_w} = \sum_{t=1}^{T} I_{D_{t,w}=1}$ and $D_{t,w}$ is the dummy U.S. Holidays at time t.

2.4.2 Discussion of the Results

In Table 2.8, we present the results for the DOW effect in the mean, variance, skewness, and kurtosis equations for each cryptocurrency. Considering the mean equation for the DOW effect, we observe a Tuesday, Friday, and Saturday effect for Bitcoin and a Friday effect for Litecoin and Dash. Dogecoin displays a Monday, Friday, and Saturday effect, while Ripple and Stellar returns show a Thursday effect. This would suggest that the average returns of all cryptocurrencies, except for Ripple and Stellar, are higher on

Fridays. Dogecoin tends to experience negative returns on Mondays, while Ripple and Stellar record negative "blue" returns on Thursdays. Our results for Bitcoin differ from Aharon and Qadan (2019), Ma and Tanizaki (2019) and Caporale and Plastun (2019), who detected a day-of-the-week effect on Monday, suggesting significantly higher mean return at the start of the week than other weekdays, but it is more in line with Bush et al. (2020).

Table 2.8: Estimates of the Day of the Week Effect in the Mean, Variance, Skewness, and Kurtosis

Mean Equation	Bitcoin	Dash	Dogecoin	Litecoin	Ripple	Stellar
Monday	0.0012	-0.0008	-0.0023*	-0.0015	-0.0012	-0.0012
Tuesday	0.0031**	-0.0018	-0.0010	0.0011	-0.0011	-0.0021
Wednesday	0.0003	0.0009	-0.0013	-0.0006	-0.0003	-0.0026
Thursday	0.0003	-0.0031	-0.0021	-0.0001	-0.0038***	-0.0037**
Friday	0.0020**	0.0042*	0.0037***	0.0026*	0.0009	0.0022
Saturday	0.0013*	0.0024	0.0018*	0.0016	0.0001	0.0023
Sunday	0.0005	-0.0027	-0.0014	-0.0009	-0.0017	-0.0005
Variance Equation						
Monday	2e-04	6e-04**	4e-04*	1.71e-07	3e-04	2.49e-05
Tuesday	2.85e-07	6.77e-08	1.69e-05	7.03e-08	6.85e-08	3.01e-05
Wednesday	3.52e-08	2.57e-08	7.86e-06	7.87e-08	1.30e-07	2.43e-08
Thursday	1.12e-08	3.18e-08	2.16e-07	2.07e-06**	2.33e-08	1.93e-08
Friday	2.08e-09	2.58e-09	1.98e-08	8.67e-10	6.83e-09	2.05e-09
Saturday	2.79e-11	4.43e-13	5.61e-13	1.30e-12	1.33e-18	6.90e-12
Sunday	1.84e-08	5.00e-08	3.55e-08	4.86e-08	1.42e-08	2.44e-08
Skewness Equation						
Monday	0.0021	-0.0308	0.0446***	0.0216	0.0143	0.0094
Tuesday	-0.0119	-0.0077	0.0062	-0.0023	0.0124	0.0110*
Wednesday	0.0004	-0.0275	0.0064	0.0001	-0.0254*	0.0025
Thursday	0.0002	0.0479**	0.0319	0.0088	0.0337**	0.0411**
Friday	0.0028	-0.0254	-0.0211	-0.0114	0.0190	0.0156
Saturday	-0.0054	-0.0287	-0.0053	-0.0141**	0.0061	-0.0436
Sunday	0.0118	0.0890***	0.0376**	0.0306	0.0224	0.0224
Kurtosis Equation						
Monday	0.1501	0.1878	0.0294	0.0005	0.2674	1.8373**
Tuesday	1.5715***	1.1652	0.3433	0.2351	1.4425*	1.8781***
Wednesday	1.5418**	0.9522	0.1468	0.1058	0.7156	1.7282**
Thursday	1.0532	0.9916	0.7032**	0.6106	1.6630*	2.3049***
Friday	1.9533***	0.8938	0.6845**	0.0162	1.2370	2.0873**
Saturday	7.6630	2.1048	1.0935***	1.1729	3.8102**	2.7475***
Sunday	0.0182	0.7984	0.0803	0.0050	0.6785	2.4920**

Note: *** = 1% significance, **= 5% significance, * = 10% significance

The variance equation, which provides an indication of the cryptocurrency's volatility, suggests that Dash and Dogecoin show a Monday effect (higher volatility) and Litecoin a Thursday effect. We do not find DOW anomalies in the variance of Bitcoin, Ripple, and Stellar returns.

The estimated skewness equation, which gives information about the asymmetries in the returns, shows that Bitcoin does not show a DOW effect, i.e. it is not possible to spot any systematic pattern regarding any likely abnormal value in the third moment of the distribution We observe a Thursday effect in Dash, Ripple, and Stellar's return,

suggesting that, tendentially, these cryptocurrencies record frequent small losses and a few extreme gains on Thursdays. The same pattern is recorded for Dash and Dogecoins on Sundays. Litecoin and Ripple tend instead to experience recurrent abnormal level of skewness on Saturdays and Wednesdays, respectively.

The estimated kurtosis equation, which reveals the probability of experiencing extreme returns, shows the Tuesday, Wednesday, and Friday effects in Bitcoin return with the highest likelihood of experiencing severe tail events on Fridays. We do not find a DOW effect for Dash and Litecoin. We detect Thursday, Friday, and Saturday effects in Dogecoin return. Ripple returns show Tuesday, Thursday, and Saturday effects, with the highest probability of registering strong tail events on Saturdays. For Stellar, we observe that all the days of the week dummies are significant and the highest risk of extreme events is on the weekend, especially on Saturdays.

Table 2.9: Estimates of the Month of the Year Effect in the Mean, Variance, Skewness, and Kurtosis

Mean Equation	Bitcoin	Dash	Dogecoin	Litecoin	Ripple	Stellar
January	0.0014	0.0037	-0.0012	9e-04	-0.0017	0.0023
February	0.0024	0.0033	-0.0014	9e-04	-0.0019	-0.0018
March	0.0013	0.0006	4e-04	0.0010	6e-04	0.0029
April	0.0031***	0.0004	0.0028	0.0010	1.10e-05	0.0012
May	0.0021	0.0014	-1e-04	0.0031	-0.0015	-0.0011
June	0.0015	-0.0016	3e-04	-2.36e-05	-5e-04	-0.0006
July	0.0001	0.0006	-0.0017	-0.0012	-4e-04	-0.0005
August	-0.0005	-0.0012	-9e-04	-0.0017	-0.0018	-0.0032**
September	0.0006	-0.0001	-2.66e-05	2e-04	-2.03e-05	-0.0004
October	0.0019*	-0.0022*	-4e-04	2e-04	-5e-04	-0.0004
November	0.0011	-0.0017	-9e-04	2e-04	-0.0011	-0.0028
December	0.0008	-0.0008	-9e-04	-9e-04	-0.0039* *	-0.0051***
Variance Equation						
January	0.0040	-0.0018	0.0386*	0.0100	0.0248***	0.0091
February	0.0033	0.0098***	0.0247	0.0273	0.0123	0.0053
March	-0.0083	0.0198	0.0303*	-0.0063	0.0162	0.0064
April	-0.0270	-0.0037	0.0093	0.0059	0.0074	-0.0202
May	-0.0187	-0.0125	0.0221	-0.0051	-0.0069	-0.0005
June	-0.0143	-0.0080	-0.0008	-0.0027	-0.0239	-0.0165
July	0.0228	0.0093	0.0303**	0.0481**	0.0143	0.0299*
August	0.0042	0.0001	0.0200	0.0164	0.0164* *	0.0200
September	0.0055	-0.0168	0.0032	0.0092	0.0044	0.0091
October	0.0295	0.0188	0.0243	0.0498*	0.0023***	0.0389*
November	-0.0128	0.0217	0.0199	0.0192	-0.0059	0.0176
December	0.0182	0.0118	0.0265	0.0343**	0.0357**	0.0284*
Skewness Equation						
January	4.20e-08	1e-04	1e-04	6.74e-09	1.39e-07	4.82e-08
February	3.38e-08	3e-04**	8.43e-08	3.50e-09	1.88e-08	2.34e-08
March	1.20e-09	2.32e-08	4.49e-07	4.89e-09	1.58e-08	5.66e-09
April	5.92e-07	1e-04	7.91e-09	2.45e-08	6.32e-09	1.62e-17
May	2.69e-07	1e-04	2.13e-11	1.96e-08	6.53e-13	1.75e-08
June	1.67e-08	1e-04	1.32e-05	4.01e-09	4.14e-09	1.11e-07
July	6.08e-09	1e-04	7.78e-09	1.53e-13	5.68e-09	1.25e-08
August	1.06e-08	1e-04	1.94e-07	1.72e-08	2.15e-08	5.74e-08
September	7.63e-16	3.66e-13	3.71e-05	5.67e-08	1e-04	1.29e-05
October	1.33e-05	1e-04*	7.43e-06	6.55e-06***	1.77e-07	2.73e-07
November	1.13e-07	1e-04*	2.56e-05	6.06e-09	2.53e-05	1.18e-07
December	4.03e-08	1e-04	1.06e-05	1.54e-08	1.33e-07	4.80e-08
Kurtosis Equation						
January	0.0748	0.0230	0.4591***	0.0435	0.1296*	1.6953***
February	0.0010	0.0025	0.3968**	0.0237	0.1124	1.3333***
March	0.1230***	0.0052	0.5190***	0.1002***	0.1810	1.6912***
April	7e-04	0.0211	0.4313***	0.0153	0.1140*	1.5582***
May	4.07e-05	0.0266	0.4771***	0.0550**	0.1204	1.6377***
June	0.0481	0.0154	0.5060***	0.0854***	0.2038**	1.6577***
July	0.0749*	0.0059	0.5837***	0.0504*	0.1163	1.8402***
August	0.0644	0.0290	0.5348***	0.0487*	0.1815	1.8636***
September	0.1342***	0.0483*	0.6348***	0.1276***	0.1494	1.7863***
October	7e-04	0.0005	0.6651***	0.0357	0.1338	2.0400***
November	0.0392	0.0184	0.4538**	0.0396	0.1014	1.8107***
December	0.0670	0.0022	0.4867***	0.0714**	0.1431	1.9770***

Note: *** = 1% significance, **= 5% significance, * = 10% significance

Table 2.9 presents the MOY effect for each cryptocurrency. We observe anomalies in the mean of Bitcoin returns in April and October, Dash in October, Ripple in December, and Stellar in August and December. In particular, the average returns are higher for Bitcoins in April and October and lower for Dash in October, Ripple and Stellar in December, and Stellar in August. We do not find MOY anomalies in the means of Dogecoin and Litecoin returns. In any case, for all cryptocurrencies and differently from the stock market, there is no evidence of a "January effect".

Moreover, there are no systematic patterns in the volatility for Bitcoin in the months of the year. Instead, the variance equation of Dash shows anomalies, i.e. higher return volatility, in February, and Dogecoin in January, March, and July. We also observe anomalies in the variance of Litecoin and Stellar returns in July, October, and December and in January, August, October, and December for Ripple.

We do not single out a MOY anomaly in the skewness of Bitcoin, Dogecoin, Ripple, and Stellar returns. Instead, we document anomalies with likely large jumps in October for Litecoin's return and mainly in February for Dash's returns. The kurtosis equation shows several significant risks of tail events, especially for Dogecoin, Stellar and Litecoin, pointing to the high likelihood of experiencing dramatic changes in their returns. The more intense tail events are detected in September for Bitcoin, Dash and Litecoin, October for Dogecoin and Stellar, and June for Ripple.

Table 2.10: Estimate of the Quarter of the Year in the Mean, Variance, Skewness, and Kurtosis

Mean Equation	Bitcoin	Dash	Dogecoin	Litecoin	Ripple	Stellar
Q1	0.0016*	0.0025	-0.0006	-0.0010	-0.0010	0.0012
Q2	0.0024**	-1.65e-05	0.0008	-0.0008	-0.0008	-0.0002
Q3	0.0001	-3e-04	-0.0005	-0.0008	-0.0008	-0.0016
Q4	0.0014*	-0.0018	-0.0007	-0.0018*	-0.0018*	-0.0027***
Variance Equation						
Q1	1.81e-08	1.24e-07	1.33e-07	4.51e-08	4.51e-08	5.20e-08
Q2	4.30e-08	1.71e-13	1.28e-12	3.51e-11	3.51e-11	7.65e-07
Q3	9.11e-15	7.13e-06	1.18e-05***	8.91e-06***	8.91e-06***	9.55e-06*
Q4	8.40e-08	4.51e-05**	2.46e-05**	2.06e-05**	2.06e-05**	1.07e-05
Skewness Equation						
Q1	-0.0046	0.0056	0.0309***	0.0060	0.0164*	0.0059
Q2	-0.0201*	-0.0107	0.0078	-0.0065	-0.0064	-0.0154
Q3	0.0061	-0.0055	0.0142*	0.0090	0.0112	0.0211*
Q4	0.0043	0.0141	0.0206**	0.0210*	0.0101	0.0300**
Kurtosis Equation						
Q1	0.1112*	0.0122	0.4160	0.0619***	0.9568***	1.6276***
Q2	0.0229	0.0178	0.4251	0.0608***	0.9690***	1.6558***
Q3	0.1292*	0.0274***	0.5213	0.0842***	1.1114***	1.8480***
Q4	0.0524	0.0139	0.4677	0.0633***	0.8790***	1.9930***

Note: *** = 1% significance, **= 5% significance, * = 10% significance
Q1 = 1^{st} quarter, Q2 = 2^{nd} quarter, Q3 = 3^{rd} quarter, Q4 = 4^{th} quarter

We present in Table 2.10 the results concerning the QOY effect for the mean, variance, skewness, and kurtosis equations for each cryptocurrency. Our results show calendar effects in the 4^{th} quarter of the year for Litecoin, Ripple, and Stellar. In particular, these cryptocurrencies systematically lessen their average returns in October, November, and December. Conversely, Bitcoin tends to experience systematic positive returns especially in the 2^{nd} quarter of the year. No calendar effects regarding average returns have been detected for Dash and Dogecoin.

From the estimated variance equations, we identify anomalies in the 4^{th} quarter of the year for Dash, in the 3^{rd} and 4^{th} quarters for Dogecoin, Litecoin, and Ripple, and in the 3^{rd} quarter of the year for Stellar. Put differently, we identify the highest volatility, especially in the last quarter of the year, for all cryptocurrencies except for Bitcoin and Stellar. There are no calendar effects in volatility for Bitcoin returns, since the QOY effect in the Bitcoin's variance is never significant. For the skewness, Dash's return does not show any QOY anomaly. Instead, we observe relevant systematic asymmetries for Dogecoin and an anomaly in the 2^{nd} quarter of the year for Bitcoin returns. In particular, the negative skewness suggests that frequent small gains and a few utmost losses tend to occur for Bitcoin in the months of April, May and June. We observe the most substantial anomalies in the kurtosis in the 3^{rd} quarter of the year for all cryptocurrencies, except for Stellar, which registers the highest anomalies in October, November and December and for Dogecoin, which does not disclose any tail anomaly.

Table 2.11: Estimates of the Holiday Effect in the Mean, Variance, Skewness, and Kurtosis

Mean Equation	Bitcoin	Dash	Dogecoin	Litecoin	Ripple	Stellar
Holiday	0.0024*	0.0045	0.0002	0.0042	0.0045*	0.0034
Variance Equation						
Holiday	1e-04***	7e-04	2.09e-13	6.02e-12	1.12e-07	2e-04***
Skewness Equation						
Holiday	-0.0200	-0.0111	0.0222	-0.0458	-0.0442	-0.0193
Kurtosis Equation						
Holiday	0.0293	1.61e-06	3.4364	0.0085	0.3740	1.3044

Note: *** = 1% significance, **= 5% significance, * = 10% significance

Table 2.11 displays the results of the Holiday effect in the cryptocurrency market. We observe significant anomalies for Bitcoin and Ripple mean returns around holidays. We do not uncover any holiday anomalies in the mean returns of Dash, Dogecoin, Litecoin, and Stellar. The implication is that Bitcoin and Ripple prices tend to increase

during holidays, especially Christmas and New Year's Day, due to increased demand from investors and traders. The estimated variance equations show the presence of calendar effects; that is, Bitcoin and Stellar are more volatile during the holidays. The estimated skewness and kurtosis equations show no asymmetric or extreme returns occurring for any cryptocurrency during holidays.

Table 2.12: Estimates of the Weekend Effect in the Mean, Variance, Skewness, and Kurtosis

Mean Equation	Bitcoin	Dash	Dogecoin	Litecoin	Ripple	Stellar
SatSun	0.0009	-0.0002	0.0004	0.0004	-0.0007	0.0010
Variance Equation						
SatSun	2.72e-12	1e-04***	5.76e-12	3.82e-12	4.17e-12	7.11e-12
Skewness Equation						
SatSun	-0.0006	0.0192	0.0193	0.0193	0.0094	-0.0108
Kurtosis Equation						
SatSun	5.9875**	3.0167***	3.2487***	0.2386	3.9039***	2.6744***

Note: *** = 1% significance, **= 5% significance, * = 10% significance

To complete the analysis, we report the results for the Weekend effect in Table 2.12. We do not detect any anomaly in mean returns and volatility on the weekend days for all the cryptocurrencies except for Dash, which registers more volatility on Saturdays and Sundays. Instead, we document weekend anomalies in the kurtosis for all cryptocurrencies, excluding Litecoin. This finding highlights that returns' extremeness tends to materialise on the weekends.

2.5 Conclusion

This study has investigated different types of calendar anomalies in the cryptocurrency market at higher moments. In particular, we have scrutinized for the day-of-the-week, the month-of-the-year, the quarter-of-the-year, the US Holidays, and the Weekend calendar anomalies for Bitcoin, Dash, Dogecoin, Litecoin, Ripple, and Stellar. For this purpose, we have employed the ACD model with dummy variables for the period 2015-2023. Our results suggest that the cryptocurrency market presents some sfumato, as the effect of Leonardo's Mona Lisa[4], and in some periods, it tends to violate the Efficient Market Hypothesis, hence creating an opportunity to earn abnormal returns.

In particular, almost all cryptocurrencies experience a calendar effect on Fridays,

[4]At first glance, in the famous painting, Mona Lisa seems to be smiling, but at a second glance, her smile fizzles out, and then it appears again but in a different shape. This ambiguous effect is created with the sfumato technique, for which Leonardo blurred the contours of Mona Lisa's face.

with mean returns above the average. Unlike stocks, all cryptocurrencies, excluding Dogecoin, do not exhibit significant Monday anomaly. No cryptocurrency registers any January effect, while Bitcoin shows an April and October effect with higher mean returns in these months. In terms of volatility, Dash and Dogecoin display marked return oscillations on Mondays, while Litecoin on Thursdays. The other cryptocurrencies do not show any DOW anomaly in the variance. Except for Bitcoin, we also found the DOW effect in the estimated skewness equations of the considered cryptocurrencies. We further observe anomalies in the kurtosis of Bitcoin, Dogecoin, Ripple, and Stellar returns. We find significant anomalies for Bitcoin and Ripple mean returns around holidays, while a higher probability of extreme returns for all cryptocurrencies characterizes weekends and, excluding Ripple, the months of September and October.

Our study holds significance for the diverse array of participants in the cryptocurrency market. Those engaged in the crypto market may find it valuable to consider calendar anomalies at higher moments to inform their decision-making. The insights from our study can aid investors in developing trading strategies to capitalize on abnormal returns and crafting risk management strategies. Both institutional and retail traders have the opportunity to construct diversified portfolios of various cryptocurrencies by leveraging seasonal information, thereby formulating strategies based on the seasonal patterns observed in the cryptocurrency market. Our findings also shed light on the impact of retail traders' weekend and holiday trading on the portfolio performance of institutional traders, albeit to a modest extent. This awareness is crucial for institutional traders as they navigate the dynamics of the market.

All in all, our study emphasizes the need and the importance of incorporating higher-order moments into the modeling process of cryptocurrencies for a more comprehensive understanding of their returns and market dynamics. This would also support policymakers in understanding risks more accurately and institute closer surveillance of those risks by institutions such as Central Banks.

Chapter 3

Forecasting Cryptocurrencies Returns: Do Macroeconomic and Financial Variables Improve Tail Expectation Predictions?

3.1 Introduction

The global crypto market capitalisation exploded to a record of more than $2.6 trillion on Oct. 30 2021—roughly equivalent to twice the nominal GDP of Canada[1]. This rapid growth of the cryptocurrency market has revealed the increasingly important value of digital currencies as an electronic payment system and an attractive financial asset. Thus, accurate forecasts for the price and return of cryptocurrencies are essential for determining digital currency price trends and making informed decisions regarding asset allocation and risk management strategies.

Since the global financial crisis of 2008, the financial sector has seen tight regulatory measures put in place. For instance, a stricter capital requirement has been enforced by the Basel III international regulatory framework for banks, and improved risk management systems have been developed. However, the introduction of decentralized cryptocurrencies as a purely peer-to-peer version of electronic cash, allowing online payments to be sent directly from one party to another without using a financial institution, has posed a new challenge to the international financial system.

[1]Source: https://coinmarketcap.com/

Cryptocurrencies, unlike traditional currencies provides many advantages over traditional payment methods, such as high liquidity, lower transaction costs, and anonymity. Each transaction of the electronic coin is defined by a chain of digital signatures that each owner transfers to the next by digitally signing a hash of the previous transaction and the next owner's public key and adding these to the coin's end (Nakamoto, 2009).

Among asset classes, Bitcoin, the world's first cryptocurrency, has had one of the most volatile trading history with strong price movements. Some analysts even drew parallels between Bitcoin and the Dutch Tulipmania in the 17th century and the South Sea Bubble in the 18th century to indicate excessive greed and speculation in the crypto market. Notwithstanding the risks (including the collapse in November 2022 of FTX, a Bahama-based crypto exchange), the interest in Bitcoin and other cryptocurrencies has risen considerably in recent years as they provide high returns, thus attracting more and more new retail and institutional investors. With major exchanges, for example, the Chicago Mercantile Exchange and the Chicago Board Options Exchange, trading Bitcoin futures, central banks have been debating whether or not to regulate cryptocurrencies, given the numerous technical and legal issues involved.

All these issues have given the analysis of cryptocurrencies momentum. For instance, Mikhaylov (2020) examined the prospects and risks of cryptocurrency as a financial system element while also providing a theoretical foundation for predicting crypto market prices. The author explored the theoretical basis of digital currencies, assessing the chronology of blockchain technology and cryptocurrency development, analysing the current market state, and evaluating the potential threats and prospects for cryptocurrency within the global financial system. A series of academic studies have investigated models for predicting the price (e.g. Singh et al., 2023; Rathore et al., 2022; Jaquart et al., 2021; Pabuçcu et al., 2020; Adcock and Gradojevic, 2019) and volatility of cryptocurrencies (e.g. Kim et al., 2021; Ardia et al., 2019; Borri, 2019; Caporale and Zekokh, 2019; Katsiampa, 2019; Feng et al., 2018; Chu et al., 2017; Gronwald, 2014; Singh et al., 2023). Some studies have used the GARCH family models to estimate the volatility of digital currencies (e.g. Kim et al., 2021; Katsiampa, 2019; Chu et al., 2017; Gronwald, 2014). Other researchers have instead adopted extreme value theory (EVT) and machine learning approach for estimating risk measures such as Value-at-Risk (VaR) and Expected Shortfall (ES) for cryptocurrencies (e.g. Lahmiri and Bekiros, 2019; Tiwari et al., 2019; Feng et al., 2018; Peng et al., 2018). We discuss

all these studies in more detail in the review of related literature.

The aim of this work is to jointly predict conditional quantiles and tail expectations for the returns of the most popular cryptocurrencies, namely Bitcoin, Ethereum, Ripple, Dogecoin and Litecoin, using financial and macroeconomic indicators as explanatory variables. Methodologically, we first fit a Monotone Composite Quantile Regression Neural Network model (MCQRNN) for each of the considered cryptocurrencies to estimate a one-step ahead prediction of VaR and ES using a rolling window technique. The superior set of models is then chosen using the Model Confidence Set procedure. We also compare the performance of different MCQRNN models against two benchmark models - Historical simulation (HS) and the GARCH model.

We contribute to the extant literature in several ways. First, we provide the forecasts of large negative and positive returns (i.e. located on the left and right tails of the distributions) for the major leading digital currencies, since we consider long and short trading positions. While the literature has generally provided forecasts for Bitcoin prices (Basher and Sadorsky, 2022; Rathore et al., 2022; Jaquart et al., 2021; Kim et al., 2021; Pabuçcu et al., 2020; Adcock and Gradojevic, 2019), there is less attention to extreme return forecast (Borri, 2019; Caporale and Zekokh, 2019; Ardia et al., 2019; Feng et al., 2018); thus, our work broadens the attention by focusing on tail risk predictions of a comprehensive set of cryptocurrencies using a novel approach.

Second, we apply, for the first time, the MCQRNN model proposed by Cannon (2018) to the case of digital currencies to predict their returns on the two tails. Ignoring the quantile crossing problem may lead to unrealistic distribution forecasting of response variables. The MCQRNN allows us to impose the monotonicity constraints, thus solving the quantile crossing problem. Our research shows that the MCQRNN model can produce quantile forecasts that are more accurate, robust, and realistic.

Third, we introduce a set of explanatory variables to check whether their inclusion improves the forecasting performance. Similar to the studies of Basher and Sadorsky (2022); Wang et al. (2022); Bakas et al. (2022), we aim to forecast tail risk (VaR and Expected Shortfall) not just for Bitcoin but four additional cryptocurrencies using exogenous (macroeconomic and financial) variables. Our results indicate that some macroeconomic and financial variables are useful in forecasting the tail risk of cryptocurrencies. In particular, the VIX index, yield spread and inflation expectations tend to sharpen the predictions of tail returns. Our findings appear robust, considering dif-

ferent significance levels and benchmark models.

Our analysis is important since the high volatility behaviour of cryptocurrencies with the consequent ups and downs in returns necessitates a high level of risk management from institutional investors and individuals who include these new digital assets in their portfolios. In addition, accuracy in the predictions would help policy authorities to make more informed decisions. We also contribute to the growing literature on risk forecasting by employing a method that allows for estimating VaR by considering more quantiles at the same time and treating the quantiles as a monotone covariate while ensuring no quantile crossing.

This paper is organised as follows: Section 2 reviews the related work in volatility modelling of cryptocurrencies, Section 3 presents our proposed models, Section 4 shows the empirical analysis, and Section 5 concludes.

3.2 Literature Review

Many studies have examined the price dynamics and volatility of cryptocurrencies. We have grouped the analyses into three main strands. The first strand discusses studies on modelling and forecasting volatility, including a group of analyses using the GARCH family models and studies considering other parametric methods. The second strand of the literature concerns those analyses that predict cryptocurrency volatility and tail risks using non-parametric models, such as machine learning. Finally, the third strand focuses on studies that use various parametric and non-parametric methods to predict cryptocurrency price movements.

The literature for modelling the volatility of financial time series and estimating VaR and ES started from the seminal work by Bollerslev (Bollerslev, 1986), which introduced the Generalized AutoRegressive Conditional Heteroskedasticity (GARCH) model as an extension of the original ARCH model proposed by Engle (1982). Since then, many additional specifications have been developed for the GARCH model: the Student's t-GARCH model of Bollerslev (1987), the exponential GARCH (EGARCH) model of Nelson (1991), the GJR-GARCH model of Glosten et al. (1993), the threshold GARCH (TGARCH) model of Zakoian (1994) are just a few examples.

Regarding the volatility of cryptocurrencies, Gronwald (2014) showed that an autoregressive jump-intensity GARCH fits Bitcoin's data more accurately than a standard

GARCH model. Chu et al. (2017) modelled seven cryptocurrencies with 12 GARCH specifications having different distributions; an IGARCH (1, 1) model with normal innovations generated the smallest values of information criteria like AIC, BIC, HQC and the Consistent AIC (CAIC) for Bitcoin, Dash, Litecoin, Maidsafecoin and Monero. In contrast, the GJR-GARCH (1, 1) and GARCH (1, 1) models with normal innovations yielded the smallest values for Dogecoin and Ripple, respectively. Extending the study by Ardia et al. (2019) to test the presence of regime changes in the GARCH volatility dynamics of cryptocurrencies, Caporale and Zekokh (2019) documented that using standard GARCH models may yield incorrect VaR and ES predictions. Instead, adopting ES and joint loss functions within the Model Confidence Set procedure advanced by Hansen et al. (2011) allows the selection of the best model or set of models for modelling volatility of Bitcoin, Ethereum, Ripple, and Litecoin.

Some studies employed exogenous variables for studying Bitcoin volatility. Wang et al. (2022) used 17 macroeconomic variables and 18 technical indicators to forecast the realized volatility of Bitcoin. Their result showed that technical indicators have more forecasting capabilities for Bitcoin volatility during the low volatility state. Applying different models (Autoregressive model, Principal component model, Partial least squares model, Shrinkage method, and Forecast combination), they showed that shrinkage methods, including Elastic net and LASSO, can significantly improve the accuracy of Bitcoin volatility forecasting. Bakas et al. (2022) applied the dynamic Bayesian model to identify the main drivers of Bitcoin volatility and showed that Google trends, total circulation of Bitcoins, the US consumer confidence, and the S&P500 index are the most important factors for Bitcoin volatility. Their results further indicated that Bitcoin Google trends have a positive impact, while total circulation of Bitcoins, US consumer confidence, and the S&P500 index have a negative impact on Bitcoin volatility. Borri (2019) used CoVaR to estimate the conditional tail-risk within the cryptocurrency market (Bitcoin, Ethereum, Ripple, and Litecoin). The study found that cryptocurrencies are highly exposed to tail risks within crypto markets, but they are not exposed to tail risks concerning other global assets, including equities or gold. The author reported, in fact, that gold is poorly correlated with cryptocurrencies. A similar result was also documented by Lawuobahsumo et al. (2022). Borri (2019) further indicated that the VIX index has positive and significant $q-quantile$ slope coefficients on Bitcoin and Ripple, meaning that a substantial increase in the VIX index leads to

a significant drop in these cryptocurrencies.

In order to improve the forecasting beyond the GARCH for cryptocurrencies, scholars have applied several other models that provide better performance. Feng et al. (2018) used the EVT-based method to evaluate the extreme characteristics of seven representative cryptocurrencies to measure the conditional VaR and conditional ES. The authors show that cryptocurrencies are independent with four selected stock indices for left tail and cross tail. This result means that cryptocurrencies can function as a safe haven to stock indices and also their ability to serve as a diversifier for the stock market as gold, but cannot be a tail hedging instrument like gold. Katsiampa (2019) used extreme value theory to investigate the tail behaviour of Bitcoin, Ethereum, Ripple, Bitcoin Cash, and Litecoin returns, estimating VaR and ES as tail risk metrics. The main finding is that the conditional variances of all five cryptocurrencies are significantly affected by both previous squared errors and past conditional volatility.

The second strand of the literature focuses on non-parametric techniques to forecast price volatility. Unlike traditional time-series models, machine learning and deep learning models perform better at analyzing non-linear multivariate data while remaining robust to noise values. Kim et al. (2021) examined the volatility of nine cryptocurrencies based on their market capitalization using a Bayesian Stochastic Volatility (SV) model and several GARCH models. They reported that the SV model performed better than the GARCH family models when dealing with extremely volatile financial data. Based on forecasting errors, they further noted that the SV model was more accurate than the GARCH model for longer time horizons. Also, Tiwari et al. (2019) compared GARCH and SV models, discovering that the latter models performed better for both Bitcoin and Litecoin. Furthermore, their results revealed that the Stochastic Volatility-t model performs the best for Bitcoin while GARCH-t is the best for Litecoin.

Lahmiri and Bekiros (2019) used the long-short term memory neural network (LSTM) and found that the predictability is significantly higher than the generalized regression neural networks, their benchmark system. Peng et al. (2018) applied the standard GARCH model along with a machine learning approach to volatility estimates, employing Support Vector Regression (SVR) to estimate the mean and volatility equations and comparing them to GARCH family models. The authors used the Diebold-Mariano test and Hansen's Model Confidence Set to assess the models' prediction performance for low- and high-frequency data. SVR-GARCH models turned out to outperform

GARCH, EGARCH, and GJR-GARCH models with Normal, Student's t, and Skewed Student's t distributions, according to their findings.

The third strand of the literature comprises studies that adopt non-parametric and parametric methods to forecast prices and/or returns. For instance, Adcock and Gradojevic (2019) utilize the feedforward neural network to produce point and density forecasts of Bitcoin return. They argue that returns are characterized by predictive non-linear trends reflecting the speculative nature of cryptocurrency trading. Pabuçcu et al. (2020) use Support Vector Machines, the Artificial Neural Network, the Naïve Bayes, and the Random Forest machine learning model to forecast the movements of Bitcoin prices at a high degree of accuracy and compared their performance against the logistic regression model as a benchmark. They showed that the Random Forest model performed better than all the other models including the benchmark model. Basher and Sadorsky (2022) use interest rates, inflation, and market volatility as macroeconomic variables and MA50, WAD, and MACDSignal as indicator variables for forecasting Bitcoin prices. Using tree-based machine learning classifiers against traditional logit models, they reported that random forests predict Bitcoin and gold price directions better than logit models. Further results showed that MA50, WAD, MACDSignal oil volatility index and Ten-year bond yields are relevant variables for predicting Bitcoin price direction.

Jaquart et al. (2021) used machine learning models to predict short-term price movements of the bitcoin market, gold, oil, and minute levels for the total return variants of the indices MSCI World, S&P 500, and VIX. Model predictions were compared based on the accuracy scores, the Gradient boosting classifier, and recurrent neural networks were the best-performing methods across all prediction horizons. Rathore et al. (2022) used the Fbprophet model to predict Bitcoin closing price, opening price, day high, day low, day volume, and market capitalization on a particular day. This method relies on using deep learning algorithms and various concepts of machine learning, which can find hidden patterns in data, combine them, and make considerably more accurate predictions. Fleischer et al. (2022) apply the LSTM model to learn the patterns within cryptocurrency closing prices and to predict future prices. Using the root-mean-squared error to compare the predictive ability of alternative models, the LSTM model significantly outperformed the ARIMA model due to its ability to handle trends and seasonality. Similarly, Singh et al. (2023) employ the generalized grey model EGM (1,

1, α, θ) to predict the closing prices of Bitcoin, Bionic, Cardano, Dogecoin, Ethereum, and Ripple. They compare the accuracy of the generalized model (EGM (1, 1, α, θ) with the classical model (EGM (1,1)), linear regression, and exponential regression. The research findings show that the generalized model (EGM(1, 1, α, θ)) generally outperforms the classical model in forecast accuracy.[2] Their works show the importance of considering various forecasting methods when making investment decisions and selecting the best-performing model. Due to the high volatility nature of cryptocurrencies, the paper emphasizes the need for dependable and accurate prediction methods to guide investment decisions in the cryptocurrency market.

Contrary to Rathore et al. (2022); Jaquart et al. (2021); Pabuçcu et al. (2020); Adcock and Gradojevic (2019); Fleischer et al. (2022); Singh et al. (2023), our aim is to forecast cryptocurrencies tail risk similar to Borri (2019); Basher and Sadorsky (2022); Wang et al. (2022); Bakas et al. (2022) using exogenous macroeconomic and financial market variables. Our method allows for estimating VaR and ES jointly. The novelty of our work is the ability of our model to estimate more quantiles simultaneously while treating the quantiles as a monotone covariate and ensuring no quantile crossing. In addition, we assess whether the hypothesis according to which macroeconomic and financial variables can improve the predictions of extreme cryptocurrency returns holds.

3.3 Models

Let P_t denote the time-t price of a given cryptocurrency so that the time-t log-return is $y_t = \log(P_t) - \log(P_{t-1})$. For $h \geq 1$, we denote by $Y_{t+h} = \sum_{j=0}^{h-1} y_{t+j}$ the h-period return.

In the case of a long position in one of the cryptocurrencies, VaR, denoted by $Q_{t,h}(\tau)$ is the τ-conditional quantile of Y_{t+h} at time t, meaning that $\tau = P\left(Y_{t+h} \leq Q_{t,h}(\tau)|\Omega_t\right)$, where Ω_t denotes the information set available at time t. We also consider the following tail

[2]Singh et al. (2023) also used the EGM (1,1, α, θ) grey model to predict the surface temperature and CO2 emissions for six significant CO2-contributing countries: China, the USA, India, Russia, Japan, and Germany. Comparisons with other grey models suggest that the EGM (1,1, α, θ) model performs better for forecasting CO2 emissions. Pandey et al. (2022) compared the performance of four grey forecasting models -DGM (1,1,α), EGM (1,1), EGM (1,1,α, θ), and DGM (1,1) and found that DGM (1,1,α) was suitable for the forecasting in almost all cases for renewable and non-renewable energy generation sources.

expectation, known as expected shortfall (ES):

$$ES_{t,h}(\tau) = \mathbb{E}_t \left[Y_{t+h} | Y_{t+h} \leq Q_{t,h}(\tau) \right],$$

where $\mathbb{E}_t(\cdot)$ denotes expectation conditional on Ω_t. In the case of short positions, instead, we compute the two risk measures on $-Y_{t+h}$, or, equivalently, look at the right tail of Y_{t+h}.

3.3.1 Quantile Regression Neural Networks

Taylor (2000) proposed the Quantile Regression Neural Network (QRNN), a nonlinear nonparametric method combining quantile regression and neural networks. In the QRNN model, the τ-quantile is specified as

$$Q_{t,h}(\tau) = \sum_{i=1}^{I} H_{i,t}(\tau) \exp(w_i(\tau)) + b(\tau) \tag{3.1}$$

where $w_i(\tau)$ is a I-parameter vector of the output layer, $b(\tau)$ is the intercept parameter of the output layer and the hidden layer $H_{i,t}(\tau)$ outputs are given by

$$H_{i,t}(\tau) = f\left(\sum_{j=1}^{p} w_{i,j}^{(H)}(\tau) x_{j,t} + b_i^{(H)}(\tau) \right). \tag{3.2}$$

In (3.2), $w_{i,j}^{(H)}(\tau)$ is a $I \times p$ parameter matrix, $x_{j,t}$ represents j-th explanatory variable at time t and $f(x) = \tanh(x/2)$.

The parameters $w_{i,j}^{(H)}(\tau)$, $b_i^{(H)}(\tau)$, $w_i(\tau)$, and $b(\tau)$ are estimated by minimizing the asymmetric absolute value error function given as

$$E_\tau = \frac{1}{T} \sum_{t=1}^{T} \rho_\tau(Y_{t+h} - Q_{t,h}(\tau)). \tag{3.3}$$

where $\rho_\tau(u) = u \cdot (\tau - \mathbb{I}(u < 0))$ and $\mathbb{I}(\cdot)$ is the indicator function. The fundamental quantity of interest in this context is the magnitude of the conditional quantile associated with the quantile probability τ ($0<\tau<1$). The asymmetric absolute value function gives different weights to positive or negative deviations.

Since the derivative of (3.3) is not defined at the origin, Chen (2007) and Cannon (2011) suggest replacing, for small values of ϵ, the quantile regression error function by

$$\rho_{\tau}^{(A)}(u) = \begin{cases} \tau\varphi(u) & \text{if} \quad u \geq 0 \\ (\tau - 1)\varphi(u) & \text{if} \quad u < 0 \end{cases} \tag{3.4}$$

where

$$\varphi(u) = \begin{cases} \frac{u^2}{2\epsilon} & \text{if} \quad 0 \geq |u| \geq \epsilon \\ |u| - \frac{\epsilon}{2} & \text{if} \quad |u| > \epsilon \end{cases}$$

is the Huber norm. The smooth transition of the Huber norm from the square error ensures differentiability. As $\epsilon \to 0$, the approximated error function tend to converge to the exact quantile regression error function. The QRNN optimization method uses a quasi-Newton algorithm to minimize E_{τ}, see Amalia et al. (2018).

Regularization terms λ can be added to the error function to penalize the magnitude of the parameters which limits the nonlinear modeling capacity of the model. The penalized loss function has the form

$$\widetilde{E}_{\tau}^{(A)} = \frac{1}{T}\sum_{t=1}^{T}\rho_{\tau}^{(A)}(Y_{t+h} - Q_{t,h}(\tau)) + \lambda^{H}\frac{1}{I \cdot p}\sum_{i=1}^{I}\sum_{j=1}^{p}\left(w_{i,j}^{(H)}(\tau)\right)^2 + \lambda\sum_{i=1}^{I}\left(w_i(\tau)\right)^2 \tag{3.5}$$

where $\lambda^{H} \geq 0$ and $\lambda \geq 0$. These hyperparameters are typically set by minimizing the out-of-sample generalization error as a control for $w^{(H)}$, and w. As suggested by Cannon (2018), λ was set to zero in our estimation.

It is possible to minimize quantile crossing in the standard QRNN model by selecting and implementing appropriate weight penalties, but multiple quantiles guaranteed to be non-crossing cannot be estimated synchronously.

3.3.2 Monotone Composite Quantile Regression Neural Network

The Monotone Composite Quantile Regression Neural Network (MCQRNN) method was first proposed by Cannon (2018). MCQRNN model is more robust than traditional QRNN model, especially for non-normal error distribution. The main advantage of MCQRNN, in addition to non-crossing, is that the multiple quantile functions estimated simultaneously are more approximate to the actual conditional quantile function.

MCQRNN is created by combining elements from the traditional QRNN model, the monotone multi-layer perceptron, the composite quantile regression neural network

(CQRNN), the expected regression neural network, and the generalized additive neural network. The MCQRNN model is the first neural network-based implementation of quantile regression that estimates multiple non-crossing, nonlinear conditional quantile functions while improving regression quantile estimation accuracy Cannon (2018). The MCQRNN of Cannon (2018) is obtained by considering $K > 1$ quantiles at the same time and treating the quantile levels as a monotone covariate. To be more precise, in the CQRNN model, the function to be minimised (ignoring for simplicity the penalty terms) is

$$\widetilde{E}_{C\tau}^{(A)} = \frac{1}{U} \sum_{k=1}^{K} \sum_{t=1}^{T} \rho_{\tau_k}^{(A)}(Y_{t+h} - Q_{t,h}(\tau_k)), \tag{3.6}$$

where $U = T \cdot K$ and C stands for composite.

The vector $(\tau_1, \ldots, \tau_K)$ is first added to the model as a covariate. To this end, we create the covariate vector $x_{0,u}^{(S)}$, $u = 1, \ldots, U$, by repeating each τ_k T times and stacking. Here (S) denotes stacked data. Next, we concatenate the newly created vector with K copies of the original $T \times p$ covariate matrix, $\mathbf{X}$. At the same time, we stack K copies of the response variable to obtain $\mathbf{y}^{(S)}$ The new covariate matrix and response variable we consider in the MCQRNN model are

$$\mathbf{X}^{(S)} = \begin{bmatrix} \tau_1 & x_{1,1} & \cdots & x_{p,1} \\ \vdots & \vdots & \ddots & \vdots \\ \tau_1 & x_{1,T} & \cdots & x_{p,T} \\ \tau_2 & x_{1,1} & \cdots & x_{p,1} \\ \vdots & \vdots & \ddots & \vdots \\ \tau_2 & x_{1,T} & \cdots & x_{p,T} \\ \vdots & \vdots & \vdots & \vdots \\ \tau_K & x_{1,1} & \cdots & x_{p,1} \\ \vdots & \vdots & \ddots & \vdots \\ \tau_K & x_{1,T} & \cdots & x_{p,T} \end{bmatrix}, \quad \mathbf{Y}^{(S)} = \begin{bmatrix} Y_{1+h} \\ \vdots \\ Y_{T+h} \\ Y_{1+h} \\ \vdots \\ Y_{T+h} \\ \vdots \\ Y_{1+h} \\ \vdots \\ Y_{T+h} \end{bmatrix}$$

Using the stacked data above, we minimise the function

$$\widetilde{E}_{C\tau}^{(A,S)} = \frac{1}{U} \sum_{u=1}^{U} \rho_{\tau(u)}^{(A)} \left(Y_u^{(S)} - Q_{u,h}^{(S)}(\tau(u)) \right), \tag{3.7}$$

where $\tau(u) = x_{0,u}$ for $u = 1, \ldots, U$. Penalty terms can be added as in (3.5). Finally,

the vector $x_0^{(S)}$ is treated as a monotone covariate by changing the associated coefficient in (3.2) to $\exp\left(w_{i,j}^{(H)}\right)$. Since $f(\cdot)$ is an increasing function, we are guaranteed that quantiles do not cross, in the sense that if $\tau_l < \tau_k$ then $Q_{t,h}(\tau_l) < Q_{t,h}(\tau_k)$. Hence, we can estimate ES using the following approximation (see for instance Khalaf et al., 2021)

$$ES_{t,h}(\tau) \simeq \frac{1}{K}\sum_{j=1}^{K} Q_{t,h}\left(j\frac{\tau}{K}\right) \tag{3.8}$$

3.3.3 Assessing Quantile and Tail Expectation Forecasts

We use the Model Confidence Set procedure of Hansen et al. (2011) to classify the models based on their out-of-sample performance. The MCS procedure is based on an optimality criterion so that the resulting set M^* (Superior Set Models, SSM) will contain the best model with a given confidence level α.

It uses the idea of sequential testing, for which the generic set M^0, containing m_0 competing models, gets reduced in the number of elements by an elimination rule if the Equal Predictive Ability (EPA) null hypothesis is rejected. The procedure is iterated until the EPA hypothesis is not rejected for all the models left in the set, constituting the optimal model confidence set $M^*_{1-\alpha}$.

Let $l_{i,t}$ be a loss function associated with model i at time t. ES is not elicitable[3] on its own but jointly elicitable along with VaR provided a set of suitable scoring functions. We jointly assess quantile and ES forecasts considering the following functional form for the loss function proposed by Fissler et al. (2015):

$$\begin{aligned} l_{i,t,h} = \rho_\tau\left(Y_{t+h} - Q^i_{t,h}(\tau)\right) - \tau Y_{t+h} \\ + \frac{ES^i_{t,h}(\tau)}{1+\exp\left(ES^i_{t,h}(\tau)\right)} \times \Big(ES^i_{t,h}(\tau) - Q^i_{t,h}(\tau) + I(Y_{t+h} \le Q^i_{t,h}(\tau)) \\ \times \frac{Q^i_{t,h}(\tau) - Y_{t+h}}{\tau}\Bigg) + \log\left(\frac{2}{1+\exp\left(ES^i_{t,h}(\tau)\right)}\right). \end{aligned} \tag{3.9}$$

The function enables us to compare forecast from different methods with the best method having the lowest value.

For simplicity, we remove the dependence of the loss function on the horizon h and define the relative performance variables as the differential between the i and j models

[3] A measure is said to be elicitable if there exists at least one scoring function such that the correct forecast of the measure is the unique minimizer of the expectation of the scoring function.

as

$$d_{ij,t} = l_{i,t} - l_{j,t} \qquad \forall i, j \in M^0 \quad t = 1, \ldots, n. \tag{3.10}$$

and the simple average loss of model i relative to the other models $j \in M$ at time t as

$$d_{i\cdot,t} = (m-1)^{-1} \sum_{j \in M \setminus i} d_{ij,t}. \tag{3.11}$$

For the elimination of inferior elements within the set M^0, two alternative sets of hypothesis are available to test the EPA:

$$\begin{cases} H_0 : \mathbb{E}(d_{ij}) = 0 \quad \forall i, j = 1, \ldots, m, & \text{against} \\ H_1 : \mathbb{E}(d_{ij}) \neq 0 \end{cases} \tag{3.12}$$

or

$$\begin{cases} H_0 : \mathbb{E}(d_{i\cdot}) = 0 \quad \forall i = 1, \ldots, m, & \text{against} \\ H_1 : \mathbb{E}(d_{i\cdot}) \neq 0 \end{cases} \tag{3.13}$$

Two statistics are then constructed to test the hypotheses:

$$T_{ij} = \frac{\bar{d}_{ij}}{\sqrt{var(d_{ij})}} \qquad T_{i\cdot} = \frac{\bar{d}_{i\cdot}}{\sqrt{var(d_{i\cdot})}} \tag{3.14}$$

where $\bar{d}_{ij}$ is the relative average losses between i and j models and $\bar{d}_{i\cdot}$ represents the average losses of the i^{th} model relative to the average losses across the models belonging to the set M.

$$\bar{d}_{ij} = n^{-1} \sum_{t=1}^{n} d_{ij,t} \qquad \bar{d}_{i\cdot} = (m-1)^{-1} \sum_{j \in M \setminus i} \bar{d}_{ij} \tag{3.15}$$

The standard errors are constructed by block bootstrap where p is the maximum number of significant parameters obtained by fitting an $AR_{(p)}$ process to the d_{ij} terms.

The two hypotheses from (3.12) and (3.13) can be tested using

$$T_R = \max_{i,j \in M} T_{ij} \qquad T_{max} = \max_{i \in M} T_{i\cdot}. \tag{3.16}$$

Because the distributions of the two test statistics under the null are not known,

they are simulated using the bootstrap.

Bernardi and Catania (2016) summarised the algorithm for the procedure as follows:

1. Set $M = M_0$.

2. Compute the test statistics under the null EPA hypothesis. If it is not rejected, set $M^*_{1-\alpha} = M$ and terminate the algorithm. If it is rejected use the elimination rule to determine the worst model.

3. Discard the model and repeat step 2.

The elimination rule defines a sequence of sets $M = M_0 \supset M_1 \cdots \supset M_m$, where $M_i = (e_{M_i}, \ldots, e_{M_m})$, each of which has a p-value associated with EPA test. Let $P_{H_{0,M_i}}$ be the p-value associated with the null hypothesis H_{0,M_i}. The MCS p-value for model $e_{M_j} \supset M$ is defined as $\hat{p}_{e_{M_j}} = max_{i \leq j} P_{H_{0,M_i}}$.

3.4 Empirical Analysis

To jointly compute VaR and ES, we consider daily returns for the five most popular cryptocurrencies, namely Bitcoin (BTC), Ethereum (ETH), Ripple (XRP), Litecoin (LTC) and Dogecoin (DOGE). The period of the analysis goes from February 10, 2015, to September 27, 2021, for a total of 1,500 daily observations. We set $\tau = 1\%$ and 5% for both in the case of a long and short position in a given cryptocurrency. We also set $K = 8$ so that ES is obtained as the average of 8 quantiles. Finally, we move a window of 1000 observations and use each window to fit the models and make predictions. Hence, for each model, we end up with 500 out-of-sample forecasts for the quantiles and tail expectations. We consider a one-day ($h = 1$) and a one-week ($h = 5$) forecast horizon for the two risk measures of interest. To further compare the performance of our model, we use two benchmarks: the historical simulation and a popular conditional volatility model. The first method does not make any assumption about the return distribution and is simple to implement since it estimates VaR and ES using their empirical counterparts. The second benchmark is the ARMA(1,1)-GARCH(1,1) model with normal innovations.

Table 3.1 reports the explanatory variables and their various transformations used in our study. In particular, we consider explanatory business cycle variables such as interest rates, inflation, and market volatility to forecast extremely large cryptocurrency

Table 3.1: Explanatory Variables

Ticker	Description	Data Transformation
DGS10	Market Yield on US Treasury Securities at 10-Year Constant Maturity	first differences
GOLD	Gold Fixing Price 3:00 P.M. (London time) in London Bullion Market	log-returns
T10Y3M	10-Year Treasury Constant Maturity Minus 3-Month Treasury Constant Maturity	first differences
T10YIE	10-Year Breakeven Inflation Rate	first differences
T5YIFR	5-Year, 5-Year Forward Inflation Expectation Rate	first differences
VIXCLS	CBOE Volatility Index (VIX)	log-returns
DXY	US Dollar Index	log-returns
CL1	Generic 1st Crude Oil WTI Futures	log-returns
IXIC	NASDAQ Composite Index	log-returns

returns in line with Basher and Sadorsky (2022). We further include the dollar-effective exchange rate, the NASDAQ index and the prices of gold and crude oil. The US dollar-effective exchange rate (DXY) is a trade-weighted index that tracks the price of the US dollar against the main foreign currencies and is a significant indicator of international competitiveness (Algieri, 2014). The NASDAQ Composite Index includes almost all equities listed on the NASDAQ stock exchange. Gold and crude oil prices reflect the developments of the main precious metal and energy commodity markets. Interest rates are measured using the term spread, which is calculated as the spread between 10-Year Treasury Constant Maturity and 3-Month Treasury Constant Maturity, and using the US generic government 10-year yield (Algieri et al., 2017). Inflation variables comprise the expected five-year inflation and breakeven inflation. The latter is computed as the difference between the nominal yield on a fixed-rate 10-Year Treasury bond and the real yield on the inflation-linked investment with the same maturity. Market volatility is captured by the VIX index derived from the volatility implied from the prices of options on the S&P 500 index. This index is a sentiment variable that reflects the equity market's perception of risk and tends to be lower (higher) in bull (bear) markets (Algieri and Leccadito, 2021; Jaquart et al., 2021; Adcock and Gradojevic, 2019).[4]

We have used the MCQRNN model to jointly predict conditional quantiles and tail expectations for the returns of the five cryptocurrencies. We have constructed six MCQRNN models and compared them to both benchmark models. The specifics of the models are in Table 3.2. In detail, we consider three different sets of explanatory

[4]A detailed analysis of our data is presented in Section 1. The data used in this chapter and preceding chapters are a subset of the dataset analyzed in Chapter 1.5.

variables and either two or three hidden layers in the MCQRNN model. Results for the HS benchmark are presented in Tables 3.3–3.6, whereas those for the ARMA(1,1)-GARCH(1,1) model are displayed in Tables 3.7–3.10.

Specifically, we report the Score Ratio, i.e. the ratio between the average loss function (3.9) for model i and the one for the benchmark model,

$$\text{ScoreRatio}_i = \frac{\sum_{t=1}^{T_h} l_{i,t,h}}{\sum_{t=1}^{T_h} l_{\text{Benchmark},t,h}}$$

where T_h is the number of predictions we can make for the horizon h. If a model has a Score Ratio lower than one, then it produces better VaR and ES forecasts for the cumulated return Y_{t+h} than the benchmark model. We also test whether a given model produces significantly better forecasts than the benchmark model by testing the null hypothesis of equal predictability with the test of Diebold and Mariano (2002). Hence we report p-values for the test of equal predictability between model i and the benchmark model. P-values smaller than a prespecified significance level (e.g. 5%) suggest that model i is more accurate than the benchmark model in jointly forecasting VaR and ES for cryptocurrencies. Finally, we use the MCS procedure to assess the accuracy of the considered models. We present under the column 'SSM Y/N' whether model i belongs (Y) or not (N) to the Superior Set Models.

Table 3.2: MCQRNN Models

Model ID	Hidden Layers	Explanatory Varaiables
M1	2	Gold, CL1, DXY, IXIC, Cryptocurrency Return (Lag 1)
M2	3	Gold, CL1, DXY, IXIC, Cryptocurrency Return (Lag 1)
M3	2	VIX, T10Y3M, T10YIE, T5YIFR, DGS10, Cryptocurrency Return (Lag 1)
M4	3	VIX, T10Y3M, T10YIE, T5YIFR, DGS10, Cryptocurrency Return (Lag 1)
M5	2	VIX, CL1, DXY, IXIC, Cryptocurrency Return (Lag 1)
M6	3	VIX, CL1, DXY, IXIC, Cryptocurrency Return (Lag 1)

3.4.1 Discussion of Results

In Tables 3.3 - 3.6, we report the performance of our model against the Historical simulation method used as the first benchmark for estimating VaR and ES. Our results show that the MCQRNN model performs better than the HS method. In all cases (1% and 5% confidence level) and for both long and short positions, the benchmark model does not enter the Superior Set Model for the one-step ahead forecast for joint VaR and

ES. The superior forecasting performance of our model is also confirmed considering the score ratio and the reported p-values of Diebold and Mariano (2002) test of equal predictability between model i and the HS benchmark (being the p-values close to zero for all i models). We observe similar results for the five-step-ahead predictions. The benchmark model enters the Superior Set Model for Dogecoin in the short position at 1% (see panel 2a of Table 3.4), suggesting equal predictability between MCQRNN and HS models, as confirmed by the DM p-value close to 1. Also, in panel 5a of Table 3.6 for Litecoin, the Superior Set Model includes the benchmark model.

Table 3.3: Joint 1%-VaR and 1%-ES Forecast, Long Position, Benchmark: Historical Simulation

	Five-step-ahead Quantile_ES			One-step-ahead Quantile_ES		
Model	Score Ratio	DM Pvalue	SSM Y/N	Score Ratio	DM Pvalue	SSM Y/N
			BITCOIN			
M1	0.2073	0.0000	Y	0.3915	0.0000	N
M2	0.2151	0.0000	Y	0.2650	0.0000	Y
M3	0.2477	0.0000	Y	0.2910	0.0000	Y
M4	0.1897	0.0000	Y	0.2036	0.0000	Y
M5	0.7859	0.3373	Y	0.3394	0.0000	N
M6	0.1718	0.0000	Y	0.3447	0.0000	N
Benchmark	1	-	N	1	-	N
			DOGECOIN			
M1	0.2904	0.0000	Y	0.2635	0.0000	Y
M2	0.3880	0.0000	N	0.2549	0.0000	Y
M3	0.2788	0.0000	Y	0.2473	0.0000	Y
M4	0.3375	0.0000	Y	0.2729	0.0000	Y
M5	0.3797	0.0000	Y	0.3417	0.0000	N
M6	0.3545	0.0000	Y	0.282	0.0000	Y
Benchmark	1	-	N	1	-	N
			ETHEREUM			
M1	0.2731	0.0000	N	0.2767	0.0000	Y
M2	0.1666	0.0000	Y	0.3882	0.0000	N
M3	0.1740	0.0000	Y	0.2341	0.0000	Y
M4	0.1560	0.0000	Y	0.2884	0.0000	Y
M5	0.2407	0.0000	N	0.2650	0.0000	Y
M6	0.1545	0.0000	Y	0.4401	0.0000	N
Benchmark	1	-	N	1	-	N
			RIPPLE			
M1	0.1116	0.0000	Y	0.1680	0.0000	Y
M2	0.1274	0.0000	Y	0.2209	0.0000	Y
M3	0.1142	0.0000	Y	0.1627	0.0000	Y
M4	0.1215	0.0000	Y	0.3745	0.0000	N
M5	0.1439	0.0000	Y	0.1050	0.0000	Y
M6	0.1151	0.0000	Y	0.1780	0.0000	Y
Benchmark	1	-	N	1	-	N
			LITECOIN			
M1	0.2419	0.0000	Y	0.2738	0.0000	Y
M2	0.1574	0.0000	Y	0.2457	0.0000	Y
M3	0.2212	0.0000	Y	0.2009	0.0000	Y
M4	0.1009	0.0000	Y	0.2951	0.0000	Y
M5	0.0992	0.0000	Y	0.2262	0.0000	Y
M6	0.1143	0.0000	Y	0.3487	0.0000	Y
Benchmark	1	-	N	1	-	N

* DM Pvalue = "Diebold Mariano p-value", SSM = "Superior Set Model"

Considering the ARMA(1,1)-GARCH(1,1) model as the second benchmark, the results show that the MCQRNN models have superior performance in most cases when predicting VaR and ES for both long and short positions in crypto trading (Tables 3.7 - 3.10). For all instances of a one-day-ahead forecast, the benchmark model was not eliminated from the Superior Set Model for 1% τ short position forecast of Dogecoin (Table 3.8 panel 2b). Nevertheless, the score ratio and the Diebold and Mariano test

Table 3.4: Joint 1%-VaR and 1%-ES Forecast, Short Position, Benchmark: Historical Simulation

	Five-step-ahead Quantile_ES			One-step-ahead Quantile_ES		
Model	Score Ratio	DM Pvalue	SSM Y/N	Score Ratio	DM Pvalue	SSM Y/N
			BITCOIN			
M1	0.2464	0.0000	Y	0.3182	0.0000	Y
M2	0.2523	0.0000	Y	0.3066	0.0000	Y
M3	0.3476	0.0000	N	0.3207	0.0000	Y
M4	0.2517	0.0000	Y	0.2609	0.0000	Y
M5	0.2652	0.0000	Y	0.3566	0.0000	Y
M6	0.3064	0.0000	Y	0.3777	0.0000	Y
Benchmark	1	-	N	1	-	N
			DOGECOIN			
M1	0.3218	0.7585	Y	0.2336	0.0504	Y
M2	0.1086	0.7815	Y	0.0736	0.0216	Y
M3	0.2358	0.7652	Y	0.2878	0.1019	Y
M4	0.1167	0.7833	Y	0.0146	0.0071	Y
M5	0.4142	0.7272	Y	0.1254	0.0067	Y
M6	0.5121	0.7134	Y	0.196	0.0407	Y
Benchmark	1	-	Y	1	-	N
			ETHEREUM			
M1	0.3211	0.0000	Y	0.3995	0.0000	N
M2	0.2360	0.0000	Y	0.4506	0.0000	N
M3	0.2348	0.0000	Y	0.3133	0.0000	Y
M4	0.2343	0.0000	Y	0.3020	0.0000	Y
M5	0.3361	0.0000	Y	0.4194	0.0000	N
M6	0.3649	0.0000	N	0.5221	0.0000	N
Benchmark	1	-	N	1	-	N
			RIPPLE			
M1	0.1362	0.0000	Y	0.2753	0.0000	Y
M2	0.1720	0.0000	N	0.1470	0.0000	Y
M3	0.1364	0.0000	Y	0.2654	0.0000	Y
M4	0.1436	0.0000	Y	0.2392	0.0000	Y
M5	0.1378	0.0000	Y	0.2720	0.0000	Y
M6	0.1408	0.0000	Y	0.3011	0.0000	Y
Benchmark	1	-	N	1	-	N
			LITECOIN			
M1	0.1426	0.0000	Y	0.2134	0.0000	Y
M2	0.2172	0.0000	Y	0.1866	0.0000	Y
M3	0.1559	0.0000	Y	0.1553	0.0000	Y
M4	0.1336	0.0000	Y	0.2109	0.0000	Y
M5	0.1473	0.0000	Y	0.2353	0.0000	Y
M6	0.1858	0.0000	Y	0.3091	0.0000	Y
Benchmark	1	-	N	1	-	N

* DM Pvalue = "Diebold Mariano p-value", SSM = "Superior Set Model"

Table 3.5: Joint 5%-VaR and 5%-ES Forecast, Long Position, Benchmark: Historical Simulation

	Five-step-ahead Quantile_ES			One-step-ahead Quantile_ES		
Model	Score Ratio	DM Pvalue	SSM Y/N	Score Ratio	DM Pvalue	SSM Y/N
			BITCOIN			
M1	0.4888	0.0000	N	0.4844	0.0000	N
M2	0.4535	0.0000	Y	0.4655	0.0000	Y
M3	0.5707	0.0000	N	0.5710	0.0000	N
M4	0.4721	0.0000	Y	0.4722	0.0000	Y
M5	0.4688	0.0000	Y	0.4754	0.0000	N
M6	0.4662	0.0000	Y	0.4634	0.0000	Y
Benchmark	1	-	N	1	-	N
			DOGECOIN			
M1	0.5933	0.0000	Y	0.5763	0.0000	Y
M2	0.5996	0.0000	Y	0.5538	0.0000	Y
M3	0.6788	0.0014	Y	0.5859	0.0000	Y
M4	0.4876	0.0000	Y	0.5144	0.0000	Y
M5	0.4906	0.0000	Y	0.5866	0.0000	Y
M6	0.6677	0.0000	N	0.5434	0.0000	Y
Benchmark	1	-	N	1	-	N
			ETHEREUM			
M1	0.5542	0.0000	Y	0.5775	0.0000	N
M2	0.5240	0.0000	Y	0.5895	0.0000	N
M3	0.6188	0.0000	Y	0.4444	0.0000	Y
M4	0.5425	0.0000	Y	0.7029	0.0000	N
M5	0.5662	0.0000	Y	0.6493	0.0000	N
M6	0.5226	0.0000	Y	0.7690	0.0000	N
Benchmark	1	-	N	1	-	N
			RIPPLE			
M1	0.4144	0.0000	N	0.4109	0.0000	Y
M2	0.5103	0.0000	N	0.4628	0.0000	N
M3	0.4109	0.0000	Y	0.4732	0.0000	N
M4	0.4283	0.0000	N	0.5925	0.0000	N
M5	0.4134	0.0000	N	0.4052	0.0000	Y
M6	0.4930	0.0000	N	0.5610	0.0000	N
Benchmark	1	-	N	1	-	N
			LITECOIN			
M1	0.5689	0.0000	Y	0.4742	0.0000	Y
M2	0.5050	0.0000	Y	0.4712	0.0000	Y
M3	0.5856	0.0000	Y	0.4876	0.0000	N
M4	0.5056	0.0000	Y	0.5425	0.0000	N
M5	0.5210	0.0000	Y	0.5244	0.0000	N
M6	0.5700	0.0000	Y	0.5998	0.0000	N
Benchmark	1	-	N	1	-	N

* DM Pvalue = "Diebold Mariano p-value", SSM = "Superior Set Model"

Table 3.6: Joint 5%-VaR and 5%-ES Forecast, Short Position, Benchmark: Historical Simulation

	Five-step-ahead Quantile_ES			One-step-ahead Quantile_ES		
Model	Score Ratio	DM Pvalue	SSM Y/N	Score Ratio	DM Pvalue	SSM Y/N
			BITCOIN			
M1	0.5518	0.0000	Y	0.5506	0.0000	Y
M2	0.5361	0.0000	Y	0.4770	0.0000	Y
M3	0.6384	0.0000	N	0.5482	0.0000	Y
M4	0.5307	0.0000	Y	0.5349	0.0000	Y
M5	0.6955	0.0003	Y	0.4931	0.0000	Y
M6	0.5767	0.0000	Y	0.5767	0.0000	Y
Benchmark	1	-	N	1	-	N
			DOGECOIN			
M1	0.6674	0.0703	N	0.6131	0.0000	Y
M2	0.3662	0.0176	Y	0.6856	0.0318	Y
M3	0.3054	0.0018	Y	0.5075	0.0000	Y
M4	0.3854	0.0066	Y	0.566	0.0001	Y
M5	0.5354	0.0270	N	0.5957	0.0000	Y
M6	0.7126	0.1930	N	0.5641	0.0000	Y
Benchmark	1	-	N	1	-	Y
			ETHEREUM			
M1	0.4665	0.0000	Y	0.6014	0.0000	N
M2	0.5444	0.0000	N	0.5289	0.0000	N
M3	0.4546	0.0000	Y	0.4995	0.0000	N
M4	0.4575	0.0000	Y	0.4768	0.0000	Y
M5	0.5514	0.0000	N	0.6006	0.0000	N
M6	0.5106	0.0000	N	0.7144	0.0000	N
Benchmark	1	-	N	1	-	N
			RIPPLE			
M1	0.3577	0.0000	N	0.4637	0.0000	N
M2	0.3952	0.0000	N	0.4007	0.0000	Y
M3	0.3270	0.0000	Y	0.5963	0.0000	N
M4	0.3735	0.0000	N	0.4142	0.0000	Y
M5	0.3623	0.0000	N	0.4347	0.0000	Y
M6	0.3843	0.0000	N	0.4072	0.0000	Y
Benchmark	1	-	N	1	-	N
			LITECOIN			
M1	0.3968	0.0000	Y	0.4557	0.0000	Y
M2	0.3837	0.0000	Y	0.5069	0.0000	Y
M3	0.3953	0.0000	Y	0.3881	0.0000	Y
M4	0.4088	0.0000	Y	0.5042	0.0000	Y
M5	0.4106	0.0000	Y	0.5189	0.0000	Y
M6	0.3934	0.0000	Y	0.4843	0.0000	Y
Benchmark	1	-	Y	1	-	N

* DM Pvalue = "Diebold Mariano p-value", SSM = "Superior Set Model"

p-values indicate that the MCQRNN model has a better predictive ability than the ARMA(1,1)-GARCH(1,1) benchmark.

The results of the superior predictive performance of MCQRNN models hold, with a few exceptions, for the five-day-ahead forecast at 1% and 5% for long or short positions. We observe that the benchmark model is not eliminated from the Superior Set Model for Dogecoin, Ethereum, Ripple, and Litecoin. We document a high score ratio and high p-values for the Diebold and Mariano test (panel 2b of Tables 3.7 and panel 2b - 2e of Table 3.8). This result implies equal predictability among the models for forecasting jointly the 1%-VaR and ES of long and short positions. For Ethereum, as shown in panel 2c of Table 3.9, the benchmark model performs better than the MCQRNN models with score ratios greater than 1 and Diebold and Mariano test p-values equal to 1.

In a nutshell, the MCQRNN models augmented with macroeconomic and financial variables can improve the predictions of extreme cryptocurrency returns for both long and short-trading positions. The best performing models are M3 and M4, with 2 and 3 layers containing the VIX index, Treasury Yield Spread, the 5-Year Forward Inflation Expectation Rate and the 10-Year Breakeven Inflation Rate.

Our findings differ from Adcock and Gradojevic (2019), who reported that the VIX index failed to improve their model performance for predicting returns but are consistent with previous research results, according to which VIX is an important macroeconomic variable for predicting Bitcoin price direction and tail risks (Borri, 2019; Basher and Sadorsky, 2022; Wang et al., 2022)[5]. However, our results hold not only for Bitcoin but also for Ethereum, Ripple and Litecoin. Moreover, differently from the extant empirical literature, we point to the role of expected inflation as a possible variable to add when predicting extreme returns of cryptocurrencies.

3.4.2 Policy Implications

The above findings provide crucial implications for the cryptocurrency market participants. Our results suggest that traders and investors can use macroeconomic and financial market indicators such as 5-Year Forward Inflation Expectation Rate, 10-

[5]For instance, Borri (2019) showed that VIX and US equity market indices have the ability to forecast future tail-risk at all time horizons for cryptocurrencies. Basher and Sadorsky (2022) also reported that the 10-year bond yield, VIX, and the oil volatility index are important macroeconomic variables for predicting Bitcoin price direction. Wang et al. (2022) suggested that macroeconomic indicators such as the realized volatility, the global real economic activity index, and the trade-weighted USD index return strongly drive Bitcoin volatility.

Table 3.7: Joint 1%-VaR and 1%-ES Forecast, Long Position, Benchmark: ARMA-GARCH (1, 1)

	Five-step-ahead Quantile_ES			One-step-ahead Quantile_ES		
Model	Score Ratio	DM Pvalue	SSM Y/N	Score Ratio	DM Pvalue	SSM Y/N
			BITCOIN			
M1	0.3683	0.0002	Y	0.7150	0.0000	N
M2	0.3821	0.0000	Y	0.4839	0.0000	Y
M3	0.4401	0.0000	Y	0.5315	0.0000	Y
M4	0.3370	0.0000	Y	0.3719	0.0000	Y
M5	1.3962	0.6690	Y	0.6200	0.0000	N
M6	0.3052	0.0000	Y	0.6295	0.0000	N
Benchmark	1	-	N	1	-	N
			DOGECOIN			
M1	0.6568	0.1223	Y	0.3630	0.0000	Y
M2	0.8775	0.3395	Y	0.3510	0.0000	Y
M3	0.6305	0.1655	Y	0.3406	0.0000	Y
M4	0.7633	0.2573	Y	0.3758	0.0000	Y
M5	0.8588	0.3331	Y	0.4705	0.0000	N
M6	0.8016	0.2932	Y	0.3883	0.0000	Y
Benchmark	1	-	Y	1	-	N
			ETHEREUM			
M1	0.3202	0.0000	N	0.4708	0.0000	Y
M2	0.1953	0.0000	Y	0.6607	0.0000	N
M3	0.2040	0.0000	Y	0.3984	0.0000	Y
M4	0.1829	0.0000	Y	0.4909	0.0000	Y
M5	0.2822	0.0000	N	0.4511	0.0000	Y
M6	0.1811	0.0000	Y	0.7490	0.0000	N
Benchmark	1	-	N	1	-	N
			RIPPLE			
M1	0.1432	0.0000	Y	0.2850	0.0000	Y
M2	0.1634	0.0000	Y	0.3749	0.0001	Y
M3	0.1465	0.0000	Y	0.2762	0.0000	Y
M4	0.1558	0.0000	Y	0.6356	0.0297	N
M5	0.1846	0.0000	Y	0.1782	0.0000	Y
M6	0.1476	0.0000	Y	0.3021	0.0000	Y
Benchmark	1	-	N	1	-	N
			LITECOIN			
M1	0.2604	0.0000	Y	0.4873	0.0000	Y
M2	0.1694	0.0000	Y	0.4374	0.0000	Y
M3	0.2381	0.0000	Y	0.3576	0.0000	Y
M4	0.1086	0.0000	Y	0.5253	0.0000	Y
M5	0.1068	0.0000	Y	0.4027	0.0000	Y
M6	0.1230	0.0000	Y	0.6207	0.0001	Y
Benchmark	1	-	N	1	-	N

* DM Pvalue = "Diebold Mariano p-value", SSM = "Superior Set Model"

Table 3.8: Joint 1%-VaR and 1%-ES Forecast, Short Position, Benchmark: ARMA-GARCH (1, 1)

	Five-step-ahead Quantile_ES			One-step-ahead Quantile_ES		
Model	Score Ratio	DM Pvalue	SSM Y/N	Score Ratio	DM Pvalue	SSM Y/N
			BITCOIN			
M1	0.3909	0.0000	Y	0.5011	0.0000	Y
M2	0.4002	0.0000	Y	0.4828	0.0000	Y
M3	0.5515	0.0000	N	0.5049	0.0000	Y
M4	0.3993	0.0000	Y	0.4108	0.0000	Y
M5	0.4208	0.0000	Y	0.5615	0.0000	Y
M6	0.4861	0.0000	N	0.5947	0.0272	Y
Benchmark	1	-	N	1	-	N
			DOGECOIN			
M1	0.5620	0.9493	Y	0.5229	0.2387	Y
M2	0.1897	0.9356	Y	0.1647	0.0427	Y
M3	0.4119	0.9318	Y	0.6442	0.2996	Y
M4	0.2038	0.9281	Y	0.0327	0.0026	Y
M5	0.7234	0.8229	Y	0.2806	0.0046	Y
M6	0.8945	0.8245	Y	0.4388	0.1079	Y
Benchmark	1	-	Y	1	-	Y
			ETHEREUM			
M1	1.3433	0.9973	Y	0.5999	0.0000	N
M2	0.9871	0.4104	Y	0.6766	0.0000	N
M3	0.9821	0.3681	Y	0.4705	0.0000	Y
M4	0.9799	0.3813	Y	0.4535	0.0000	Y
M5	1.4057	0.8881	Y	0.6298	0.0000	N
M6	1.5263	0.9925	N	0.7841	0.0000	N
Benchmark	1	-	Y	1	-	N
			RIPPLE			
M1	0.7191	0.0687	Y	0.6258	0.0000	Y
M2	0.9077	0.2977	N	0.3342	0.0000	Y
M3	0.7200	0.0844	Y	0.6032	0.0000	Y
M4	0.7580	0.1114	Y	0.5437	0.0000	Y
M5	0.7276	0.0867	Y	0.6182	0.0000	Y
M6	0.7433	0.0825	Y	0.6845	0.0004	Y
Benchmark	1	-	Y	1	-	N
			LITECOIN			
M1	0.7560	0.1718	Y	0.4773	0.0000	Y
M2	1.1517	0.7387	Y	0.4173	0.0000	Y
M3	0.8267	0.1909	Y	0.3474	0.0000	Y
M4	0.7084	0.0653	Y	0.4717	0.0000	Y
M5	0.7810	0.2123	Y	0.5263	0.0000	Y
M6	0.9852	0.4695	Y	0.6913	0.0487	Y
Benchmark	1	-	Y	1	-	N

* DM Pvalue = "Diebold Mariano p-value", SSM = "Superior Set Model"

Table 3.9: Joint 5%-VaR and 5%-ES Forecast, Long Position, Benchmark: ARMA-GARCH (1, 1)

	Five-step-ahead Quantile_ES			One-step-ahead Quantile_ES		
Model	Score Ratio	DM Pvalue	SSM Y/N	Score Ratio	DM Pvalue	SSM Y/N
			BITCOIN			
M1	0.6208	0.0000	N	0.6912	0.0000	Y
M2	0.5760	0.0000	Y	0.5989	0.0000	Y
M3	0.7248	0.0000	N	0.6882	0.0000	Y
M4	0.5996	0.0000	Y	0.6715	0.0000	Y
M5	0.5954	0.0000	Y	0.6191	0.0000	Y
M6	0.5922	0.0000	Y	0.7240	0.0000	Y
Benchmark	1	-	N	1	-	N
			DOGECOIN			
M1	0.8666	0.3180	Y	0.5821	0.0000	Y
M2	0.8759	0.3309	Y	0.5593	0.0000	Y
M3	0.9915	0.4871	Y	0.5917	0.0000	Y
M4	0.7122	0.0085	Y	0.5195	0.0000	Y
M5	0.7166	0.1920	Y	0.5925	0.0000	Y
M6	0.9753	0.4650	N	0.5489	0.0000	Y
Benchmark	1	-	Y	1	-	N
			ETHEREUM			
M1	1.3797	1.0000	N	0.7096	0.0000	N
M2	1.1903	1.0000	N	0.7244	0.0000	N
M3	1.2308	1.0000	N	0.5461	0.0000	Y
M4	1.2042	1.0000	N	0.8638	0.0000	N
M5	0.6431	0.2624	Y	0.7978	0.0000	N
M6	1.1776	1.0000	N	0.9449	0.0046	N
Benchmark	1	-	Y	1	-	N
			RIPPLE			
M1	0.8275	0.0041	N	0.4352	0.0000	Y
M2	1.0190	0.6312	N	0.4902	0.0000	N
M3	0.8205	0.0017	Y	0.5011	0.0000	N
M4	0.8552	0.0097	N	0.6275	0.0000	N
M5	0.8255	0.0023	N	0.4291	0.0000	Y
M6	0.9843	0.4358	N	0.5941	0.0000	N
Benchmark	1	-	N	1	-	N
			LITECOIN			
M1	0.5505	0.0000	Y	0.5804	0.0000	Y
M2	0.4887	0.0000	Y	0.5767	0.0000	Y
M3	0.5668	0.0000	Y	0.5967	0.0000	N
M4	0.4893	0.0000	Y	0.6639	0.0000	N
M5	0.5042	0.0000	Y	0.6418	0.0000	N
M6	0.5516	0.0000	Y	0.7341	0.0000	N
Benchmark	1	-	N	1	-	N

* DM Pvalue = "Diebold Mariano p-value", SSM = "Superior Set Model"

Table 3.10: Joint 5%-VaR and 5%-ES Forecast, Short Position, Benchmark: ARMA-GARCH (1, 1)

	Five-step-ahead Quantile_ES			One-step-ahead Quantile_ES		
Model	Score Ratio	DM Pvalue	SSM Y/N	Score Ratio	DM Pvalue	SSM Y/N
			BITCOIN			
M1	0.6816	0.0000	Y	0.6952	0.0000	Y
M2	0.6623	0.0000	Y	0.6024	0.0000	Y
M3	0.7886	0.0000	N	0.6922	0.0000	Y
M4	0.6556	0.0000	Y	0.6754	0.0000	Y
M5	0.8592	0.0922	Y	0.6227	0.0000	Y
M6	0.7124	0.0000	Y	0.7282	0.0000	Y
Benchmark	1	-	N	1	-	N
			DOGECOIN			
M1	1.4990	0.9564	N	0.7148	0.0032	Y
M2	0.8225	0.3039	Y	0.7993	0.1716	Y
M3	0.6860	0.1365	Y	0.5916	0.0000	Y
M4	0.8657	0.3337	Y	0.6598	0.0084	Y
M5	1.2026	0.7658	N	0.6945	0.0025	Y
M6	1.6007	0.9857	N	0.6576	0.0090	Y
Benchmark	1	-	Y	1	-	N
			ETHEREUM			
M1	0.5951	0.0000	Y	0.7846	0.0000	N
M2	0.6945	0.0000	N	0.6900	0.0000	N
M3	0.5799	0.0000	Y	0.6517	0.0000	N
M4	0.5836	0.0000	Y	0.6221	0.0000	Y
M5	0.7034	0.0000	N	0.7836	0.0000	N
M6	0.6513	0.0000	N	0.9322	0.0653	N
Benchmark	1	-	N	1	-	N
			RIPPLE			
M1	0.4767	0.0216	N	0.6911	0.0000	N
M2	0.5265	0.0421	N	0.5971	0.0000	Y
M3	0.4357	0.0221	Y	0.8887	0.1084	N
M4	0.4977	0.0191	N	0.6172	0.0000	Y
M5	0.4827	0.0245	N	0.6478	0.0000	Y
M6	0.5121	0.0429	N	0.6069	0.0000	Y
Benchmark	1	-	N	1	-	N
			LITECOIN			
M1	0.5674	0.0000	Y	0.6515	0.0000	Y
M2	0.5486	0.0000	Y	0.7248	0.0067	Y
M3	0.5652	0.0000	Y	0.5549	0.0000	Y
M4	0.5844	0.0000	Y	0.7209	0.0000	Y
M5	0.5870	0.0000	Y	0.7419	0.0063	Y
M6	0.5624	0.0000	Y	0.6924	0.0001	Y
Benchmark	1	-	N	1	-	N

* DM Pvalue = "Diebold Mariano p-value", SSM = "Superior Set Model"

Year Breakeven Inflation Rate, 10-Year Treasury Constant Maturity Minus 3-Month Treasury Constant Maturity, and the VIX index to forecast cryptocurrency tail risk. However, they should care about which combination of variables to include in the model. We recommend that traders and investors train the model on an array of indicators before deciding which to enter into the final model. Based on the relevance of forecasting tail risk for investment, decision-makers must consider various forecasting methods before selecting the appropriate one. Due to the predictive ability of the MCQRNN model compared to the industrially used Historical simulation and the standard ARMA-GARCH model, institutional investors, regulators, and academicians can use this model as an additional tool for forecasting cryptocurrencies' tail risk. These results, together with increased transparency of market operations (Mikhaylov et al., 2023), may guide policymakers to make informed risk management decisions and investors to choose what other assets to include in the portfolio along with cryptocurrencies.

3.5 Conclusion

This study has employed the Model Confidence Set technique to determine the optimal model for predicting the returns of the major cryptocurrencies, namely Bitcoin, Ethereum, Ripple, Litecoin and Dogecoin. Our goal has been to jointly forecast the Quantile and Expected Shortfall using Monotone Composite Quantile Regression Neural Network models. First, we constructed six MCQRNN models for the considered cryptocurrencies, and then we compared their performances against the traditional Historical simulation method and ARMA(1,1)-GARCH(1,1) benchmark models. Our results show that the MCQRNN models outperform the benchmark for all the investigated cryptocurrencies. Both the Historical Simulation method and the ARMA(1,1)-GARCH(1,1) model do not enter the superior set of models for the one-day-ahead predictions of cryptocurrency returns. This finding holds for $\tau = 1\%$ and $\tau = 5\%$, both in case of long or short positions in cryptocurrencies. The exception is for the short positions in Dogecoin when $\tau = 1\%$.

As a robustness check, we have forecast the five-day-ahead returns for the five cryptocurrencies using the same models. For all τ-quantiles and trading positions in Bitcoin, the MCQRNN models turn out to be superior to the other benchmarks. Furthermore, for all trading positions in Dogecoin, the EPA was not rejected for all

the considered MCQRNN models, both with $\tau = 1\%$ and $\tau = 5\%$.

Our results, thus, show that MCQRNN models augmented with economic and financial data allow us to improve the forecasting performances of cryptocurrencies' extreme returns and hedge the risks of investing in this new type of asset. In particular, the VIX index, Treasury Yield Spread, the 5-Year Forward Inflation Expectation Rate and the 10-Year Breakeven Inflation Rate are relevant when predicting tail risks. Notwithstanding the limitations due to the peculiar nature of cryptocurrencies, that exhibit attributes of both commodities and money, our methodology could be applied to other areas, including the forecast of the e-commerce sector (Moiseev et al., 2023) and CO2 emissions (Algieri et al., 2023; Singh et al., 2022).

Chapter 4

Exploring Dependence Relationships between Bitcoin and Commodity returns: An assessment using the Gerber Cross-Correlation

4.1 Introduction

This study investigates the cross-dependence between the returns of cryptocurrencies and commodities in order to determine how strongly the assets are interlinked and how they can influence each other. We focus on the most renowned cryptocurrency, Bitcoin, and compute robust measures of non-linear dependence between Bitcoin's returns and the leads/lags returns of four different commodities. These latter belong to the categories of precious metals (platinum and gold), energy (crude oil WTI) (West Texas Intermediate [1] and agricultural products (wheat).

Previous studies investigating the relationship and volatility spillover (see Almeida and Gonçalves (2022) for a comprehensive literature overview) between Bitcoin and gold/oil prices (or returns) have produced mixed findings. Kristoufek (2015) explores the linkages between Bitcoin and gold prices while Kjærland et al. (2018) investigates the connection between (i) Bitcoin and (ii) crude oil and gold prices. Both studies conclude that the dynamics of gold (and oil) prices do not have a significant impact

[1] (WTI) crude oil is a light, sweet, high-quality crude oil sourced primarily from inland Texas that serves as a global benchmark in oil pricing along with the European BRENT extracted in the North Sea

on cryptocurrencies' returns. Using transfer entropy, Huynh et al. (2020) investigates the link between gold and cryptocurrency prices and shows that gold could be a good hedging instrument for cryptocurrencies. These results are in line with the findings of Klein et al. (2018), who evaluates the time-varying conditional correlations between Bitcoin and gold returns using the BEKK-GARCH model. Huynh et al. (2020) shows that Bitcoin and stock market returns are positively correlated during financial market downturns, in sharp contrast to the behaviour of gold returns, which is widely believed to be a hedging instrument against stock market downfalls. These findings are challenged by (i) Wu (2021); Elsayed et al. (2022), who show that gold is very sensitive to uncertainty shock from cryptocurrency markets, and by (ii) Elsayed et al. (2022), who employs a time-varying parameter vector autoregressive model to show that gold is vulnerable to return and volatility spillovers from cryptocurrency uncertainty measures. The difference in behaviour between Bitcoin and commodities returns is carried out also for higher-order moments. Conrad et al. (2018) reports a significant difference in the long-term volatility of Bitcoin compared to gold returns. Conrad et al. (2018) attribute this result to the fact that since Bitcoin does not have an income stream or an intrinsic value, its price tends to be more sensitive to non-fundamental financial markets news/sentiment. Finally, Dai et al. (2022) assesses the impact of global economic policy uncertainty and natural resource prices (oil and gold in particular) on Bitcoin returns. By employing an autoregressive distributed lagged (ARDL) model and a nonlinear ARDL model for evaluating the symmetric and asymmetric long- and short-run effects, Dai et al. (2022) observes that oil price had a negative relationship with Bitcoin. Furthermore, using a partial sum of positive and negative changes in global policy uncertainty, gold price, and oil price as the asymmetric long-run equation of Bitcoin return, Dai et al. (2022) reports that (i) asymmetry shocks in oil price positively impact Bitcoin returns and that (ii) a positive (negative) shock in the gold price is negatively (positively) related to Bitcoin returns.

We use the Gerber statistic as a tool to capture the dependence between the time series of Bitcoin log returns and (leads/lags) of the time series of commodities log returns. The measure we employ was introduced by Gerber et al. (2022), and it is a robust measure of pairwise movements of two series of returns. In particular, it counts the proportion of co-movements in the series of interest, i.e., when both series simultaneously pierce the thresholds specified by the econometrician. As such, it rep-

resents an extension of Kendall's Tau. The Gerber statistics have two key advantages regarding other measures of dependence. First, since only joint co-movements larger than the chosen thresholds enter the statistic, the Gerber correlation is insensitive to small movements in the series that may simply be noise. Second, in contrast to product-moment-based measures, such as the Pearson correlation, the Gerber statistic is insensitive to extreme movements because it relies on the number of times the returns jointly exceed the thresholds and not on the extent to which the thresholds are pierced, Algieri et al. (2021a) introduces a time-varying version of the Gerber statistic, which is used with the aim of identifying co-movements in commodity prices over the period 2006–2020. Another application of the Gerber correlation to commodity markets is represented by Zaremba et al. (2021). The authors use rolling windows estimations for Gerber correlation using monthly data over 170 years. Similar to Algieri et al. (2021a) and contrary to Zaremba et al. (2021), where spot commodity prices are employed, we use daily data for futures prices of each of the four commodities; Ref. Algieri et al. (2021a), however, is concerned only with the Gerber correlation for contemporaneous values of each pair of commodities, whereas here we consider what we call the Gerber cross-correlation.

The paper makes the following contributions. It is the first study using Gerber correlation to analyse the dependence between Bitcoin and commodities. Secondly, it considers a cross-correlation version of the measure, i.e., the Gerber statistic between the cryptocurrency and leads or lags log price changes of four commodities of interest. Finally, it relies on the bootstrap to derive confidence intervals for the newly introduced measure and to test the null that all the Gerber cross-correlations up to lag $k_{\max}$ are zero.

The remainder of the study is organised as follows. Section 4.2 presents the Gerber correlation and cross-correlation statistics and inference methods for the two measures. Section 4.3 shows the results of the empirical application involving log returns. Section 4.4 concludes.

4.2 Methodology

4.2.1 The Gerber Statistic

Let $\{(y_{1,t}, y_{2,t}) : t \in \mathbb{Z}\}$ be a strictly stationary bivariate time series. The Gerber statistic is defined as

$$\frac{\mathbb{E}\left[I^U_{1,t}I^U_{2,t} + I^D_{1,t}I^D_{2,t}\right] - \mathbb{E}\left[I^U_{1,t}I^D_{2,t} + I^D_{1,t}I^U_{2,t}\right]}{\mathbb{E}\left[I^U_{1,t}I^U_{2,t} + I^D_{1,t}I^D_{2,t}\right] + \mathbb{E}\left[I^U_{1,t}I^D_{2,t} + I^D_{1,t}I^U_{2,t}\right]} \tag{4.1}$$

where for $i = 1, 2$

$$I^U_{i,t} = I(y_{i,t} \geq H_{i,t}) = \begin{cases} 1 & \text{if } y_{i,t} \geq H_{i,t} \\ 0 & \text{if } y_{i,t} < H_{i,t} \end{cases}$$

$$I^D_{i,t} = I(y_{i,t} \leq -H_{i,t}) = \begin{cases} 1 & \text{if } y_{i,t} \leq -H_{i,t} \\ 0 & \text{if } y_{i,t} > -H_{i,t} \end{cases},$$

$H_{1,t}$ and $H_{2,t}$ are the thresholds for the two series, and $I(A)$ denotes the indicator function for the event A. The sample counterpart of (4.1) based on T observations is

$$\widehat{g}(0) = \frac{f^c_0 - f^d_0}{f^c_0 + f^d_0} \tag{4.2}$$

where

$$\begin{aligned} f^c_0 &= \frac{1}{T}\sum_{t=1}^{T} I\left(y_{1,t} \geq H_{1,t}\right) I\left(y_{2,t} \geq H_{2,t}\right) + \frac{1}{T}\sum_{t=1}^{T} I\left(y_{1,t} \leq -H_{1,t}\right) I\left(y_{2,t} \leq -H_{2,t}\right) \\ &= f^{UU} + f^{DD} \\ f^d_0 &= \frac{1}{T}\sum_{t=1}^{T} I\left(y_{1,t} \geq H_{1,t}\right) I\left(y_{2,t} \leq -H_{2,t}\right) + \frac{1}{T}\sum_{t=1}^{T} I\left(y_{1,t} \leq -H_{1,t}\right) I\left(y_{2,t} \geq H_{2,t}\right) \\ &= f^{UD} + f^{DU}. \end{aligned}$$

Hence, f^c_0 denotes the proportion of concordant pairs, i.e., the number of times both series pierce their thresholds while moving in the same direction divided by T. Indeed, f^c_0 is equal to the sum of f^{UU}, the proportion of pairs in the sample for which both series are larger than their threshold, and f^{DD}, the proportion of pairs for which

both y_1 and y_2 are smaller than their threshold times minus one. On the other hand, $f_0^d = f^{UD} + f^{DU}$ represents the frequency of discordant pairs in the sample, i.e., the number of times both series pierce their thresholds while moving in the opposite direction divided by T. Note that the statistic in (4.2) coincides with Kendall's Tau if the thresholds $H_{1,t}$ and $H_{2,t}$ are equal to zero for all t.

4.2.2 The Gerber Cross-Correlation

In this study, we examine the Gerber statistic between $y_{1,t}$ and $y_{2,t-k}$, which we define as Gerber cross-correlation. The sample Gerber cross-correlation is hence defined by making some straightforward changes to (4.2):

$$\widehat{g}(k) = \frac{f_k^c - f_k^d}{f_k^c + f_k^d} \tag{4.3}$$

where for $k = 0, \pm 1, \pm 2, \ldots$

$$f_k^c = \frac{1}{T-k} \sum_{t=k+1}^{T} \left[I\left(y_{1,t} \geq H_{1,t}\right) I\left(y_{2,t-k} \geq H_{2,t-k}\right) + I\left(y_{1,t} \leq -H_{1,t}\right) I\left(y_{2,t-k} \leq -H_{2,t-k}\right) \right]$$

$$f_k^d = \frac{1}{T-k} \sum_{t=k+1}^{T} \left[I\left(y_{1,t} \geq H_{1,t}\right) I\left(y_{2,t-k} \leq -H_{2,t-k}\right) + I\left(y_{1,t} \leq -H_{1,t}\right) I\left(y_{2,t-k} \geq H_{2,t-k}\right) \right].$$

The Gerber cross-correlation is a non-linear pairwise dependence measure counting simultaneously the number of piercings of the thresholds. Similarly to the Pearson's correlation coefficient (and Kendall's Tau coefficient), the Gerber statistics lies in the interval $[-1, 1]$. However, contrarily to the Pearson's statistics, the Gerber correlation coefficient does not include all available data points in its computation. In contrast, it is computed by including only meaningful (i.e., above the threshold) co-movement of the pairs of returns, thus being more robust to small positive/negative co-movements.

Inference Methods

We use the stationary bootstrap of Politis and Romano (1994) to obtain the confidence intervals for the Gerber cross-correlation and to test its significance. This method consists in a block bootstrap where blocks have random lengths. In particular, we assume that the block length has a geometric distribution. The optimal (average) block length for the stationary bootstrap is selected based on the criterion discussed

by Patton et al. (2009). The adopted resampling scheme is needed to preserve the time-series dependence between variables y_1 and y_2. Gerber cross-correlation based on the stationary bootstrap resample is defined as follows:

$$\widehat{g}^*(k) = \frac{f_k^{c*} - f_k^{d*}}{f_k^{c*} + f_k^{d*}} \tag{4.4}$$

with

$$f_k^{c*} = \frac{1}{T-k} \sum_{t=k+1}^{T} \left[I\left(y_{1,t}^* \geq H_{1,t}^*\right) I\left(y_{2,t-k}^* \geq H_{2,t-k}^*\right) + I\left(y_{1,t}^* \leq -H_{1,t}^*\right) I\left(y_{2,t-k}^* \leq -H_{2,t-k}^*\right) \right]$$

$$f_k^{d*} = \frac{1}{T-k} \sum_{t=k+1}^{T} \left[I\left(y_{1,t}^* \geq H_{1,t}^*\right) I\left(y_{2,t-k}^* \leq -H_{2,t-k}^*\right) + I\left(y_{1,t}^* \leq -H_{1,t}^*\right) I\left(y_{2,t-k}^* \geq H_{2,t-k}^*\right) \right].$$

where $(y_{1,t}^*, y_{2,t}^*)$ is the bootstrap sample and H_1^* and H_2^* are the thresholds based on the bootstrap sample. To test the null $H_0 : g(1) = g(2) = \ldots = g(k_{\max}) = 0$ we consider the Box–Pierce test statistic

$$\widehat{Q}(k_{\max}) = T \sum_{k=1}^{k_{\max}} \widehat{g}^2(k)$$

and construct B-centred bootstrap realisations of $\widehat{Q}(k_{\max})$, namely

$$\widehat{Q}^*(k_{\max}) = T \sum_{k=1}^{k_{\max}} \left[\widehat{g}^*(k) - \widehat{g}(k)\right]^2.$$

Iterating the stationary bootstrap procedure B times, we end up with B sets of Gerber cross-correlation, $[\widehat{g}_b^*(1), \ldots, \widehat{g}_b^*(k_{\max})]_{b=1}^B$, and the corresponding test statistics

$$\left[\widehat{Q}_b^*(k_{\max}) = T \sum_{k=1}^{k_{\max}} \left[\widehat{g}_b^*(k) - \widehat{g}(k)\right]^2 \right]_{b=1}^{B}.$$

To carry out the test, we compute the bootstrap p-value as

$$\widehat{p}(k_{\max}) = \frac{1}{B} \sum_{b=1}^{B} I\left[\widehat{Q}_b^*(k_{\max}) \geq \widehat{Q}(k_{\max})\right].$$

4.3 Empirical Results

We compute the daily log returns, i.e., changes in log prices, for Bitcoin and the futures prices of the commodities listed in Table 4.1. Commodities prices are based on the first generic futures contracts series extracted from Bloomberg. We focus our attention on commodity futures prices since they are the sources of many forward-looking decisions of economic agents and represent important price signals to guide future spot prices Ameur et al. (2022); Algieri and Leccadito (2017). Indeed, futures prices account for the expectations of supply and demand of the selected commodities. For instance, producers may define their supply strategy based on the price of futures contracts, and investors could outline their asset allocation strategy based on the trend of futures prices. With future prices, we can hence capture market sentiments regarding the commodities since a future contract obligates the seller and a potential buyer to transact at a specified future date and an agreed-upon price. In addition, futures contracts are widespread speculation vehicles, so the link with cryptocurrency markets is more straightforward. Data cover the period from 18 September 2014 to 17 June 2022 for a total of 1954 observations per series.

Table 4.1: Commodity futures (Bloomberg Tickers)

Selected Commodities	
Ticker	**Description**
CL1 Comdty	Generic 1st Crude Oil WTI Futures
PL1 Comdty	Generic 1st Platinum futures
W1 Comdty	Generic 1st Wheat futures
GC1 Comdty	Generic 1st Gold futures

Each panel of Figure 4.1 reports the full-sample Gerber statistics for leads and lags, $k = -25, \ldots, +25$ days, between the Bitcoin returns, $y_{1,t}$ in Equation (4.3), and $y_{2,t-k}$, the second variable of Equation (4.3), which is the crude oil WTI (top-left), platinum (top-right), wheat (bottom-left) and gold (bottom-right), respectively. Since for negative values of k for the pair $(y_{1,t}, y_{2,t-k})$ are equivalent to the pair $(y_{2,t}, y_{1,t-j})$, with $j = -k$, Figure 4.1 provides the whole picture of the cross dependence of Bitcoin (commodities) returns on lagged commodities (Bitcoin) returns.

There are two main messages arising from Figure 4.1. First, independent of the lags/leads or commodity type, the cross-correlation with Bitcoin returns are mild,

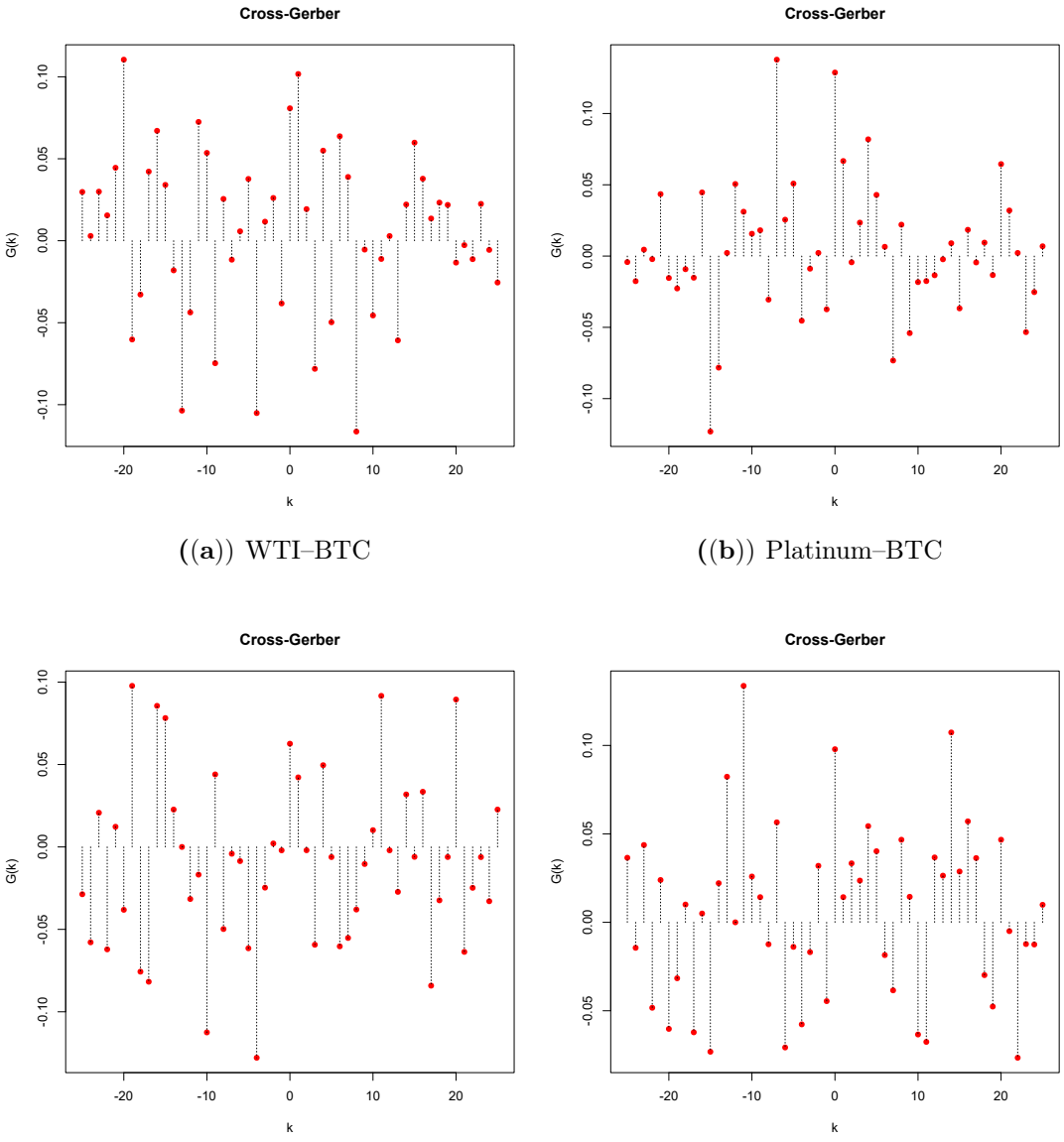

((**a**)) WTI–BTC

((**b**)) Platinum–BTC

((**c**)) Wheat–BTC

((**d**)) Gold–BTC

Figure 4.1: Whole Sample Gerber cross-correlations between Bitcoin (BTC) and each commodity. Note: Thresholds are $H_i = \sigma_i/2$ where σ_i are the (unconditional) return volatilities for $i = 1, 2$.

mostly below 0.1 in absolute value. This result would signal that Bitcoin is widely different from commodity markets, in line with the analysis by Klein et al. (2018); Baur et al. (2018). Second, as the lags/leads change, correlations tend to switch sign with no clear pattern. In the next section, we assess if these cross-correlations are time varying via a rolling window analysis.

4.3.1 Rolling Window Estimation of Gerber Cross-Correlations

In this section, we use a rolling window procedure to obtain time-varying estimates of the statistic (4.3). We set (i) the window size to roughly three years, corresponding to 750 daily observations, (ii) k to -25, -5, -1, 0, 1, 5, and 25, corresponding to leads/lags of one day, one week and (roughly) one month, and (iii) the thresholds to one-half of the unconditional volatilities of the original series. For the block bootstrap procedure, we perform 1000 replications by re-sampling blocks of data, instead of individual values, to preserve the cross-sectional dependence of the original series. The time-varying cross-correlations are reported in Figures 4.2–4.9. Focusing on the contemporaneous cross-correlation, the top-left panel of each figure, one notices that the cross-correlations have turned (significantly) positive for WTI and precious metals after the COVID-19 crisis. This indicates that the health and economic-financial turmoil increases the connectedness between Bitcoin and the other asset classes—in our case, commodities. Indeed, contagion effects across markets can trigger the increased connectedness of returns during hectic market periods, and this would have a major impact on risk and investment portfolio management, and policy making.

Turning to lags/leads correlations, Figure 4.2 reports a small, positive correlation between Bitcoin at time t and WTI one week or one month lagged. Conversely, the correlation is negative when WTI is one day lagged, except for the period of pandemics, when the cross-correlation becomes positive.

When the correlation is computed between WTI at time t and BTC one day lagged, we observe a low but positive correlation (Figure 4.3b) before the COVID-19 crisis, contrary to when WTI is one day lagged (Figure 4.2b). In Figure 4.3c, we detect a higher correlation (around 0.1) between the WTI at time t and Bitcoin at time $t-5$, compared to a very low correlation (around 0) when instead WTI is one week lagged (Figure 4.2c). In both cases, we can also notice a sharp change in the correlation during the COVID-19 pandemic.

The contemporaneous Gerber correlations between Bitcoin and platinum's returns are generally positive but low. The same positive nexus exists when Bitcoin is evaluated at time t, and platinum's returns are one week or month lagged (Figure 4.4). When instead the Bitcoin's returns are lagged, the situation is almost similar to WTI (Figure 4.5). In both cases, we see a generally increasing trend after the Coronavirus

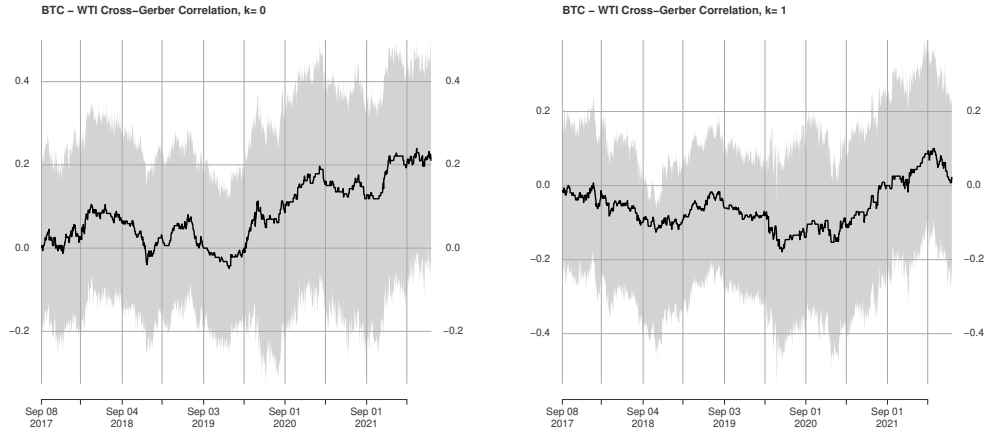

((**a**)) $k = 0$ ((**b**)) $k = 1$

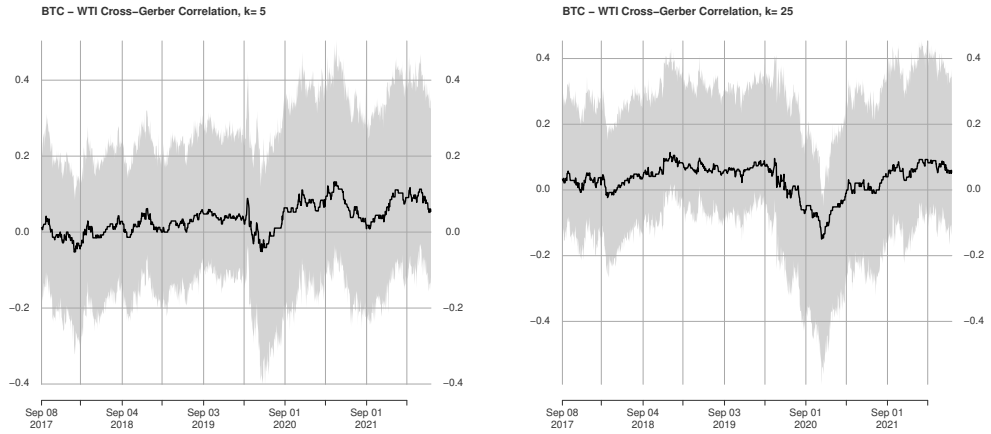

((**c**)) $k = 5$ ((**d**)) $k = 25$

Figure 4.2: The 3-year trailing Gerber cross-correlations and 99% confidence bands, y_1 = BTC, y_2 = WTI. Note: Thresholds are $H_i = \sigma_i/2$ where σ_i are the (unconditional) return volatilities for $i = 1, 2$.

pandemic. The cross-correlation between contemporaneous Bitcoin and wheat is positive and declining between 2017 and 2020. It started rising during the pandemic, but overall it remains low and consistently below 0.15 (Figures 4.6 and 4.7). Bitcoin and gold display a contained and, only at times, negative Gerber correlation (Figures 4.8 and 4.9).

This latter result, coupled with the fact that Bitcoin returns' volatility is five times higher than that of gold, highlights the fundamental differences between the two assets. First, while gold is considered a safe haven in times of financial or political uncertainty, the same cannot be said for Bitcoin. Given the low/contrasting correlations between the two assets, investors do not see the two assets as a substitute for each other. Second, given the high(er) volatility of Bitcoin returns, this asset cannot be considered

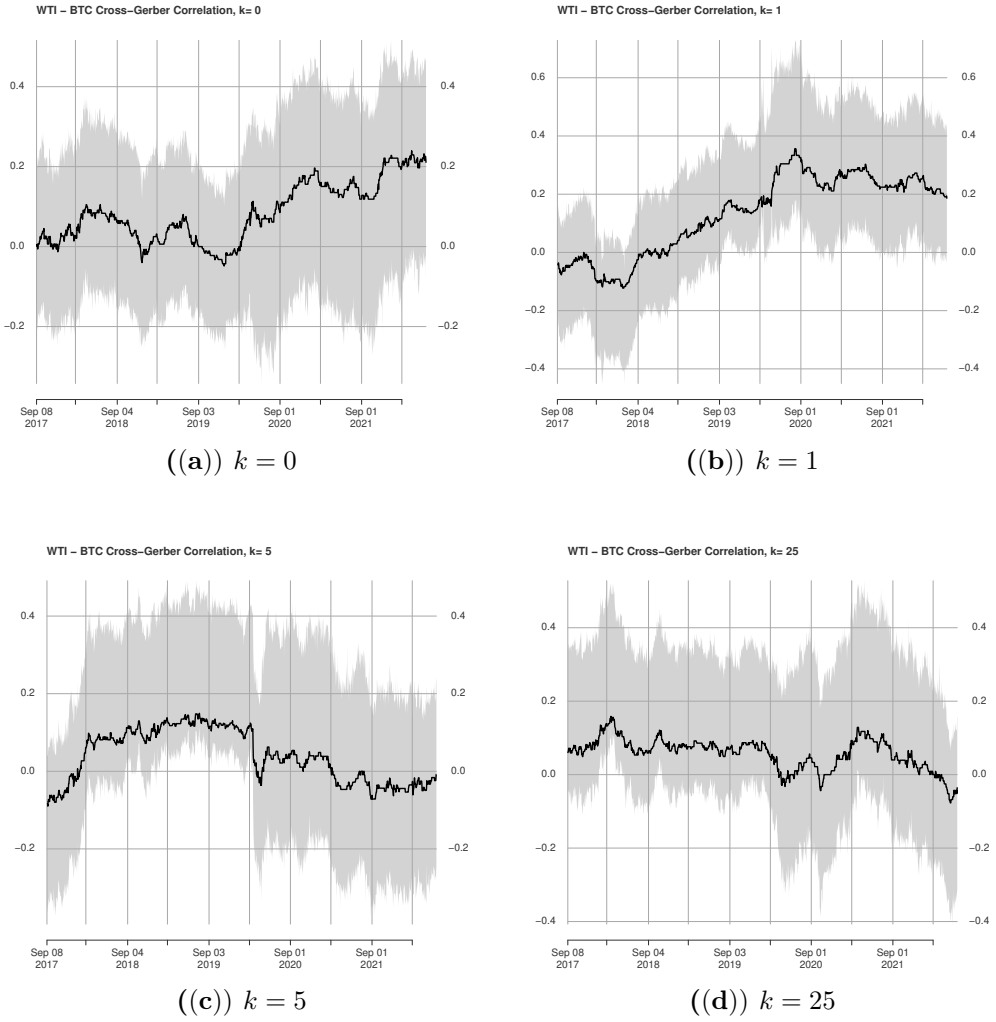

((**a**)) $k = 0$ ((**b**)) $k = 1$

((**c**)) $k = 5$ ((**d**)) $k = 25$

Figure 4.3: The 3-year trailing Gerber cross-correlations and 99% confidence bands, y_1 = WTI, y_2 = BTC. Note: Thresholds are $H_i = \sigma_i/2$ where σ_i are the (unconditional) return volatilities for $i = 1, 2$.

an investment to rely on in turbulent times, as is the case for gold.

These considerations support the findings by Baur and Hoang (2021) that pointed out how Bitcoin cannot be considered the "new digital gold", i.e., Bitcoin cannot provide a store of value similar to gold nor can it be considered a safe haven like the yellow metal. Our results differ from the study by Bouri et al. (2018), who documented a negative relation between gold price and Bitcoin. Our findings also diverge from Jareño et al. (2021), which detected a significant positive connectedness between Bitcoin and gold. The positive connectedness would suggest that Bitcoin has a potential hedging ability like gold, which is opposite to our results.

Our analysis indicates that the cross-correlation between Bitcoin's and commodities' returns is relatively scanty, even if it has increased during the recent turbulent

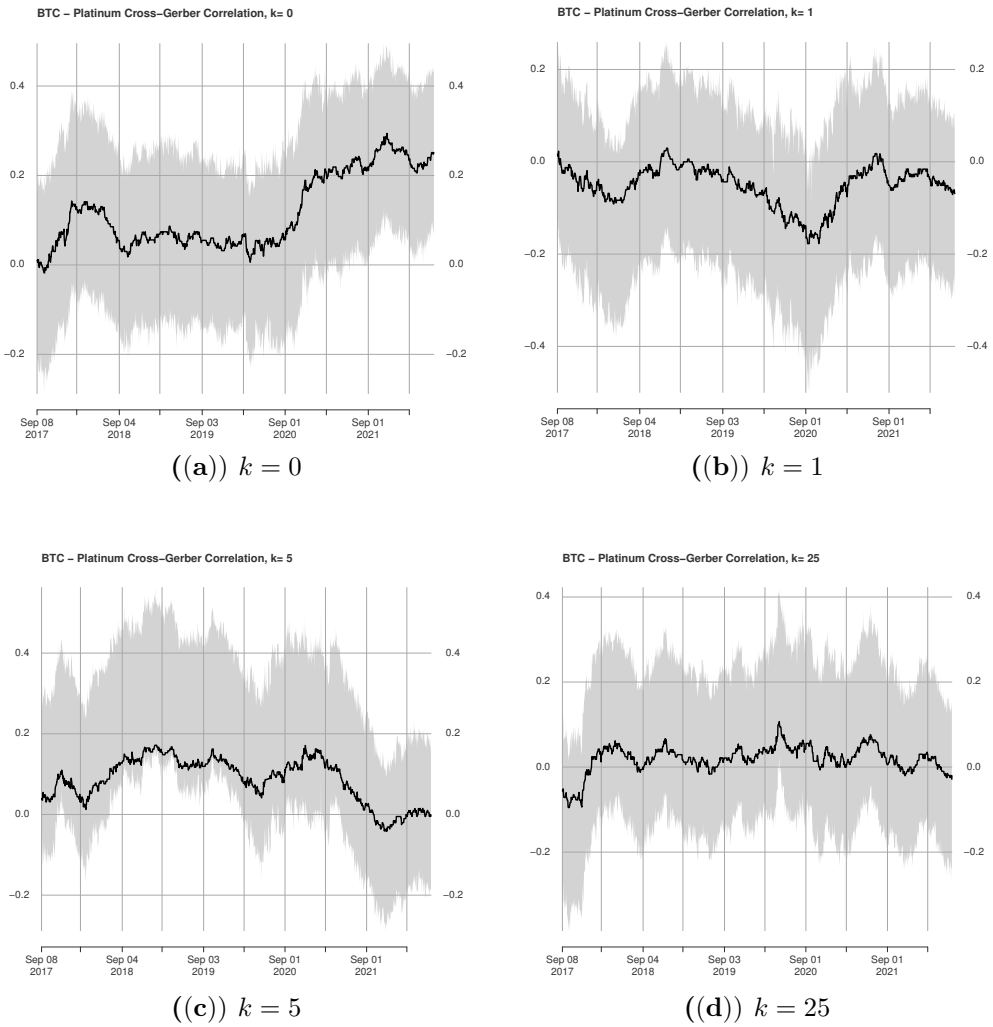

((**a**)) $k = 0$ ((**b**)) $k = 1$

((**c**)) $k = 5$ ((**d**)) $k = 25$

Figure 4.4: The 3-year trailing Gerber cross-correlations and 99% confidence bands, y_1 = BTC,
y_2 = Platinum. Note: Thresholds are $H_i = \sigma_i/2$ where σ_i are the (unconditional) return volatilities for $i = 1, 2$.

periods. The rising interdependence between commodities and cryptocurrencies in periods of economic crisis is similar to the study by Jareño et al. (2021) that applied a nonlinear ARDL model to crude oil and Bitcoin. We can attribute our finding to the highly speculative activities of investors during periods of economic, financial, and health turmoil and to capital movements from more risky investments to safe havens. Indeed, these factors may result in high interactions between different markets (see Aloui et al. (2011)).

Finally, we test the null $H_0 : g(1) = g(2) = \ldots = g(k_{\max}) = 0$ for $k_{\max} \in \{1, 5, 10, 25\}$. Table 4.2 reports the values of the test statistic $\widehat{Q}(k_{\max})$ and the corresponding p-value $\widehat{p}(k_{\max})$. The bootstrap p-values are based on $B = 1000$ replicas. The only time when we reject the null is for the case $y_1 =$ WTI, $y_2 =$ BTC with $k_{\max} = 1$.

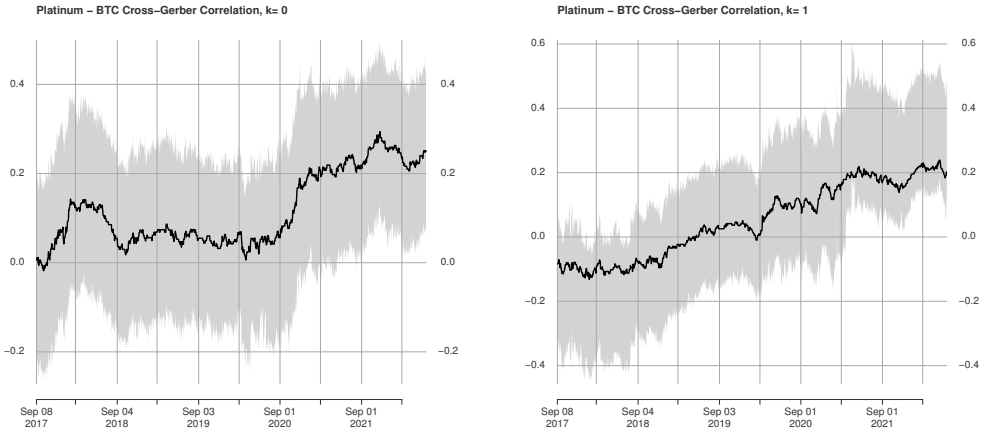

((**a**)) $k = 0$ ((**b**)) $k = 1$

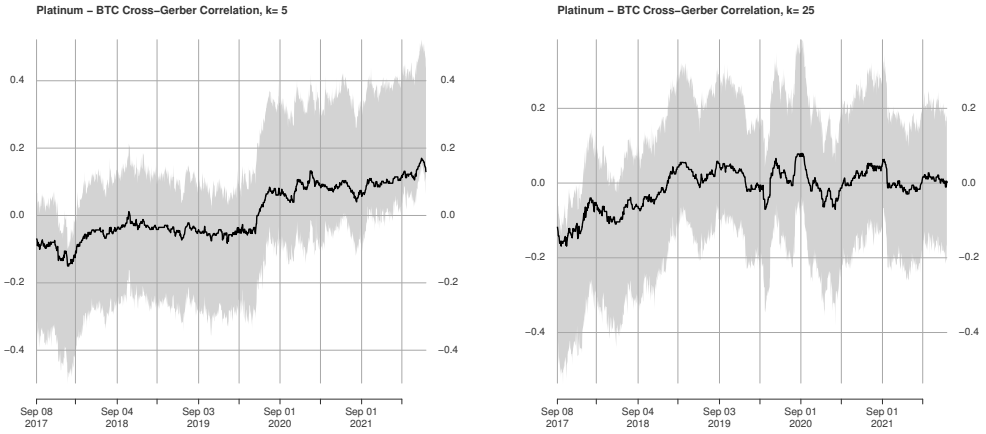

((**c**)) $k = 5$ ((**d**)) $k = 25$

Figure 4.5: The 3-year trailing Gerber cross-correlations and 99% confidence bands, y_1 = Platinum, y_2 = BTC. Note: Thresholds are $H_i = \sigma_i/2$ where σ_i are the (unconditional) return volatilities for $i = 1, 2$.

These findings imply that there is no dependence between log returns of Bitcoin and the major categories of commodities.

Table 4.2: Bootstrap test Bitcoin, Commodities

	y_1 = BTC, y_2 = WTI		y_1 = BTC, y_2 = Platinum		y_1 = BTC, y_2 = Wheat		y_1 = BTC, y_2 = Gold	
$k_{\max}$	$\widehat{Q}(k_{\max})$	$\widehat{p}(k_{\max})$	$\widehat{Q}(k_{\max})$	$\widehat{p}(k_{\max})$	$\widehat{Q}(k_{\max})$	$\widehat{p}(k_{\max})$	$\widehat{Q}(k_{\max})$	$\widehat{p}(k_{\max})$
1	2.8590	0.4570	2.7277	0.5500	0.0083	0.9600	3.8789	0.5790
5	28.8201	0.4320	11.9621	0.9000	40.5485	0.7110	13.3090	0.9120
10	46.9309	0.6870	53.2732	0.9080	74.0836	0.8400	31.3360	0.9640
25	137.9548	0.9130	112.1169	0.9880	166.4217	0.9670	120.1614	0.9920
	y_1 = WTI, y_2 = BTC		y_1 = Platinum, y_2 = BTC		y_1 = Wheat, y_2 = BTC		y_1 = Gold, y_2 = BTC	
$k_{\max}$	$\widehat{Q}(k_{\max})$	$\widehat{p}(k_{\max})$	$\widehat{Q}(k_{\max})$	$\widehat{p}(k_{\max})$	$\widehat{Q}(k_{\max})$	$\widehat{p}(k_{\max})$	$\widehat{Q}(k_{\max})$	$\widehat{p}(k_{\max})$
1	20.2080	0.0410	8.6844	0.5050	3.4788	0.4300	0.3950	0.7700
5	43.5911	0.2180	26.5014	0.8040	15.2411	0.8270	12.5860	0.8540
10	85.0695	0.2350	44.3850	0.9250	31.5308	0.9300	28.6693	0.9560
25	108.5652	0.8880	66.4093	0.9980	97.5479	0.9880	97.3701	0.9930

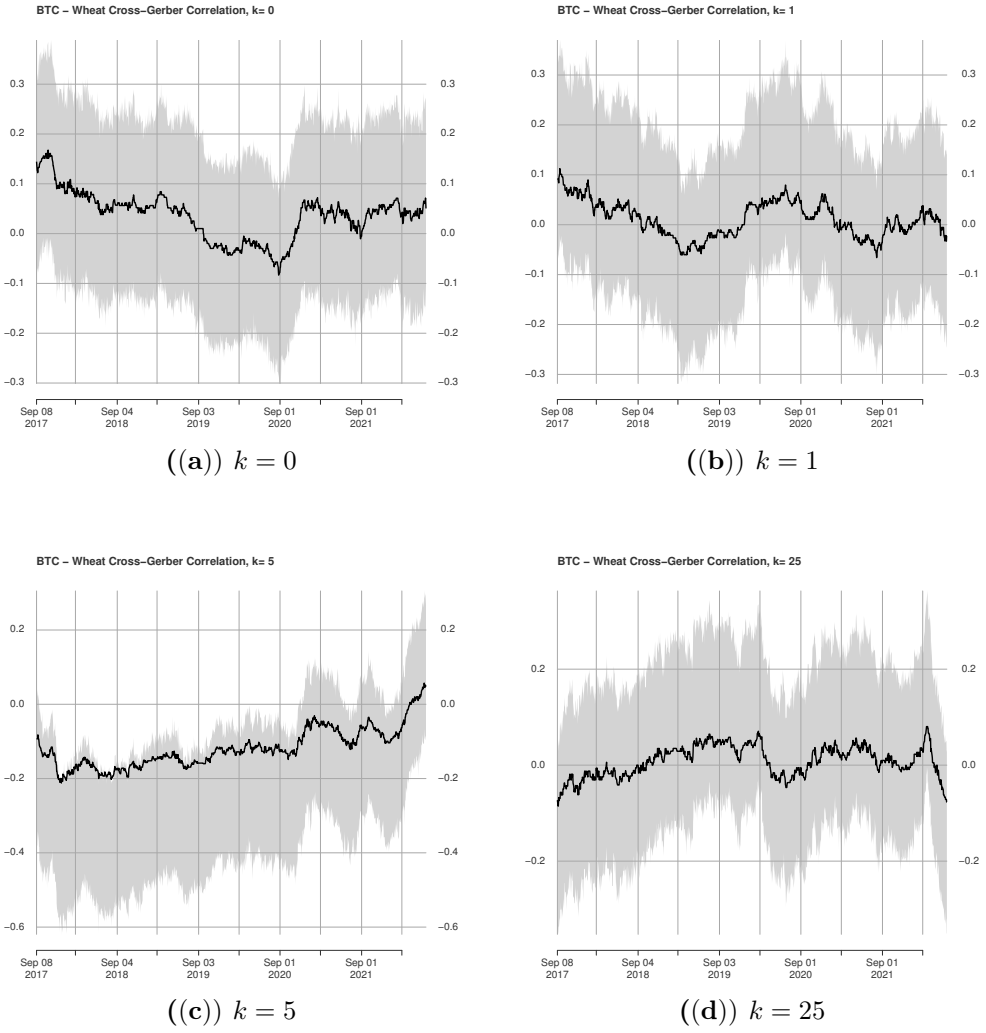

((**a**)) $k = 0$ ((**b**)) $k = 1$

((**c**)) $k = 5$ ((**d**)) $k = 25$

Figure 4.6: The 3-year trailing Gerber cross-correlations and 99% confidence bands, y_1 = BTC, y_2 = Wheat. Note: Thresholds are $H_i = \sigma_i/2$ where σ_i are the (unconditional) return volatilities for $i = 1, 2$.

We also investigate whether there is a dependence between squared Bitcoin log returns (a proxy for Bitcoin volatility) and lead/lags of log returns from the four commodities. The results are given in Table 4.3. In both cases where Bitcoin squared log returns are assumed to be the y_1 variable and the y_2 variable, we do not reject the null hypothesis. This is true for all the values of $k_{\max}$ we consider. Hence, we can conclude that there is no dependence between Bitcoin volatility (proxied by squared Bitcoin log returns) and the returns of crude oil WTI, platinum, wheat, and gold.

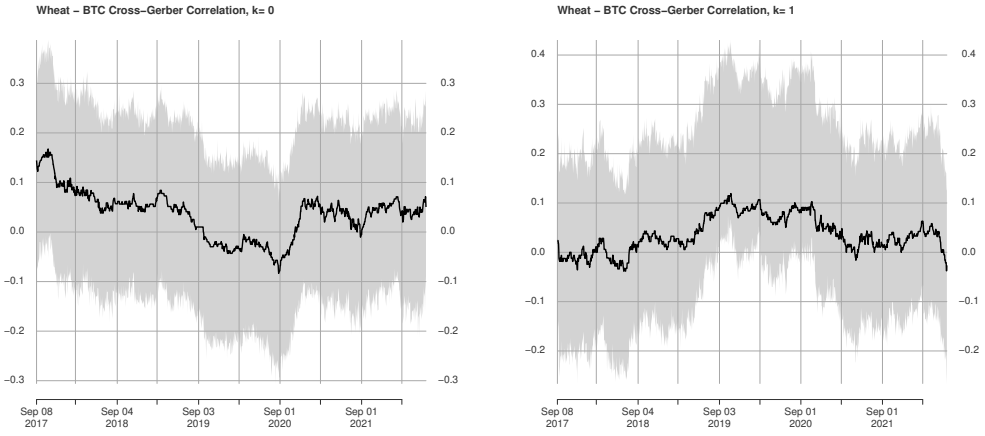

((**a**)) $k = 0$ ((**b**)) $k = 1$

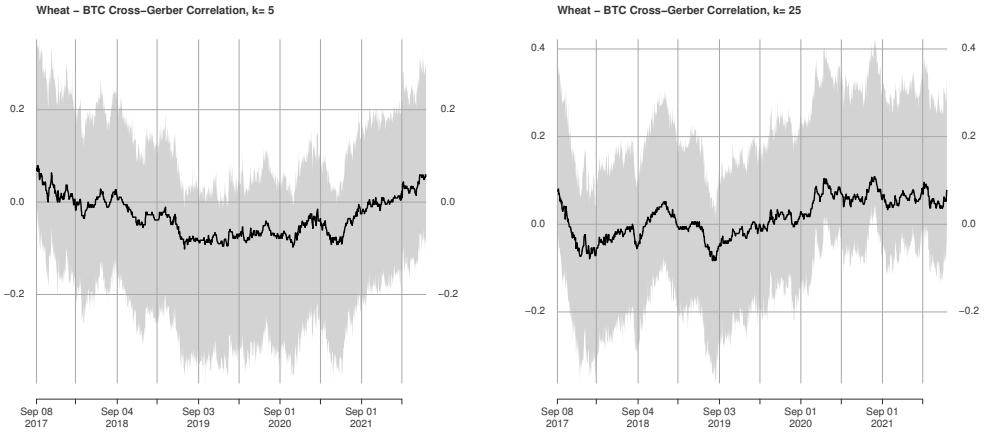

((**c**)) $k = 5$ ((**d**)) $k = 21$

Figure 4.7: The 3-year trailing Gerber cross-correlations and 99% confidence bands, y_1 = Wheat, y_2 = BTC. Note: Thresholds are $H_i = \sigma_i/2$ where σ_i are the (unconditional) return volatilities for $i = 1, 2$.

Table 4.3: Bootstrap test, Squared Bitcoin, Commodities

	$y_1 = \text{BTC}^2$, $y_2 = \text{WTI}$		$y_1 = \text{BTC}^2$, $y_2 = \text{Platinum}$		$y_1 = \text{BTC}^2$, $y_2 = \text{Wheat}$		$y_1 = \text{BTC}^2$, $y_2 = \text{Gold}$	
$k_{\max}$	$\widehat{Q}(k_{\max})$	$\widehat{p}(k_{\max})$	$\widehat{Q}(k_{\max})$	$\widehat{p}(k_{\max})$	$\widehat{Q}(k_{\max})$	$\widehat{p}(k_{\max})$	$\widehat{Q}(k_{\max})$	$\widehat{p}(k_{\max})$
1	12.0200	0.5480	0.9370	0.7950	16.1488	0.3110	13.1282	0.3170
5	58.6704	0.7580	14.5683	0.9510	52.9512	0.6780	97.1572	0.3190
10	178.7206	0.7110	75.9803	0.8770	94.2911	0.8270	260.5584	0.1840
25	672.2332	0.8990	183.1941	0.9870	275.7607	0.9490	684.0197	0.2120
	$y_1 = \text{WTI}$, $y_2 = \text{BTC}^2$		$y_1 = \text{Platinum}$, $y_2 = \text{BTC}^2$		$y_1 = \text{Wheat}$, $y_2 = \text{BTC}^2$		$y_1 = \text{Gold}$, $y_2 = \text{BTC}^2$	
$k_{\max}$	$\widehat{Q}(k_{\max})$	$\widehat{p}(k_{\max})$	$\widehat{Q}(k_{\max})$	$\widehat{p}(k_{\max})$	$\widehat{Q}(k_{\max})$	$\widehat{p}(k_{\max})$	$\widehat{Q}(k_{\max})$	$\widehat{p}(k_{\max})$
1	4.2667	0.6090	19.5400	0.1990	0.1041	0.9280	1.0248	0.7990
5	72.4407	0.6180	71.6663	0.4770	25.2471	0.8870	72.1157	0.4660
10	229.8511	0.3820	152.8596	0.5500	63.1620	0.9220	191.9757	0.2990
25	506.2262	0.5990	295.6690	0.9330	339.1286	0.8870	510.9055	0.3830

Finally, we study the dependence between squared Bitcoin log returns and lead/lags of squared log returns from the four commodities (note that when both y_1 and y_2 take

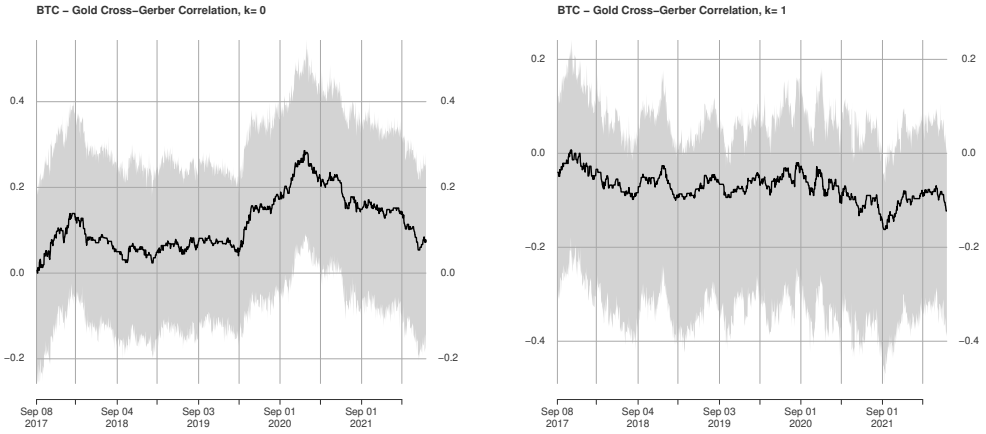

((**a**)) $k = 0$ ((**b**)) $k = 1$

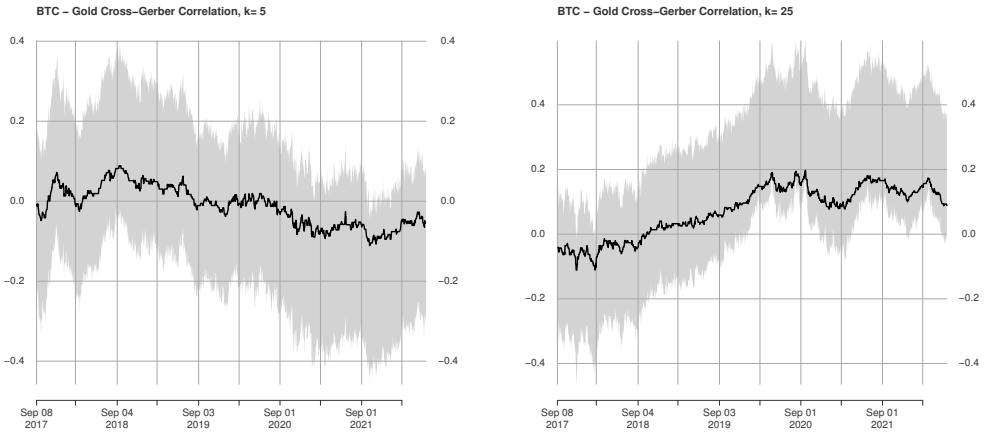

((**c**)) $k = 5$ ((**d**)) $k = 25$

Figure 4.8: The 3-year trailing Gerber cross-correlations and 99% confidence bands, y_1 = BTC, y_2 = Gold. Note: Thresholds are $H_i = \sigma_i/2$ where σ_i are the (unconditional) return volatilities for $i = 1, 2$.

on only positive values and the thresholds are positive, then $f_k^d = 0$. Therefore, in this case (4.3) is not suitable and we use an alternative version of the Gerber statistic discussed by Gerber et al. (2022). Hence, only for this final case, we change the denominator of (4.3) and use

$1 - f_k^n$ where $f_k^n = \frac{1}{T-k} \sum_{t=k+1}^{T} \left[I\left(-H_{1,t} < y_{1,t} < H_{1,t}\right) I\left(-H_{2,t-k} < y_{2,t-k} < H_{2,t-k}\right) \right]$.

Table 4.4 reports the results. From the table, it is evident that for all the levels of $k_{\max}$ and for all the pairs of squared returns we consider, we strongly reject the null hypothesis, except when y_1 is Bitcoin and y_2 is WTI and vice versa. Therefore, we can conclude that there is interdependence between Bitcoin volatility and the volatility of platinum, wheat, and gold.

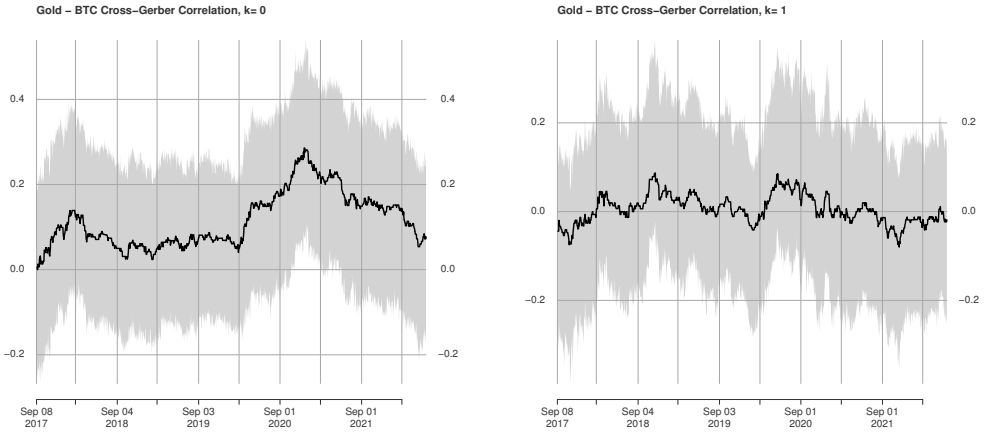

((**a**)) $k = 0$ ((**b**)) $k = 1$

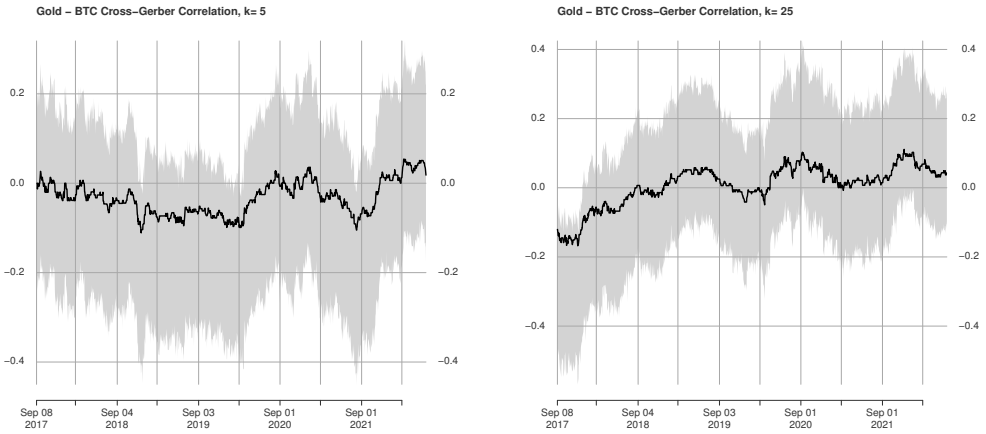

((**c**)) $k = 5$ ((**d**)) $k = 25$

Figure 4.9: The 3-year trailing Gerber cross-correlations and 99% confidence bands, y_1 = Gold, y_2 = BTC. Note: Thresholds are $H_i = \sigma_i/2$ where σ_i are the (unconditional) return volatilities for $i = 1, 2$.

Table 4.4: Bootstrap test, Squared Bitcoin, Squared Commodities

	multicolumn2l$y_1 = \mathbf{BTC^2}$, $y_2 = \mathbf{WTI^2}$		$y_1 = \mathbf{BTC^2}$, $y_2 = \mathbf{Platinum^2}$		$y_1 = \mathbf{BTC^2}$, $y_2 = \mathbf{Wheat^2}$		$y_1 = \mathbf{BTC^2}$, $y_2 = \mathbf{Gold^2}$	
$k_{\max}$	$\widehat{Q}(k_{\max})$	$\widehat{p}(k_{\max})$	$\widehat{Q}(k_{\max})$	$\widehat{p}(k_{\max})$	$\widehat{Q}(k_{\max})$	$\widehat{p}(k_{\max})$	$\widehat{Q}(k_{\max})$	$\widehat{p}(k_{\max})$
1	1.8448	0.2820	16.9378	0.0000	9.4301	0.0380	17.7234	0.0000
5	17.9767	0.2060	60.2868	0.0020	69.5256	0.0000	74.4307	0.0000
10	31.2844	0.2050	118.3702	0.0000	137.8887	0.0000	135.3187	0.0000
25	53.1649	0.2070	308.7823	0.0000	333.0107	0.0000	316.5219	0.0000
	$y_1 = \mathbf{WTI^2}$, $y_2 = \mathbf{BTC^2}$		$y_1 = \mathbf{Platinum^2}$, $y_2 = \mathbf{BTC^2}$		$y_1 = \mathbf{Wheat^2}$, $y_2 = \mathbf{BTC^2}$		$y_1 = \mathbf{Gold^2}$, $y_2 = \mathbf{BTC^2}$	
$k_{\max}$	$\widehat{Q}(k_{\max})$	$\widehat{p}(k_{\max})$	$\widehat{Q}(k_{\max})$	$\widehat{p}(k_{\max})$	$\widehat{Q}(k_{\max})$	$\widehat{p}(k_{\max})$	$\widehat{Q}(k_{\max})$	$\widehat{p}(k_{\max})$
1	3.0219	0.2290	9.8020	0.0430	9.9330	0.0470	14.4043	0.0000
5	23.6538	0.1600	71.9153	0.0000	72.8432	0.0010	73.0970	0.0000
10	44.6466	0.1700	144.1266	0.0000	138.5131	0.0010	134.3093	0.0000
25	104.3157	0.1820	326.3295	0.0030	348.7731	0.0020	308.8461	0.0000

4.4 Conclusions

The present study has explored the cross-correlation relationships between Bitcoin and the main energy, precious metal, and agricultural commodities: crude oil WTI, platinum, gold, and wheat. The analysis covers the period 2014–2022 using daily futures price data. We adopted the time-varying cross-correlation metric proposed by Gerber but readapted it to consider both contemporaneous relationships across variables and time asymmetric linkages. This means that pairs of variables have been considered at time t and $t - k$. The findings of our analysis show that Bitcoin and commodities have a low cross-correlation that stays below 0.25 over time. The low correlations between Bitcoin and other commodities might highlight that the drivers of Bitcoin's returns differ from those of other commodities. Hence, it might be challenging to understand, looking at the commodity market, what could drive sudden movements in Bitcoin prices. Generally, the cross-correlations showed a tendency to rise after the COVID-19 pandemic. Furthermore, gold tends to have a weak and sometimes negative linkage with Bitcoin. Finally, there seems to be no dependence between Bitcoin volatility (proxied by squared Bitcoin log returns) and the returns of the four commodities. Instead, we found strong dependence between Bitcoin volatility and the volatility of platinum, wheat, and gold (again proxied by their squared returns).

Overall, we show that the Gerber statistic is a straightforward and robust tool, which can give insightful indications to portfolio managers building optimal strategies. For example, in our analysis, we show that while the low average correlations between Bitcoin and commodities returns might indicate the potential diversification effects for portfolios of commodities, the time-varying and volatility analysis suggest that this might not result in a reduction in risk. In fact, in times of turmoil, the correlations between Bitcoin and other commodities returns and volatility tend to increase, hurting portfolio diversification when it is needed the most.

Our analysis also has policy implications. As more and more developing economies are embarking on the usage of cryptocurrencies-based digital assets, our findings point out that these decisions should be taken with caution. Since many developing economies are commodity export dependent, linking the currency to a highly volatile asset that tends to have a higher correlation with commodities returns in times of turmoil might add additional risks to a country's stability.

The limitations of the present study are related to the fact that we only analyse two asset classes (commodities and cryptocurrencies, namely the Bitcoin). Therefore, future research involving our novel methodology could be extended to stock and bond markets, more cryptocurrencies (Ethereum, to start with) and traditional currencies.

Chapter 5

Investigating time-varying correlations between cryptocurrency and financial markets: a GAS-based approach

5.1 Introduction

Diversifying portfolios allows investors to minimize risks. Diversification implies that operators select assets that are negatively or not correlated with each other for their portfolios. Thus, asset returns will move in different directions when the conditions in the market change. Accurately modeling the correlation between financial assets enhances portfolio performance and risk management, and reduces losses (Feder-Sempach et al., 2024; Hull et al., 2004; Longin and Solnik, 2001). When a financial instrument is uncorrelated or negatively correlated with another asset, one speaks of a hedge. When a hedge negatively correlates with the other instrument during times of distress and economic downturns, it is defined as a safe-haven asset (Bedowska-Sójka and Kliber, 2021; Baur and Lucey, 2010). Traditional correlation models, based on Pearson's correlation coefficient, often fail to capture the dynamic and non-linear relationships between financial assets, ignoring factors like volatility clustering and tail dependence (Algieri et al., 2021b; Cont, 2001). Previous research indicates that financial time series exhibit changing dependence structures, with asset interdependence intensifying during crises (Lawuobahsumo et al., 2024; Das and Uppal, 2004; Patton, 2004). This effect, known as *asymmetric dependence* (Ang and Bekaert, 2002), is prevalent in the cryptocurrency markets, which are particularly sensitive to economic changes and dif-

ferent types of news (Telli and Chen, 2020). Incorporating exogenous information like macroeconomic indicators into correlation models is crucial, as it can impact asset correlations (Bauwens et al., 2006) and enhance prediction accuracy (Diebold and Yilmaz, 2009).

To address these challenges, we propose a novel framework based on an asymmetric Student-t distribution (Azzalini, 2005), with correlations governed by a Generalized Autoregressive Score (GAS, Creal et al., 2013) dynamics. This advanced approach overcomes the limitations of traditional models by offering a more flexible and accurate representation of financial returns In particular, GAS models represent an easy and efficient way to make the parameters dynamic, as they are updated according to the maximum directional increase of the score function.

Investigating the time-varying correlation between cryptocurrencies and other financial assets is essential for understanding market dynamics, developing trading strategies and managing portfolios. Indeed, cryptocurrency prices show complex risk patterns, high volatility, asymmetries, and high tail risk. These characteristics make it challenging to model their volatility and manage portfolios containing digital assets. Moreover, given the growing popularity of cryptocurrencies, understanding their interactions with other asset classes can provide investors with valuable insights to make informed decisions in the financial markets, giving rise to several studies in the literature. While some research suggests that cryptocurrencies offer diversification and hedging benefits (Terraza et al., 2024; Colon et al., 2021; Guesmi et al., 2019; Urquhart and Zhang, 2019; Dyhrberg, 2016), others indicate their limited effectiveness as safe-havens or hedging instruments (Feder-Sempach et al., 2024; Bedowska-Sójka and Kliber, 2021; Smales, 2019; Wang et al., 2019; Klein et al., 2018; Corbet et al., 2018). For instance, Bedowska-Sójka and Kliber (2021) documented that Bitcoin and Ether can be occasionally considered as weak safe-haven against stock indices. Conversely, gold could be regarded as a strong safe haven within the years 2015-2019, but not during the coronavirus outbreak. Dyhrberg (2016) compared Bitcoin, gold and the US dollar's hedging capabilities against the stock market (FTSE Index) and showed that Bitcoin, combining some of the advantages of gold and the dollar, can be a useful tool for portfolio management and risk analysis. Bouri et al. (2017) studied the Bitcoin diversification and hedging nature and concluded that while Bitcoin may diversify portfolios, it is not a reliable hedge. However, in another study, Bouri et al. (2017) and Demir et al.

(2018) suggested that Bitcoin can serve as a short-term hedge in extreme market conditions. Corbet et al. (2018) also found that cryptocurrencies can provide short-term diversification benefits by being disconnected from traditional markets.

Klein et al. (2018) employed the multivariate volatility models of the BEKK-GARCH type to analyze the dynamic correlation between Bitcoin and gold. They reported that while gold acts as a safe haven during market distress, Bitcoin behaves inversely, positively correlating with downward market movements. Further studies have focused on the relationship between Bitcoin and commodities like crude oil. Selmi et al. (2018) used the conditional and unconditional Quantile-on-Quantile Regression (QQR) technique to study the impact of gold and Bitcoin on the crude oil market and found that gold and Bitcoin can hedge crises in oil markets. Guesmi et al. (2019) employed the VARMA-DCC-GARCH framework and reported that Bitcoin can reduce portfolio risk when included in a portfolio in addition to crude oil. Moussa et al. (2021) utilized various regression techniques to analyze Bitcoin's relationship with commodities like oil, gold, and coal, emphasizing the importance of dynamic modeling for understanding their long-term interactions. Kumah and Odei-Mensah (2022) employed wavelet techniques and quantile regressions to investigate the hedging properties of various cryptocurrencies against oil market volatility and highlighted Ethereum, Stellar, Ripple, and Monero as potential hedges. Tiwari et al. (2019) investigated time-differentiated correlations between the S&P 500 and six other cryptocurrencies. They reported that cryptocurrencies can hedge against the risks of the S&P 500 due to the low time-varying correlations observed. Conlon and McGee (2020) questioned Bitcoin's diversification potential during the COVID-19 pandemic, observing an increased correlation with the S&P 500. They concluded that Bitcoin did not act as a safe haven during the crisis, potentially increasing portfolio downside risk when held alongside equities consistent with what was observed by Klein et al. (2018) within the commodity market. Kim et al. (2020) also noted significant correlations between Bitcoin and traditional assets during the cryptocurrency crash and the COVID-19 pandemic, indicating potential correlations during market crises. Shen (2022) applied the BEKK-GARCH model to assess time-varying correlations between Bitcoin, gold, and major market indexes, revealing Bitcoin's inability to hedge market risks during crashes. Ghorbel and Jeribi (2021) emphasized the weak association between Bitcoin and conventional assets, suggesting Bitcoin's isolation from financial markets. Cortese et al. (2023) show a similar

result, using a sparse statistical jump model (Nystrup et al., 2021) to identify the main drivers of cryptomarkets, finding that momentum is the primary driver (Liu et al., 2022). Oosterlinck et al. (2023) provided evidence from the 2022 Ukraine war, indicating that gold and Bitcoin complement each other rather than serving as substitutes during crises, with Bitcoin diversifying oil risk more effectively than gold. In a nutshell, these studies highlight the complex and evolving relationship between cryptocurrencies and traditional financial assets, emphasizing the importance of dynamic modeling of correlation.

The literature on correlation models highlights the importance of dynamic distributions (e.g Bedowska-Sójka and Kliber, 2021) and non-linear methods, such as Dynamic Conditional Correlation models (DCC) initially proposed by Engle (2002) and copulas (Cherubini et al., 2004; Cortese et al., 2024), to accurately capture the asymmetries in traditional financial assets and cryptocurrency market dependencies. The main drawback with DCC is that it usually relies on normality, which is proven to be a questionable assumption in a financial context. Copula models, on the other hand, offer a more flexible framework by allowing for the modeling of dependencies between variables with different marginal distributions (Patton, 2013). However, their complexity and the difficulty in selecting the appropriate copula function can be challenging and potentially lead to model misspecification.

Several advancements in modelling dynamic correlation matrices and volatility have emerged in the recent literature. Hafner and Wang (2023) introduced a model where the dynamics of correlation matrices are driven by the likelihood score corresponding to the matrix logarithm of the correlation matrix, maintaining positive-definiteness through a transformation akin to exponential GARCH for volatility. They employed a student-t copula framework for the conditional dependence structure, facilitating separation of volatility and correlation for high-dimensional estimation. In a similar pursuit of scalability, D'Innocenzo and Lucas (2024) developed a recursive framework of bivariate partial correlation models, which uses stochastic recurrence equations to estimate partial correlations from bivariate slices, allowing for flexible restrictions. For tail risk modelling, D'Innocenzo et al. (2024) proposed a dynamic semiparametric framework based on the Generalized Pareto Distribution, capable of capturing time-varying tail shape and scale parameters, essential for evaluating market risk measures like VaR and ES. Addressing asymmetric risk transmission, Tiwari et al. (2024) explored the

spillover effects between clean and dirty energy markets, revealing significant asymmetries using time-varying and frequency-domain methods. Finally, Zheng and Ye (2024) introduced a Cholesky-based generalized autoregressive score model for large-dimensional covariance matrices, leveraging score-driven updates resembling GARCH and stochastic volatility models to ensure computational feasibility. Their method also incorporates dynamic model averaging to handle model and parameter uncertainty in high-dimensional cases. Together, these contributions enhance our understanding of dynamic dependencies, risk modelling, and high-dimensional estimation in financial econometrics.

We contribute to the existing literature by developing an asymmetric Student-t framework for modelling time-varying correlation based on the GAS framework. As argued by Creal et al. (2013), the effective way for choosing time-varying parameters is introducing a score function as a driving mechanism. This approach enables us not only to capture the first or second-order moments, but the complete density structure, and it further allows us to examine tail dependence, which is significant in understanding extreme events such as market crashes or surges. By modelling extreme events jointly, one can assess how cryptocurrencies and stock indices behave under stress conditions, and understanding the complex relationship between cryptocurrencies and traditional financial assets offers insights for portfolio management and risk assessment. Our approach is further designed to overcome the limitations of traditional models by offering a more flexible and accurate representation of financial series since it captures time-varying skewness, heavy tails, and volatility clustering, features commonly observed in financial markets. In contrast to other methods in the literature, for instance, the copula models excel in modelling dependence structures but may lack flexibility in dynamic environments, multivariate GARCH models effectively model volatility clustering but struggle with skewness and tail risk. The GAS-based models are adaptive in nature and often deliver superior performance with less computational complexity.

We also introduce explanatory variables in the model specification to examine their impact on the time-varying correlation between our considered pairs. The correlations between cryptocurrencies and other financial variables can have implications for monetary policy and financial stability therefore: our GAS-based approach can help policymakers to better understand the interconnectedness of these markets and formulate appropriate policies. Our results underscore exogenous variables' significance in

tracking time-varying correlations.

The rest of the paper is organized as follows: Section 5.2 introduces the methodology, covering the asymmetric Student-t case first and then exploring the Student-t, normal, and asymmetric normal cases as special instances. In Section 5.3, we conduct an extensive simulation study to assess the good finite sample properties of the proposed estimator. Section 5.4 shows an empirical analysis where the model is employed on real data (Bitcoin, Ripple, S&P 500 index, NASDAQ index, VIX index, and WTI crude oil). Section 5.5 concludes the paper.

5.2 Methodology

Let $y_{1,t}$ and $y_{2,t}$ be the log returns, i.e., changes in the log prices, at time t, $t = 1, \dots, T$, of two assets. Building upon the DCC model proposed by Engle (2002), our approach involves a two-stage process. Initially, we separately model the mean and variances of asset returns using ARMA-GARCH models (Engle and Bollerslev, 1986). In the second stage, we focus on the marginal standardized residuals, namely:

$$\eta_{i,t} = \frac{\hat{u}_{i,t}}{\hat{\sigma}_{i,t}} \quad i = 1, 2,$$

where $\hat{u}_{i,t}$ are the residuals in the mean equation and $\hat{\sigma}_{i,t}$ are the volatilities from the estimated GARCH model for asset i.

Given a bivariate distribution $f(\eta_{1,t}, \eta_{2,t}; \rho_t)$ for the pair $(\eta_{1,t}, \eta_{2,t})$, depending on a time-varying correlation parameter ρ_t, we assume that ρ_t is modelled via a GAS(1,1) model (Creal et al., 2013)

$$\rho_t = \Omega + A s_{t-1} + B(\rho_{t-1} - \Omega) + D X_{t-1} \tag{5.1}$$

where $s_t = S_t \nabla_t$ is the scaled score of the log-likelihood. Here, $\nabla_t = \frac{\partial \ell_t}{\partial \rho_t}$ is the score, i.e., the partial derivative of the likelihood function with respect to ρ_t, S_t is a scaling matrix, and X_t is a vector of explanatory variables. Given the information matrix $\mathcal{I}_t = -\mathbb{E}_{t-1}\left[\frac{\partial^2 \ell_t}{\partial \rho_t \rho_t'}\right] = \mathbb{E}_{t-1}\left[\nabla_t \nabla_t'\right]$, the scaling matrix is typically constructed as $S_t = \mathcal{I}_t^{-k}$, with the exponent $k \in \{0, 1/2, 1\}$. In our model, we consider only the correlation coefficient to be time-varying. In particular, to ensure that ρ_t belongs to $(-1, 1)$, we consider the inverse hyperbolic tangent transformation $\delta_t = \operatorname{atanh}(\rho_t)$.

Hence, (5.1) becomes

$$\delta_t = \omega + as_{t-1} + b(\delta_{t-1} - \omega_\delta) + \gamma' X_{t-1} \tag{5.2}$$

where X_{t-1} denotes a vector of explanatory variables and $s_t = S_t \times \frac{\partial \ell_t}{\partial \delta_t}$. Note that

$$\frac{\partial \ell_t}{\partial \delta_t} = \frac{\partial \ell_t}{\partial \rho_t} \times \frac{\partial \rho_t}{\partial \delta_t} = \frac{\partial \ell_t}{\partial \rho_t} \times (1 - \rho_t^2). \tag{5.3}$$

Below, we present various analytical forms that the density f can be assumed, starting with the asymmetric Student-t distribution. The subsequent forms can be derived as special cases of this broader distribution. For each distribution, we present the scores. It is important to note that Fisher's information is available in closed form only for models without asymmetries.

5.2.1 Bivariate Asymmetric Student-t Model

The bivariate asymmetric Student-t is a four-parameter family, where, besides the parameter related to the correlation, the remaining parameters are ν, α_1 and α_2. The ν parameter is related to the thickness of the tails of the marginal distributions, whereas α_i is the asymmetry parameter for the i-th marginal, $i = 1, 2$.

In what follows, we use the notation

$$Q(\rho, u, v) = \frac{u^2 - 2\rho uv + v^2}{1 - \rho^2}. \tag{5.4}$$

Furthermore, we denote by $T(y; \nu)$ and $t(y; \nu)$ the cumulative distribution and density function of the Student-t random variable with ν degrees of freedom, respectively.

Following Azzalini (2005), the density of the asymmetric Student-t distribution is given by

$$\begin{aligned} f(\eta_{1,t}, \eta_{2,t}) = & \frac{b_1 b_2}{\pi\sqrt{1-\rho_t^2}} \left[1 + \frac{Q(\rho_t, x_{1,t}, x_{2,t})}{\nu}\right]^{-\frac{\nu+2}{2}} \\ & \times T\left((\alpha_1 x_{1,t} + \alpha_2 x_{2,t})\sqrt{\frac{\nu+2}{\nu + Q(\rho_t, x_{1,t}, x_{2,t})}}; \nu + 2\right) \end{aligned} \tag{5.5}$$

with

$$x_{i,t} = a_i \eta_{i,t} + b_i, \quad i = 1, 2$$

$$b_\nu = \sqrt{\frac{\nu}{\pi}} \frac{\Gamma\left(\frac{\nu-1}{2}\right)}{\Gamma\left(\frac{\nu}{2}\right)}$$

$$a_i = \delta_i b_\nu$$

$$b_i = \sqrt{\frac{\nu}{\nu-2} - a_i^2}$$

$$\alpha_*^2 = \alpha_1^2 + \alpha_2^2 + 2\rho_t \alpha_1 \alpha_2$$

$$\delta_1 = \frac{\alpha_1 + \rho_t \alpha_2}{\sqrt{1+\alpha_*^2}}$$

$$\delta_2 = \frac{\rho_t \alpha_1 + \alpha_2}{\sqrt{1+\alpha_*^2}}.$$

Note that the above density implies that $\mathbb{E}_{t-1}[\boldsymbol{\eta}_t] = 0$, $\mathbb{E}_{t-1}\left[\eta_{1,t}^2\right] = \mathbb{E}_{t-1}\left[\eta_{2,t}^2\right] = 1$. Note also that ρ_t does not coincide with the correlation at time t as

$$\mathrm{corr}_{t-1}(\eta_1, \eta_2) = \frac{\frac{\nu}{\nu-2}\rho_t - b_\nu^2 \delta_1 \delta_2}{b_1 b_2}.$$

The following result gives the score to be used in eq. (5.2)

Result 1. *The derivative of the log-likelihood with respect to ρ_t is*

$$\begin{aligned}\frac{\partial \ell_t}{\partial \rho_t} =& \frac{\rho_t}{1-\rho_t^2} + \frac{b_1'}{b_1} + \frac{b_2'}{b_2} - \frac{\nu+2}{2\nu} Q' \left[1 + \frac{Q}{\nu}\right]^{-1} \\ &+ \sqrt{\frac{\nu+2}{\nu+Q}} \left[\alpha_1 x_{1,t}' + \alpha_2 x_{2,t}' - \frac{1}{2}(\alpha_1 x_{1,t} + \alpha_2 x_{2,t}) \frac{Q'}{\nu+Q}\right] \\ &\frac{t\left((\alpha_1 x_{1,t} + \alpha_2 x_{2,t})\sqrt{\frac{\nu+2}{\nu+Q}}; \nu+2\right)}{T\left((\alpha_1 x_{1,t} + \alpha_2 x_{2,t})\sqrt{\frac{\nu+2}{\nu+Q}}; \nu+2\right)}\end{aligned} \tag{5.6}$$

where

$$\begin{aligned}
\delta_1' &= \frac{\alpha_2}{\sqrt{1+\alpha_*^2}} - \frac{\alpha_1\alpha_2\delta_1}{1+\alpha_*^2} \\
\delta_2' &= \frac{\alpha_1}{\sqrt{1+\alpha_*^2}} - \frac{\alpha_1\alpha_2\delta_2}{1+\alpha_*^2} \\
a_i' &= \delta_i' b_\nu \\
b_i' &= -a_i' \frac{a_i}{b_i} \\
x_{i,t}' &= a_i'\eta_{i,t} + b_i' \quad \textit{for } i = 1,2 \\
Q &= Q(\rho_t, x_{1,t}, x_{2,t}) \\
Q' &= 2\frac{x_{1,t}'x_{1,t} + x_{2,t}'x_{2,t} - x_{1,t}x_{2,t} - \rho_t(x_{1,t}'x_{2,t} + x_{1,t}x_{2,t}') + \rho_t Q}{1-\rho_t^2}
\end{aligned}$$

5.2.2 Bivariate Student-t Model

We consider the Student-t density, derived from (5.5) with the parameters $\alpha_1 = \alpha_2 = 0$, and expressed as

$$f(\eta_{1,t}, \eta_{2,t}) = \frac{\nu}{2\pi(\nu-2)\sqrt{1-\rho_t^2}} \left(1 + \frac{1}{\nu-2} Q(\rho_t, \eta_{1,t}, \eta_{2,t})\right)^{-\frac{\nu+2}{2}}. \tag{5.7}$$

Results 2 presents the score for this model.

Result 2. *The derivative of the log-likelihood with respect to ρ_t is*

$$\frac{\partial \ell_t}{\partial \rho_t} = \frac{\rho_t}{1-\rho_t^2} - \frac{\frac{\nu+2}{(\nu-2)(1-\rho_t^2)^2}\left[\rho_t(\eta_{1,t}^2+\eta_{2,t}^2) - (1+\rho_t^2)\eta_{1,t}\eta_{2,t}\right]}{1 + \frac{1}{(\nu-2)\left(1-\rho_t^2\right)}\left[\eta_{1,t}^2 - 2\rho_t\eta_{1,t}\eta_{2,t} + \eta_{2,t}^2\right]} \tag{5.8}$$

Furthermore

$$\mathbb{E}_{t-1}\left[\left(\frac{\partial \ell_t}{\partial \rho_t}\right)^2\right] = -\frac{\rho_t^2}{(1-\rho_t^2)^2} + \mathbb{E}_{t-1}[g(\boldsymbol{\eta}_t)^2] = -\frac{\rho_t^2}{(1-\rho_t^2)^2} + \frac{\nu+2}{\nu+4}\frac{1+2\rho_t^2}{(1-\rho_t^2)^2} \tag{5.9}$$

where

$$\begin{aligned}
g(\boldsymbol{\eta}_t) &= \frac{\nu+2}{(\nu-2)(1-\rho_t^2)^2} \frac{\left[\rho_t(\eta_{1,t}^2+\eta_{2,t}^2) - (1+\rho_t^2)\eta_{1,t}\eta_{2,t}\right]}{1 + \frac{1}{(\nu-2)\left(1-\rho_t^2\right)}\left[\eta_{1,t}^2 - 2\rho_t\eta_{1,t}\eta_{2,t} + \eta_{2,t}^2\right]} \\
\mathbb{E}_{t-1}[g(\boldsymbol{\eta}_t)] &= \frac{\rho_t}{1-\rho_t^2} \\
\mathbb{E}_{t-1}[g(\boldsymbol{\eta}_t)^2] &= \frac{\nu+2}{\nu+4}\frac{1+2\rho_t^2}{(1-\rho_t^2)^2}
\end{aligned}$$

Proof. See Appendix A.2.1. □

As expected, eq. (5.8) can also be obtained setting $\alpha_1 = \alpha_2 = 0$ in (5.6).

5.2.3 Bivariate Asymmetric Normal

The density we use for the bivariate asymmetric normal distribution (Azzalini, 2005) is

$$f(\eta_{1,t}, \eta_{2,t}) = \frac{b_1 b_2}{\pi\sqrt{1-\rho_t^2}} \exp\left(-\frac{1}{2}Q(\rho_t, x_{1,t}, x_{2,t})\right) \Phi\left(\alpha_1 x_{1,t} + \alpha_2 x_{2,t}\right). \tag{5.10}$$

with

$$\begin{aligned} x_{i,t} &= a_1\eta_{i,t} + b_i \\ a_i &= \delta_i\sqrt{\frac{2}{\pi}} \\ b_i &= \sqrt{1-a_i^2} \\ \alpha_*^2 &= \alpha_1^2 + \alpha_2^2 + 2\rho_t\alpha_1\alpha_2 \\ \delta_1 &= \frac{\alpha_1 + \rho_t\alpha_2}{\sqrt{1+\alpha_*^2}} \\ \delta_2 &= \frac{\rho_t\alpha_1 + \alpha_2}{\sqrt{1+\alpha_*^2}}, \end{aligned}$$

and with $\Phi(\cdot)$ being the standard normal cumulative distribution function. The above density can be obtained by letting $\nu \to \infty$ in (5.5). Note that it implies that $\mathbb{E}_{t-1}[\boldsymbol{\eta}_t] = 0$, $\mathbb{E}_{t-1}\left[\eta_{1,t}^2\right] = \mathbb{E}_{t-1}\left[\eta_{2,t}^2\right] = 1$. Note also that ρ_t does not coincide with the correlation at time t as

$$\operatorname{corr}_{t-1}(\eta_1, \eta_2) = \frac{\rho_t - \frac{2}{\pi}\delta_1\delta_2}{b_1 b_2}.$$

The score is derived in Results 3.

Result 3. *The derivative of the log-likelihood with respect to ρ_t is*

$$\frac{\partial \ell_t}{\partial \rho_t} = \frac{\rho_t}{1-\rho_t^2} + \frac{b_1'}{b_1} + \frac{b_2'}{b_2} - \frac{1}{2}Q' + (\alpha_1 x_{1,t}' + \alpha_2 x_{2,t}')\frac{\phi(\alpha_1 x_{1,t} + \alpha_2 x_{2,t})}{\Phi(\alpha_1 x_{1,t} + \alpha_2 x_{2,t})}$$

where

$$\delta_1' = \frac{\alpha_2}{\sqrt{1+\alpha_*^2}} - \frac{\alpha_1\alpha_2\delta_1}{1+\alpha_*^2}$$

$$\delta_2' = \frac{\alpha_1}{\sqrt{1+\alpha_*^2}} - \frac{\alpha_1\alpha_2\delta_2}{1+\alpha_*^2}$$

$$a_i' = \delta_i'\sqrt{\frac{2}{\pi}}$$

$$b_i' = -a_i'\frac{a_i}{b_i}$$

$$x_{i,t}' = a_i'\eta_{i,t} + b_i' \quad i = 1, 2$$

$$Q' = 2\frac{x_{1,t}'x_{1,t} + x_{2,t}'x_{2,t} - x_{1,t}x_{2,t} - \rho_t(x_{1,t}'x_{2,t} + x_{1,t}x_{2,t}') + \rho_t Q(\rho_t, x_{1,t}, x_{2,t})}{1-\rho_t^2}.$$

5.2.4 Bivariate normal

We derive the symmetric normal distribution by setting $\alpha_1 = \alpha_2 = 0$ in (5.10):

$$f(\eta_{1,t}, \eta_{2,t}) = \frac{1}{2\pi\sqrt{1-\rho_t^2}} \exp\left(-\frac{1}{2}Q(\rho_t, \eta_{1,t}, \eta_{2,t})\right). \tag{5.11}$$

The score is derived in Results 4 along with the Fisher information.

Result 4. *The derivative of the log-likelihood with respect to ρ_t is*

$$\frac{\partial \ell_t}{\partial \rho_t} = \frac{\rho_t}{1-\rho_t^2} - \frac{1}{(1-\rho_t^2)^2}\left[\rho_t(\eta_{1,t}^2 + \eta_{2,t}^2) - (1+\rho_t^2)\eta_{1,t}\eta_{2,t}\right] \tag{5.12}$$

Furthermore

$$\mathbb{E}_{t-1}\left[\left(\frac{\partial \ell_t}{\partial \rho_t}\right)^2\right] = \frac{1+\rho_t^2}{(1-\rho_t^2)^2}. \tag{5.13}$$

Proof. See Appendix A.2.2 □

5.3 Simulation Study

In this section, we conduct a comprehensive simulation study to assess the performance of our statistical model under varying parameter configurations. The model's key parameters are systematically explored to understand their impact on estimation accuracy. The considered parameter choices, based on values fitted on real data from diverse sources (equity, debt, crypto, utilities), are given in Table 5.1.

We examine a total of 81 parameter combinations, creating a robust exploration of the model's behavior. We simulate $T = 250$, 500, and $1,000$ observations for each

Parameter	Values
ω	$[-0.12, 0, 0.12]$
a	$[-0.03, 0, 0.03]$
b	0.95
α_1	$[-0.3, 0, 0.3]$
α_2	$[-0.8, 0.2, 1.2]$
ν	4

Table 5.1: Parameter values for the simulation study.

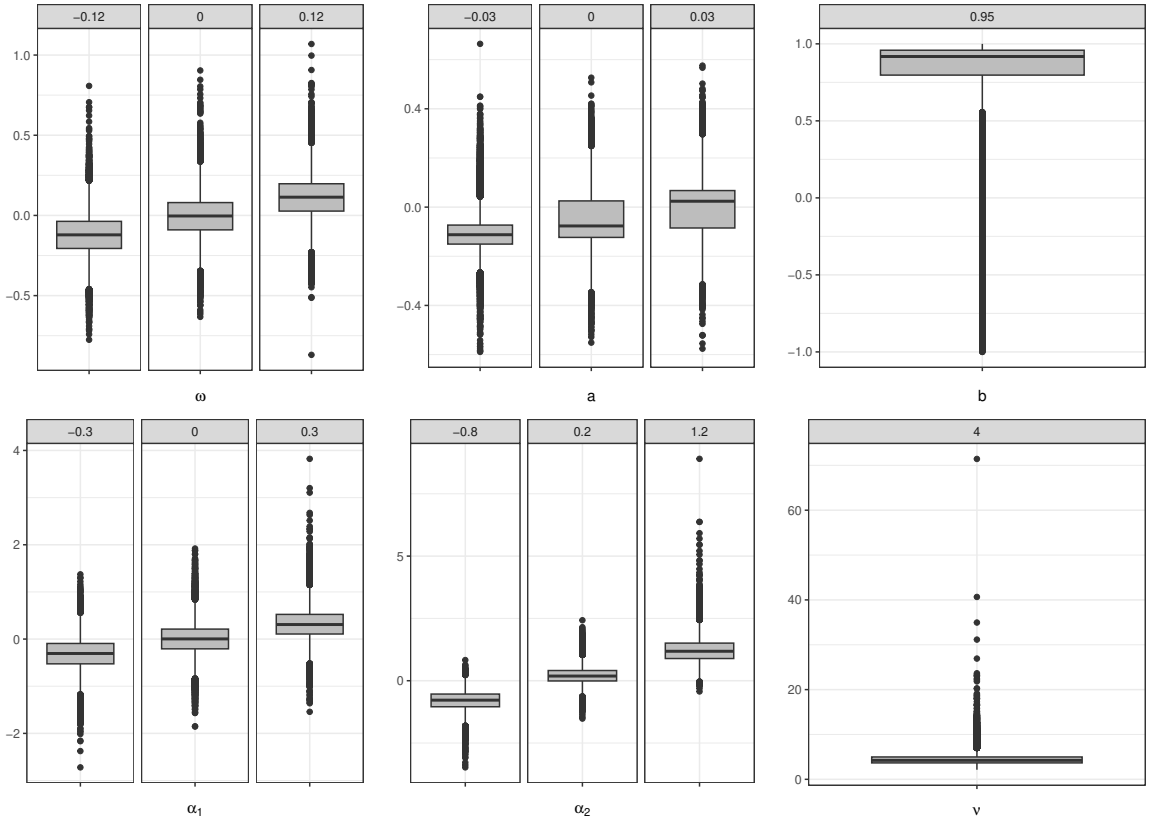

Figure 5.1: Boxplots illustrating simulation study results for $T = 250$, and across diverse parameter values.

combination. The primary objective of these simulations is to assess the convergence of the estimated parameters to their true values.

Figures 5.1, 5.2, and 5.3 show the results of the experiment. The outcomes demonstrate that the mean of the estimated values from simulated samples align with the true values in all scenarios. Estimates when T is low show higher variability, especially for ν.

Figure 5.4 illustrates the Root Mean Squared Errors (RMSE) across parameters for varying time periods T. The pattern is generally stable, with a notable decrease in RMSE for ν. The result of Figure 5.4 confirms the robustness of our estimation framework, even in datasets characterized by small sample sizes.

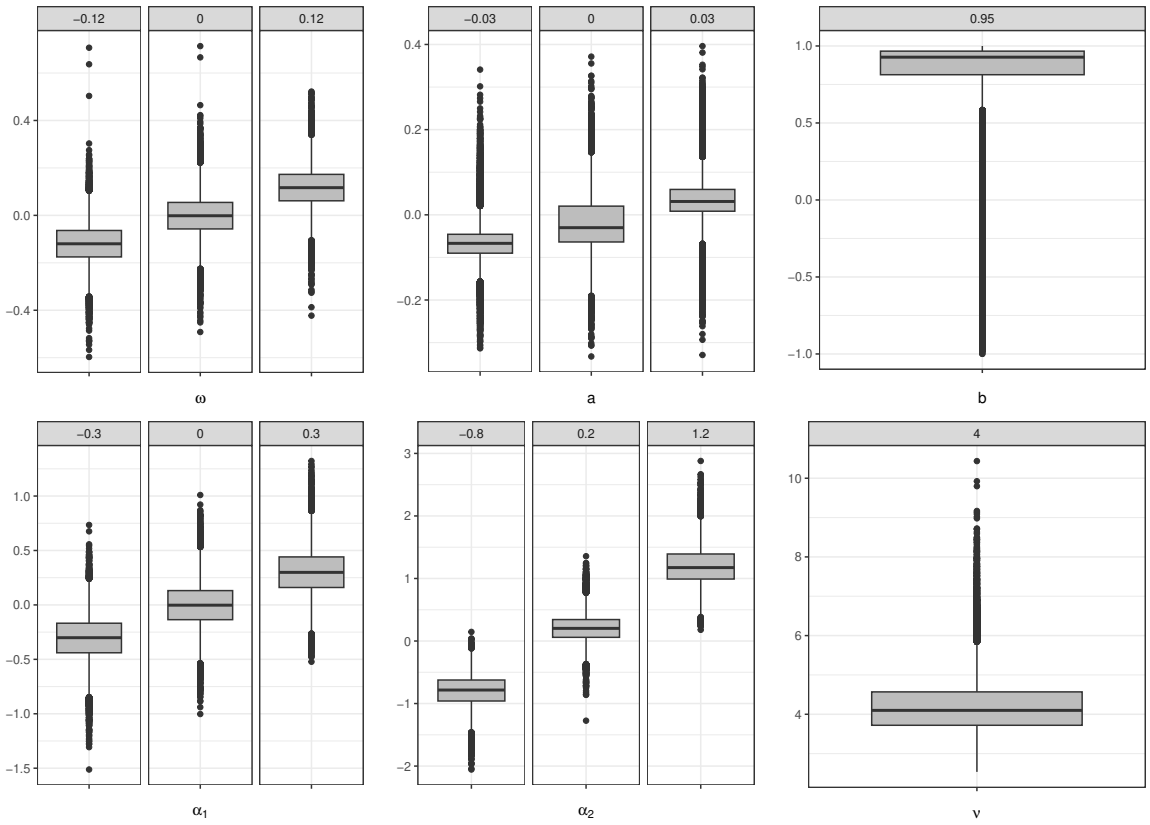

Figure 5.2: Boxplots illustrating simulation study results for $T = 500$, and across diverse parameter values.

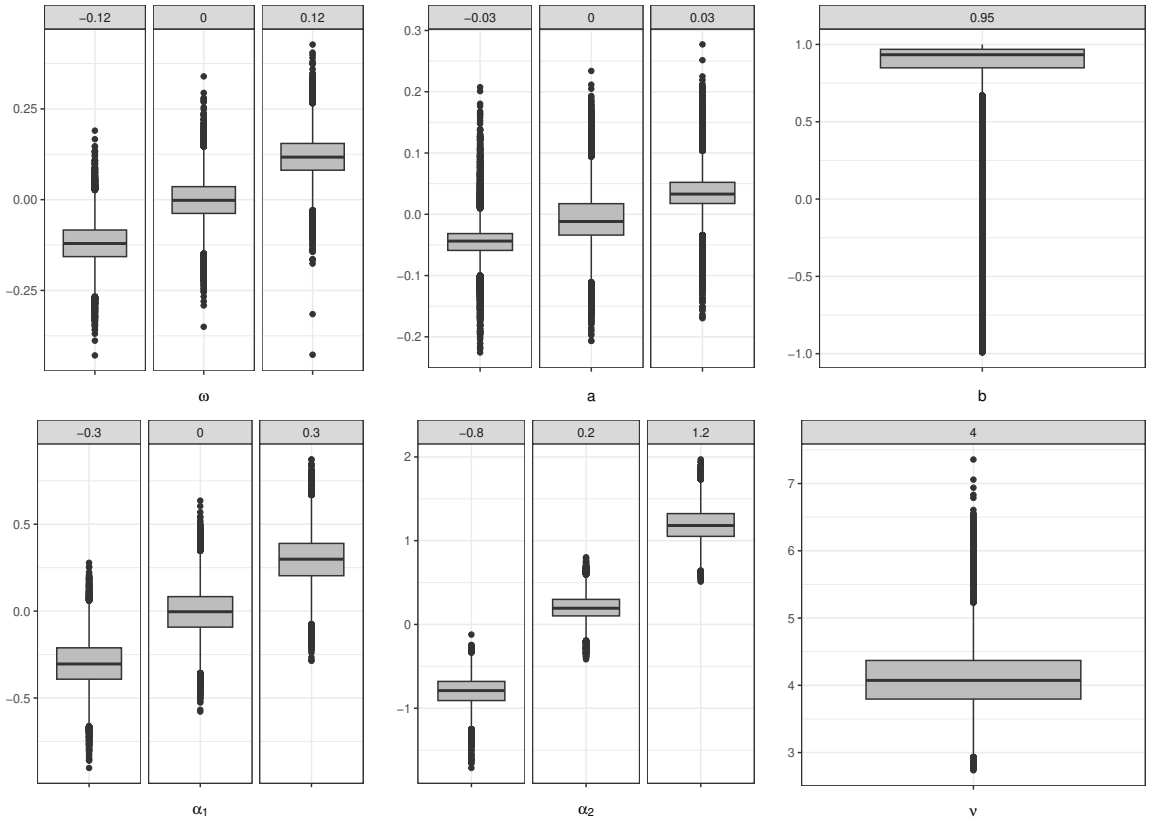

Figure 5.3: Boxplots illustrating simulation study results for $T = 1,000$, and across diverse parameter values.

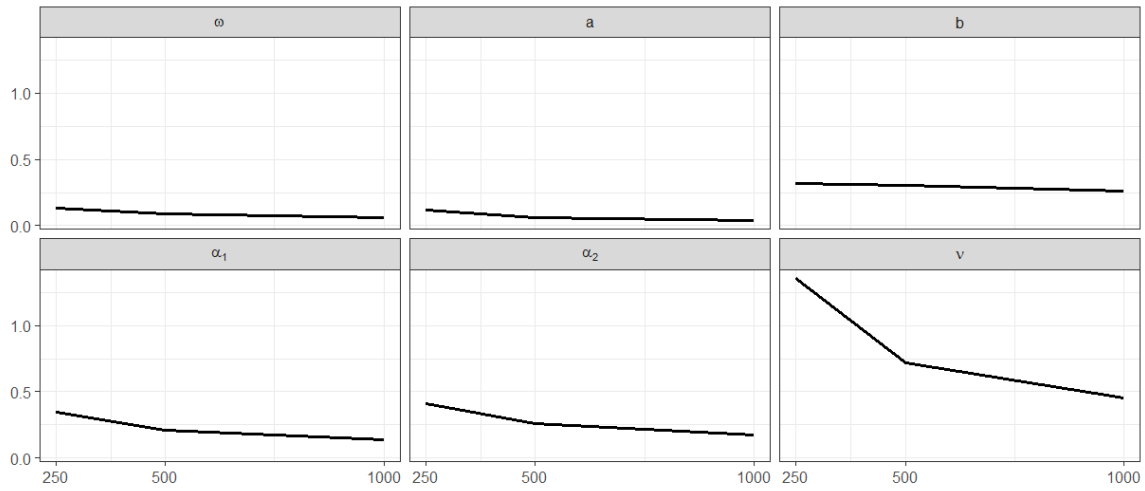

Figure 5.4: Root mean squared errors (RMSE) across different parameters and time periods $T = 250, 500, 1,000$.

5.4 Empirical Study

We consider data for Bitcoin (BTC), Ripple (XRP), S&P 500 index (S&P 500), NASDAQ index (NASDAQ), CBOE Volatility Index (VIX), West Texas Intermediate Crude Oil (WTI), Gold (Gold), Market Yield on U.S. Treasury Securities at 10-Year Constant Maturity (DGS10), 10-Year Treasury Constant Maturity Minus 3-Month Treasury Constant Maturity (T10Y3M), and 10-Year Breakeven Inflation Rate (T10YIE). We take BTC, XRP, S&P 500, NASDAQ, VIX, and WTI as the correlation variables and use Gold, DGS10, T10Y3M, and T10YIE as explanatory variables. Data covers a period going from 7 August 2015 to 7 December 2023, for a total of 2050 observations per series.

5.4.1 Model Estimation

In our analysis, we scrutinize eight sets of correlation variables and delve into the dynamic correlations between cryptocurrency and financial markets. Our focus lies in comparing how these correlations evolve across different pairs of cryptocurrency and financial market data. In particular, we consider pairs as given in Table 5.2.

We adopted the Log-Likelihood, the Akaike Information Criterion (AIC) (Akaike, 1974), and the Bayesian Information Criterion (BIC) (Schwarz, 1978) to ascertain our models performance[1]. Also, based on the significance of the estimated parameters,

[1]The AIC and BIC are popular criteria for model selection in statistical and econometric analysis, balancing goodness-of-fit against model complexity. The AIC penalizes models with more parameters

Table 5.2: Variables pairs (y_1, y_2) for which the dynamic correlation is computed

Pairs	Description
(BTC, S&P500)	Bitcoin and S&P 500 Index
(XRP, S&P500)	Ripple and S&P 500 Index
(BTC, NASDAQ)	Bitcoin and Nasdaq Index
(XRP, NASDAQ)	Ripple and Nasdaq Index
(BTC, VIX)	Bitcoin and CBOE Volatility Index (VIX)
(XRP, VIX)	Ripple and CBOE Volatility Index (VIX)
(BTC, WTI)	Bitcoin and Crude Oil WTI Futures
(XRP, WTI)	Ripple and Crude Oil WTI Futures

we can determine if our model captures relevant features regarding the data. Results in Table 5.3, 5.4, 5.5, and 5.6 show that the asymmetric Student-t model is our preferred choice in the modeling correlation dynamic for pairs BTC-SP500, XRP-SP500, BTC-NASDAQ, XRP-NASDAQ, BTC-VIX, XRP-VIX, BTC-WTI, XRP-WTI, as it provides the lowest AIC and BIC values. Accounting for asymmetry and heavy tails in modeling the relationship between cryptocurrency and financial market data provides the best fit, as our model choice captures these features effectively. In fact, the skewness and kurtosis parameters are statistically significant at the 1% confidence level.

Figure 5.5 shows the time-varying correlation between BTC and other explanatory variables, estimated using the asymmetric Student-t model. We observe that since 2020, the correlations between BTC and the S&P 500, as well as BTC and NASDAQ, show a higher positive trend. In contrast, the correlation between BTC and WTI displays a negative trend. The correlation between BTC and VIX remains relatively stable around zero. Figure 5.6 shows the time-varying correlation for XRP, which follows a similar pattern.

Relying on the definition of Baur and Lucey (2010), uncorrelated or negatively correlated assets hedge each other, and a safe haven asset is uncorrelated or negatively correlated with other assets (stocks and bonds) when the markets are in distress. From this, we can conclude that cryptocurrencies (BTC and XRP) can serve as a hedge and a safe haven for WTI and VIX, respectively, due to their negative and zero correlations, especially during the 2020 COVID-19 pandemic. Our results align with previous studies

to reduce overfitting and is often favored for predictive purposes. In contrast, the BIC imposes a stronger penalty, especially with larger datasets, making it more conservative and typically preferred when simpler, more interpretable models are desired. Both criteria aim to avoid overfitting, with the AIC focusing on improving predictive performance, while the BIC emphasizes model parsimony and consistency. Although AIC tends to deliver better predictive accuracy, BIC, grounded in Bayesian theory, is more likely to identify the true model as the sample size grows. A lower value of either criterion suggests a better model, and we use both as a robustness check.

Table 5.3: Parameter estimates for the bivariate models fitted on the pairs BTC-S&P500 (Panel A) and XRP-S&P500 (Panel B), comparing Normal, Student-t, Asymmetric Normal, and Asymmetric Student-t distributions. The table includes estimates for the degrees of freedom (ν), asymmetry parameters (α_1, α_2), and other model parameters (ω, a, b), along with log-likelihood (LogLik), AIC, and BIC values.

	Normal	Student-t	Asymmetric Normal	Asymmetric Student-t
Panel A: (BTC, S&P500)				
ν	-	4.4332 ***	-	4.5571 ***
	-	(0.2159)	-	(0.2357)
α_1	-	-	-0.9206 ***	-0.0598
	-	-	(0.1950)	(0.1145)
α_2	-	-	-1.0431 ***	-0.4110 ***
	-	-	(0.3009)	(0.1208)
ω	0.0925	0.0318	0.3207 **	0.0565
	(0.0864)	(0.1439)	(0.1308)	(0.1479)
a	0.0121 ***	0.0165 ***	0.0130 ***	0.0178 ***
	(0.0037)	(0.0059)	(0.0038)	(0.0064)
b	0.9972 ***	0.9976 ***	0.9985 ***	0.9974 ***
	(0.0021)	(0.0031)	(0.0017)	(0.0032)
LogLik	-5758.5180	-5461.9997	-5707.4198	-5454.6774
AIC	11523.0359	10931.9993	11424.8396	10921.3548
BIC	11539.9127	10954.5017	11452.9675	10955.1084
Panel B: (XRP, S&P500)				
ν	-	3.9375 ***	-	3.9906 ***
	-	(0.1479)	-	(0.1544)
α_1	-	-	1.1639 ***	0.0536
	-	-	(0.0818)	(0.1022)
α_2	-	-	-0.1598 *	-0.2685 ***
	-	-	(0.0949)	(0.1018)
ω	0.1232 **	0.1389 **	0.0873	0.1345 **
	(0.0524)	(0.0628)	(0.0769)	(0.0661)
a	0.0150 ***	0.0144 *	0.0242 ***	0.0152 *
	(0.0058)	(0.0076)	(0.0093)	(0.0078)
b	0.9884 ***	0.9931 ***	0.9885 ***	0.9931 ***
	(0.0066)	(0.0074)	(0.0064)	(0.0074)
LogLik	-5774.5301	-5374.1334	-5739.3562	-5370.1770
AIC	11555.0602	10756.2668	11488.7124	10752.3539
BIC	11571.9370	10778.7691	11516.8403	10786.1075

Note: * 10%, ** 5%, and *** 1% significance levels

(Oosterlinck et al., 2023; Lawuobahsumo et al., 2022; Kumah and Odei-Mensah, 2022; Shen, 2022; Conlon and McGee, 2020; Kim et al., 2020; Guesmi et al., 2019; Klein et al., 2018; Selmi et al., 2018; Bouri et al., 2017), confirming that BTC and XRP cannot serve as a hedge or safe haven for the stock market. In fact, they show a positive correlation with the S&P 500 and NASDAQ indices, which has become more pronounced during the COVID-19 pandemic. This contrasts with the findings of Tiwari et al. (2019); Wang et al. (2019); Corbet et al. (2018); Demir et al. (2018); Dyhrberg (2016).

5.4.2 The Impact of Explanatory Variables on Correlations

To investigate the influence of external factors on the correlation between cryptocurrency markets and traditional assets, we include interest rates (DGS10), market expectations (T10Y3M), expected inflation (T10YIE) and gold, as explanatory variables. These variables enter the models since they have a significant economic role, and they likely influence the correlation structure between assets by altering market expectations, risk perceptions, and macroeconomic fundamentals (Polizu et al., 2023; Şarkaya İçellioğlu and Öner, 2019; Dyhrberg, 2016). For instance, when interest rates change,

Table 5.4: Parameter estimates for the bivariate models fitted on the pairs BTC-NASDAQ (Panel A) and XRP-NASDAQ (Panel B), comparing Normal, Student-t, Asymmetric Normal, and Asymmetric Student-t distributions. The table includes estimates for the degrees of freedom (ν), asymmetry parameters (α_1, α_2), and other model parameters (ω, a, b), along with log-likelihood (LogLik), AIC, and BIC values.

	Normal	Student-t	Asymmetric Normal	Asymmetric Student-t
Panel A: (BTC, NASDAQ)				
ν	-	4.5494 ***	-	4.6963 ***
	-	(0.2361)	-	(0.2716)
α_1	-	-	-0.7642 **	-0.0151
	-	-	(0.3392)	(0.1129)
α_2	-	-	-1.2605 **	-0.6354 ***
	-	-	(0.5042)	(0.1194)
ω	0.1024	0.0413	0.3359 ***	0.0671
	(0.0987)	(0.1502)	(0.1129)	(0.1514)
a	0.0128 ***	0.0162 ***	0.0149 ***	0.0191 ***
	(0.0035)	(0.0052)	(0.0045)	(0.0062)
b	0.9973 ***	0.9979 ***	0.9983 ***	0.9978 ***
	(0.0022)	(0.0025)	(0.0019)	(0.0030)
LogLik	-5746.2173	-5470.4683	-5697.7899	-5454.9885
AIC	11498.4346	10948.9366	11405.5798	10921.9771
BIC	11515.3114	10971.4390	11433.7078	10955.7307
Panel B: (XRP, NASDAQ)				
ν	-	4.0616 ***	-	4.1324 ***
	-	(0.1636)	-	(0.1867)
α_1	-	-	1.1738 ***	0.0979
	-	-	(0.0836)	(0.0981)
α_2	-	-	-0.1949 *	-0.5083 ***
	-	-	(0.1059)	(0.1085)
ω	0.1427 ***	0.1486 **	0.1003	0.1354 *
	(0.0539)	(0.0660)	(0.0782)	(0.0709)
a	0.0156 ***	0.0131 *	0.0254 ***	0.0154 *
	(0.0056)	(0.0069)	(0.0098)	(0.0080)
b	0.9889 ***	0.9941 ***	0.9890 ***	0.9939 ***
	(0.0062)	(0.0061)	(0.0071)	(0.0063)
LogLik	-5770.9193	-5396.2515	-5735.2131	-5383.3826
AIC	11547.8385	10800.5029	11480.4263	10778.7652
BIC	11564.7153	10823.0053	11508.5542	10812.5187

Note: * 10%, ** 5%, and *** 1% significance levels

the global economy and financial markets, including bonds, stocks, commodities and crypto, are affected. Indeed, high interest rates lessen the appetite for assets with higher risk and higher returns, while low interest rates increase the appetite for the same types of risky assets (Polizu et al., 2023). More in detail, DGS10, as a benchmark for interest rates, influences borrowing costs within the financial system. Higher yields indicate tighter monetary policy, which may reduce the availability of cheap credit and slow economic growth, whereas lower yields can spur growth by encouraging investment and consumption. As a reflection of the opportunity cost of holding riskier assets versus risk-free government bonds, when interest rates rise, bond yields become more attractive, which can reduce demand for riskier assets, resulting in negative correlations between bonds and assets like equities or cryptocurrencies. Conversely, falling yields make riskier investments more attractive as they promise higher returns, altering their correlation with bond prices. Additionally, rising yields often signal expectations of higher inflation or economic growth, which could also impact assets that are sensitive to economic cycles or inflation protection such as cryptocurrency (Bernanke, 1990; Fama and French, 1989; Fama, 1981).

Table 5.5: Parameter estimates for the bivariate models fitted on the pairs BTC-VIX (Panel A) and XRP-VIX (Panel B), comparing Normal, Student-t, Asymmetric Normal, and Asymmetric Student-t distributions. The table includes estimates for the degrees of freedom (ν), asymmetry parameters (α_1, α_2), and other model parameters (ω, a, b), along with log-likelihood (LogLik), AIC, and BIC values.

	Normal	Student-t	Asymmetric Normal	Asymmetric Student-t
Panel A: (BTC, VIX)				
ν	-	4.7397 ***	-	4.7762 ***
	-	(0.2487)	-	(0.2491)
α_1	-	-	-1.2765 ***	-0.1801
	-	-	(0.0972)	(0.1117)
α_2	-	-	-0.1514	-0.7243 ***
	-	-	(0.1565)	(0.1317)
ω	0.0524	0.0544 *	0.1380	0.1159 **
	(0.0337)	(0.0300)	(0.0847)	(0.0468)
a	0.0031	0.0070	0.0032	0.0101
	(0.0048)	(0.0081)	(0.0045)	(0.0110)
b	0.9930 ***	0.9755 ***	0.9958 ***	0.9735 ***
	(0.0202)	(0.0387)	(0.0066)	(0.0336)
LogLik	-5818.1159	-5535.7538	-5777.3546	-5516.1544
AIC	11642.2317	11079.5076	11564.7092	11044.3088
BIC	11659.1085	11102.0100	11592.8372	11078.0624
Panel B: (XRP, VIX)				
ν	-	4.0413 ***	-	4.0483 ***
	-	(0.1550)	-	(0.1577)
α_1	-	-	1.1398 ***	0.1025
	-	-	(0.0808)	(0.0967)
α_2	-	-	-0.0436	-0.5467 ***
	-	-	(0.0881)	(0.1067)
ω	0.0432 ***	0.0309	0.0339	0.0085
	(0.0167)	(0.0249)	(0.0452)	(0.0341)
a	-0.0253 *	-0.0239	-0.0391 *	-0.0262
	(0.0146)	(0.0222)	(0.0215)	(0.0288)
b	0.8760 ***	0.6590 ***	0.8774 ***	0.6471 *
	(0.0616)	(0.2427)	(0.0609)	(0.3450)
LogLik	-5812.8406	-5418.3112	-5779.1994	-5402.9669
AIC	11631.6812	10844.6224	11568.3988	10817.9338
BIC	11648.5579	10867.1248	11596.5268	10851.6874

Note: * 10%, ** 5%, and *** 1% significance levels

The difference between the yields on the 10-year Treasury Constant Maturity and the 3-month Treasury Constant Maturity can be considered a gauge of economic expectations. In particular, a negative difference between the two yields has historically been a signal of an incoming recession and gloomy economic perspectives (Park, 2022; Estrella and Mishkin, 1998; Estrella and Hardouvelis, 1991). These unfavourable market conditions tend to reduce investors' appetite towards higher-risk assets, such as cryptocurrencies. Put differently, a steepening yield curve suggests stronger economic growth expectations, while a flattening or inverted yield curve is a precursor to an economic slowdown or recession. An inverted yield curve (short-term rates are higher than long-term rates) causes correlations between risky assets (like cryptocurrencies, equities, or commodities) to increase as all markets adjust to higher perceived risks. Conversely, during periods of steepening, correlations may shift as different assets react to positive growth expectations in varying ways (Bekaert and Engstrom, 2010; Ang et al., 2008).

The 10-year Breakeven Inflation Rate reflects the operator's expectations of future inflation, particularly what market participants expect inflation to be in the next 10

Table 5.6: Parameter estimates for the bivariate models fitted on the pairs BTC-WTI (Panel A) and XRP-WTI (Panel B), comparing Normal, Student-t, Asymmetric Normal, and Asymmetric Student-t distributions. The table includes estimates for the degrees of freedom (ν), asymmetry parameters (α_1, α_2), and other model parameters (ω, a, b), along with log-likelihood (LogLik), AIC, and BIC values.

	Normal	Student-t	Asymmetric Normal	Asymmetric Student-t
Panel A: (BTC, WTI)				
ν	-	3.9191 ***	-	4.0983 ***
	-	(0.1454)	-	(0.1656)
α_1	-	-	-0.0705	-0.0379
	-	-	(0.1236)	(0.0785)
α_2	-	-	2.5309 ***	1.1691 ***
	-	-	(0.1649)	(0.1407)
ω	-0.1457	-0.0750	-0.2379	-0.1380
	(0.1054)	(0.1457)	(0.1451)	(0.1456)
a	0.0112 ***	0.0190 **	0.0219 ***	0.0283 ***
	(0.0037)	(0.0075)	(0.0077)	(0.0105)
b	0.9976 ***	0.9968 ***	0.9976 ***	0.9960 ***
	(0.0023)	(0.0041)	(0.0022)	(0.0043)
LogLik	-5762.9108	-5349.8262	-5640.6314	-5299.0091
AIC	11531.8216	10707.6524	11291.2629	10610.0183
BIC	11548.6983	10730.1548	11319.3908	10643.7718
Panel B: (XRP, WTI)				
ν	-	3.5480 ***	-	3.6650 ***
	-	(0.1078)	-	(0.1207)
α_1	-	-	-0.1060	0.0501
	-	-	(0.0721)	(0.0753)
α_2	-	-	2.5372 ***	0.9579 ***
	-	-	(0.1607)	(0.1246)
ω	-0.1254 **	-0.1457 *	-0.2289 ***	-0.1567
	(0.0502)	(0.0831)	(0.0760)	(0.1013)
a	0.0139 **	0.0132 *	0.0286 **	0.0180 **
	(0.0063)	(0.0068)	(0.0129)	(0.0088)
b	0.9872 ***	0.9962 ***	0.9869 ***	0.9961 ***
	(0.0074)	(0.0044)	(0.0076)	(0.0044)
LogLik	-5780.4252	-5250.7161	-5657.1225	-5206.6176
AIC	11566.8504	10509.4322	11324.2449	10425.2352
BIC	11583.7272	10531.9346	11352.3729	10458.9887

Note: * 10%, ** 5%, and *** 1% significance levels

years, on average. With higher expectations of increasing prices, investors look for assets that represent an alternative way of preserving purchasing power to anticipate higher inflation in the future (Polizu et al., 2023; Orlowski and Soper, 2019). This shift can cause correlations between different asset classes to change. Higher inflation expectation reduces the real value of risk-free returns, leading to changes in the demand for riskier assets, including cryptocurrencies, which may be perceived by some as inflation hedges due to their decentralized nature (Ang et al., 2006; Estrella and Mishkin, 1996).

Gold has been considered a traditional inflation hedge and has always played the role of currency and store of value (Bedowska-Sójka and Kliber, 2021; Baur and Lucey, 2010). Explicitly, during periods of economic uncertainty, financial instability, or market stress, gold protects market participants against market volatility and currency devaluation; also, due to its intrinsic value nature, it is considered an effective hedge against inflation. Gold's correlation with risky assets such as cryptocurrencies typically becomes more negative during market downturns as investors shift into safe-haven assets. When inflation is high, the value of gold tends to increase, resulting in changing correlations with inflation-sensitive assets (Beckmann and Czudaj, 2013).

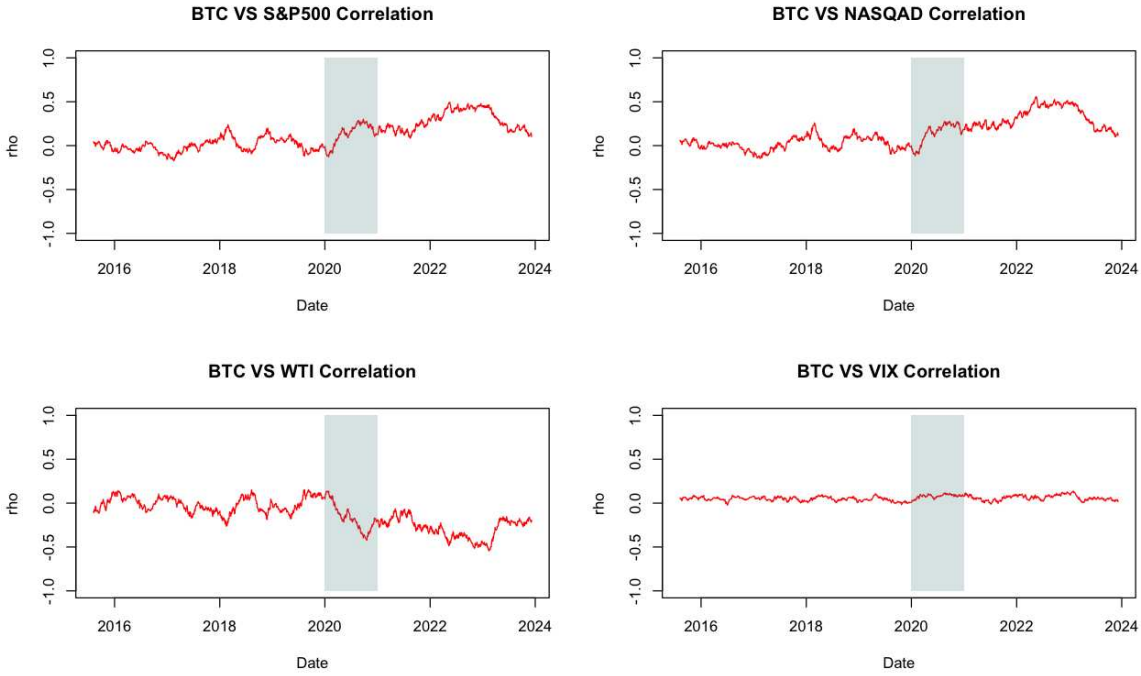

Figure 5.5: Asymmetric Student-t model Time Varying correlations Plots without Explanatory Variables for BTC-S&P 500, BTC-NASDAQ, BTC-WTI and BTC-VIX

Our approach allows for a fast and efficient assessment of the impact of the aforementioned variables on the correlation between the two assets.

Table 5.7 evaluates the significance of each explanatory variable on the correlations between BTC and S&P 500 and between XRP and S&P 500. The Student$-t$ and asymmetric Student$-t$ models outperform the Normal and asymmetric Normal models, both show lower AIC and BIC.

The coefficient for Gold is positive and significant at the 10% level for the pair BTC and S&P 500. In Panel A of Table 5.7, we show that Gold positively impacts the correlation between BTC and the S&P 500. Specifically, a unit increase in Gold returns leads to a 3.0496 unit increase in the inverse hyperbolic tangent correlation for the Student-t model and a 3.2294 unit increase for the asymmetric Student-t model.

In Panel B of Table 5.7, for the correlation between XRP and the S&P 500, Gold is significant for all models. It has positive coefficients with a 1% significance for the Normal and asymmetric Normal models, 10% for the Student-t model, and 5% for the asymmetric Student-t model. A unit increase in Gold results in a 3.0496 unit increase in the inverse hyperbolic tangent correlation for the Student-t model and a 3.2294 unit increase for the asymmetric Student-t model. Additionally, DGS10 is significant for the Normal and asymmetric Normal models at the 10% confidence level, indicating

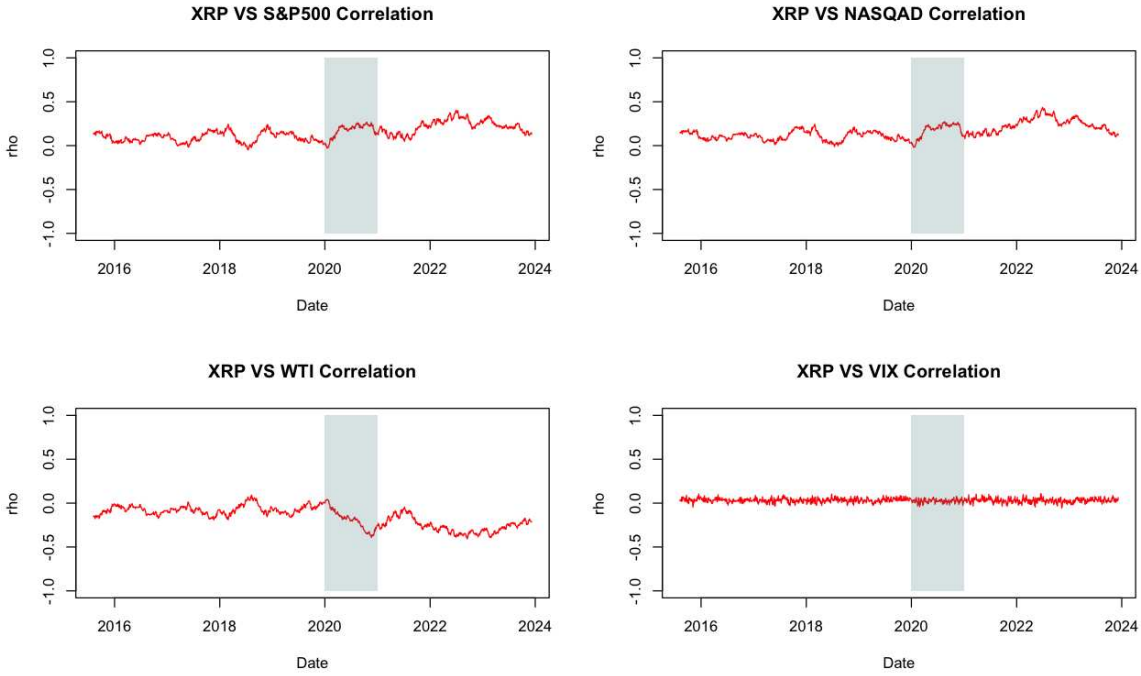

Figure 5.6: Asymmetric Student-t model Time Varying correlations Plots without Explanatory Variables for XRP-S&P 500, XRP-NASDAQ, XRP-WTI and XRP-VIX

that a 1% increase in DGS10 will increase the inverse hyperbolic tangent correlation by 40.51%.

Table 5.8 evaluates the significance of each explanatory variable on BTC and XRP against NASDAQ correlations. In Panel A and Panel B of Table 5.8, we show that the Student$-t$ and asymmetric Student$-t$ models are the preferred choices. None of the selected explanatory variables significantly impact the correlation between BTC and NASDAQ correlation. Panel B of Table 5.8 shows that Gold is significant at a 5% level for all models and that positively impacts the XRP-NASDAQ correlation. In particular, a unit increase in Gold causes a 2.4224, 2.1043, 2.9805, and 2.2713 units increase in the inverse hyperbolic tangent correlation between XRP and the NASDAQ for the Normal, asymmetric Normal, Student$-t$ and asymmetric Student$-t$ models, respectively. We also observed that DGS10 positively impacts the correlation between XRP and the NASDAQ at a 10% significance level for the asymmetric Normal model, with a 1% increase resulting in 35.91% increase in the inverse hyperbolic tangent correlation.

In Table 5.9, we show results of the models fitted considering WTI as explanatory variable for the same pairs of assets considered before. The Student$-t$ and asymmetric Student$-t$ models fit the data better than the Normal and asymmetric Normal. with lower AIC and BIC values and higher log-likelihoods. In Panel A of Table 5.9,

Table 5.7: Parameter estimates for the bivariate models with explanatory variables fitted on the pairs BTC-S&P 500 (Panel A) and XRP-S&P 500 (Panel B), comparing Normal, Student-t, Asymmetric Normal, and Asymmetric Student-t distributions. The table includes estimates for the degrees of freedom (ν), asymmetry parameters (α_1, α_2), and other model parameters (ω, a, b), along with log-likelihood (LogLik), AIC, and BIC values.

	Normal	Student-t	Asymmetric Normal	Asymmetric Student-t
Panel A: (BTC, S&P500)				
ν	-	4.4419 ***	-	4.5641 ***
	-	(0.2271)	-	(0.2381)
α_1	-	-	-0.9220 ***	-0.0545
	-	-	(0.2183)	(0.1103)
α_2	-	-	-1.0267 ***	-0.4129 ***
	-	-	(0.3246)	(0.1206)
ω	0.0311	0.0452	0.2863 ***	0.0648
	(0.0713)	(0.0627)	(0.1018)	(0.0671)
a	0.0143 **	0.0261 **	0.0145 **	0.0287 **
	(0.0059)	(0.0123)	(0.0061)	(0.0135)
b	0.9921 ***	0.9810 ***	0.9955 ***	0.9796 ***
	(0.0079)	(0.0161)	(0.0050)	(0.0179)
ρ_{GOLD}	2.0794	3.0496 *	1.4236	3.2294 *
	(1.3081)	(1.6524)	(1.1271)	(1.6580)
ρ_{DGS10}	0.2931	0.5470	0.1870	0.5888
	(0.2276)	(0.3658)	(0.1803)	(0.4105)
ρ_{T10Y3M}	-0.0302	-0.1462	-0.0299	-0.1609
	(0.1157)	(0.2127)	(0.1113)	(0.2328)
ρ_{T10YIE}	-0.2540	-0.5656	-0.1107	-0.6168
	(0.2085)	(0.3783)	(0.1566)	(0.5065)
LogLik	-5755.5913	-5458.6567	-5706.0112	-5451.3256
AIC	11525.1826	10933.3134	11430.0224	10922.6512
BIC	11564.5618	10978.3182	11480.6528	10978.9071
Panel B: (XRP, S&P500)				
ν	-	3.9457 ***	-	3.9993 ***
	-	(0.1645)	-	(0.1552)
α_1	-	-	1.1613 ***	0.0550
	-	-	(0.0832)	(0.1022)
α_2	-	-	-0.1462	-0.2710 ***
	-	-	(0.0953)	(0.0969)
ω	0.0715	0.0968 *	0.0278	0.0910 *
	(0.0539)	(0.0496)	(0.0798)	(0.0507)
a	0.0155 **	0.0146 *	0.0246 **	0.0157 *
	(0.0067)	(0.0084)	(0.0101)	(0.0087)
b	0.9830 ***	0.9828 ***	0.9831 ***	0.9827 ***
	(0.0088)	(0.0133)	(0.0075)	(0.0124)
ρ_{GOLD}	2.7660 ***	2.2929 *	3.3897 ***	2.3608 **
	(0.9957)	(1.2298)	(1.2587)	(1.1225)
ρ_{DGS10}	0.3251 *	0.3485	0.4051 *	0.3610
	(0.1662)	(0.2498)	(0.2300)	(0.2229)
ρ_{T10Y3M}	-0.0186	-0.0412	-0.0358	-0.0426
	(0.1096)	(0.1336)	(0.1491)	(0.1265)
ρ_{T10YIE}	-0.2757	-0.3084	-0.3350	-0.3241
	(0.2083)	(0.3021)	(0.2440)	(0.2415)
LogLik	-5769.7005	-5370.8153	-5734.7300	-5366.8216
AIC	11553.4010	10757.6305	11487.4600	10753.6431
BIC	11592.7802	10802.6353	11538.0904	10809.8991

Note: The significance of each explanatory variable (Gold, DGS10, T10Y3M and T10YIE) coefficient is indicated with stars. * 10%, ** 5%, and *** 1% le

we show that Gold is significant at a 5% level for all models and negatively impacts the BTC and WTI correlation. In particular, a unit increase in Gold causes a 2.6100, 2.9660, 3.5025, and 3.4686 units decrease in the inverse hyperbolic tangent correlation between BTC and the WTI for the Normal, asymmetric Normal, Student$-t$ and asymmetric Student$-t$ models, respectively. DGS10 is significant at a 5% level for the Normal model, and a 10% level for the asymmetric Normal, Student$-t$, and asymmetric Student$-t$ models. DGS10 has a negative impact on BTC and WTI correlation, where a 1% increase in DSG10 causes a 36.70%, 56.21%, 45.70% and 67.16% decrease in the inverse hyperbolic tangent correlation between BTC and the WTI for the Normal, asymmetric Normal, Student$-t$ and asymmetric Student$-t$ models, respectively. Furthermore, the T10YIE is significant at 5% for the Normal and asymmetric models.

Table 5.8: Parameter estimates for the bivariate models with explanatory variables fitted on the pairs BTC-NASDAQ (Panel A) and XRP-NASDAQ (Panel B), comparing Normal, Student-t, Asymmetric Normal, and Asymmetric Student-t distributions. The table includes estimates for the degrees of freedom (ν), asymmetry parameters (α_1, α_2), and other model parameters (ω, a, b), along with log-likelihood (LogLik), AIC, and BIC values.

	Normal	Student-t	Asymmetric Normal	Asymmetric Student-t
Panel A: (BTC, NASDAQ)				
ν	-	4.5534 ***	-	4.6996 ***
	-	(0.2407)	-	(0.2589)
α_1	-	-	-0.5478 *	-0.0161
	-	-	(0.2872)	(0.1059)
α_2	-	-	-1.5252 ***	-0.6353 ***
	-	-	(0.3414)	(0.1224)
ω	0.0292	0.0052	0.2443 *	0.0276
	(0.0907)	(0.1205)	(0.1364)	(0.1341)
a	0.0133 ***	0.0175 **	0.0170 ***	0.0206 **
	(0.0044)	(0.0072)	(0.0062)	(0.0092)
b	0.9956 ***	0.9956 ***	0.9968 ***	0.9951 ***
	(0.0042)	(0.0075)	(0.0035)	(0.0071)
ρ_{GOLD}	1.3638	1.4850	1.2627	1.6118
	(0.9965)	(1.2520)	(1.1795)	(1.2343)
ρ_{DGS10}	0.1731	0.2169	0.1488	0.2408
	(0.1608)	(0.2145)	(0.1716)	(0.2205)
ρ_{T10Y3M}	0.0062	0.0553	0.0061	0.0557
	(0.0902)	(0.1502)	(0.0963)	(0.1537)
ρ_{T10YIE}	-0.1938	-0.3701	-0.1689	-0.4077
	(0.1447)	(0.2323)	(0.1804)	(0.2588)
LogLik	-5744.0306	-5468.1402	-5696.5973	-5452.6736
AIC	11502.0612	10952.2803	11411.1947	10925.3473
BIC	11541.4403	10997.2851	11461.8250	10981.6032
Panel B: (XRP, NASDAQ)				
ν	-	4.0651 ***	-	4.1355 ***
	-	(0.1683)	-	(0.1722)
α_1	-	-	1.1707 ***	0.0987
	-	-	(0.0839)	(0.1019)
α_2	-	-	-0.1791	-0.5104 ***
	-	-	(0.1117)	(0.1079)
ω	0.0844	0.1069 **	0.0317	0.0905
	(0.0576)	(0.0523)	(0.0845)	(0.0606)
a	0.0147 **	0.0131	0.0240 **	0.0155 *
	(0.0062)	(0.0090)	(0.0098)	(0.0084)
b	0.9865 ***	0.9859 ***	0.9863 ***	0.9855 ***
	(0.0088)	(0.0114)	(0.0068)	(0.0128)
ρ_{GOLD}	2.4224 **	2.1043 **	2.9805 **	2.2713 **
	(1.0166)	(1.0354)	(1.1828)	(1.1038)
ρ_{DGS10}	0.2824	0.3194	0.3591 *	0.3485
	(0.1861)	(0.2042)	(0.2098)	(0.2423)
ρ_{T10Y3M}	0.0087	0.0027	-0.0067	-0.0006
	(0.1392)	(0.1255)	(0.1443)	(0.1520)
ρ_{T10YIE}	-0.2812	-0.3866	-0.3420	-0.4228
	(0.1828)	(0.2764)	(0.2395)	(0.2656)
LogLik	-5766.5960	-5392.9277	-5731.1201	-5380.0065
AIC	11547.1919	10801.8554	11480.2401	10780.0130
BIC	11586.5711	10846.8601	11530.8705	10836.2689

Note: The significance of each explanatory variable (Gold, DGS10, T10Y3M and T10YIE) coefficient is indicated with stars. * 10%, ** 5%, and *** 1% le

Panel B of Table 5.9 shows results for the pair XRP-WTI. Gold, DSG10, and T10YIE are significant at a 1% level for the Normal and asymmetric Normal models. Results indicate that an increase in Gold and DGS10 returns causes a decrease in XRP-WTI correlation, while an increase in T10YIE increases in the XRP and WTI correlation. The coefficients for Student$-t$ and asymmetric Student$-t$ models are significant at 5% level for Gold.

Finally, we consider the impact of the explanatory variables on the correlation between the cryptocurrencies and the VIX, and we show results in Table 5.10. We do not observe a significant impact from the selected explanatory variables for the BTC-VIX correlation. Considering model performance, the asymmetric Student$-t$ model best fits the data. When considering XRP and the VIX, Gold and T10YIE are

Table 5.9: Parameter estimates for the bivariate models with explanatory variables fitted on the pairs BTC-WTI (Panel A) and XRP-WTI (Panel B), comparing Normal, Student-t, Asymmetric Normal, and Asymmetric Student-t distributions. The table includes estimates for the degrees of freedom (ν), asymmetry parameters (α_1, α_2), and other model parameters (ω, a, b), along with log-likelihood (LogLik), AIC, and BIC values.

	Normal	Student-t	Asymmetric Normal	Asymmetric Student-t
Panel A: (BTC, WTI)				
ν	-	3.9342 ***	-	4.1129 ***
	-	(0.1576)	-	(0.1779)
α_1	-	-	-0.1136	-0.0334
	-	-	(0.1121)	(0.0794)
α_2	-	-	2.5194 ***	1.1737 ***
	-	-	(0.1743)	(0.1463)
ω	-0.0388	-0.0512	-0.0867	-0.0837
	(0.0853)	(0.0638)	(0.1412)	(0.0793)
a	0.0119 **	0.0254 **	0.0218 *	0.0361 ***
	(0.0047)	(0.0099)	(0.0115)	(0.0135)
b	0.9935 ***	0.9834 ***	0.9945 ***	0.9826 ***
	(0.0050)	(0.0112)	(0.0052)	(0.0119)
ρ_{GOLD}	-2.6100 **	-2.9660 **	-3.5025 **	-3.4686 **
	(1.0294)	(1.3306)	(1.4633)	(1.6348)
ρ_{DGS10}	-0.3670 **	-0.5621 *	-0.4570 *	-0.6716 *
	(0.1759)	(0.3038)	(0.2386)	(0.3765)
ρ_{T10Y3M}	0.0126	0.1523	0.0012	0.1846
	(0.0819)	(0.1732)	(0.1171)	(0.2157)
ρ_{T10YIE}	0.3486 **	0.4328	0.4639 **	0.5502
	(0.1598)	(0.3273)	(0.2345)	(0.4185)
LogLik	-5755.9246	-5345.4034	-5633.5289	-5294.5868
AIC	11525.8492	10706.8068	11285.0578	10609.1737
BIC	11565.2283	10751.8116	11335.6882	10665.4296
Panel B: (XRP, WTI)				
ν	-	3.5552 ***	-	3.6732 ***
	-	(0.1108)	-	(0.1219)
α_1	-	-	-0.1075	0.0537
	-	-	(0.0793)	(0.0746)
α_2	-	-	2.5458 ***	0.9626 ***
	-	-	(0.1619)	(0.1381)
ω	-0.1703 ***	-0.0825	-0.2916 ***	-0.0847
	(0.0298)	(0.0583)	(0.0483)	(0.0708)
a	0.0517 ***	0.0136 *	0.1144 ***	0.0193 *
	(0.0098)	(0.0071)	(0.0268)	(0.0101)
b	0.8321 ***	0.9866 ***	0.8208 ***	0.9856 ***
	(0.0605)	(0.0132)	(0.0567)	(0.0145)
ρ_{GOLD}	-4.5435 ***	-2.5325 **	-6.9377 ***	-2.9712 **
	(1.5352)	(1.2208)	(2.1651)	(1.4937)
ρ_{DGS10}	-1.7973 ***	-0.4054	-2.7988 ***	-0.5034
	(0.6023)	(0.3267)	(0.8664)	(0.3774)
ρ_{T10Y3M}	0.3079	0.0520	0.7551	0.0696
	(0.4727)	(0.1385)	(0.7311)	(0.1641)
ρ_{T10YIE}	1.0650 ***	0.2657	1.6265 ***	0.3520
	(0.3494)	(0.3088)	(0.4848)	(0.3546)
LogLik	-5772.9531	-5246.3971	-5648.8003	-5202.2376
AIC	11559.9062	10508.7941	11315.6005	10424.4753
BIC	11599.2854	10553.7989	11366.2309	10480.7312

Note: The significance of each explanatory variable (Gold, DGS10, T10Y3M and T10YIE) coefficient is indicated with stars. * 10%, ** 5%, and *** 1% le

significant at a 10% level for the Normal and asymmetric Normal models. The DSG10 is significant at 10% level for the Normal model. The coefficients for Gold and DGS10 are positive, while those for T10YIE are negative.

Figures 5.7 and 5.8 plot the time-varying correlation between the BTC and S&P 500, NASDAQ, WTI and VIX, and XRP and S&P 500, NASDAQ, WTI and VIX considering the impact of explanatory variables. Compared to the plot for the time-varying correlation without explanatory variables, Figures 5.5 and 5.6 show higher correlation values, suggesting that these explanatory variables significantly impact the correlation between these asset classes.

We compared the performance of our models along with the DCC model of Engle (2002) for all pairs based on AIC and BIC. Based on AIC, the asymmetric Student$-t$

Table 5.10: Parameter estimates for the bivariate models with explanatory variables fitted on the pairs BTC-VIX (Panel A) and XRP-VIX (Panel B), comparing Normal, Student-t, Asymmetric Normal, and Asymmetric Student-t distributions. The table includes estimates for the degrees of freedom (ν), asymmetry parameters (α_1, α_2), and other model parameters (ω, a, b), along with log-likelihood (LogLik), AIC, and BIC values.

	Normal	Student-t	Asymmetric Normal	Asymmetric Student-t
Panel A: (BTC, VIX)				
ν	-	4.7458 ***	-	4.7815 ***
	-	(0.2643)	-	(0.2466)
α_1	-	-	-1.2741 ***	-0.1801 *
	-	-	(0.0900)	(0.0969)
α_2	-	-	-0.1740	-0.7235 ***
	-	-	(0.1756)	(0.1289)
ω	0.0411	0.0323	0.1376	0.0921 **
	(0.0307)	(0.0316)	(0.0884)	(0.0444)
a	0.0075	0.0069	0.0116	0.0104
	(0.0067)	(0.0117)	(0.0112)	(0.0145)
b	0.9643 ***	0.9548 ***	0.9653 ***	0.9546 ***
	(0.0215)	(0.0445)	(0.0229)	(0.0369)
ρ_{GOLD}	1.4942	1.6100	1.6265	1.7492
	(1.1158)	(1.3137)	(1.2972)	(1.5691)
ρ_{DGS10}	0.3026	0.3993	0.3424	0.4383
	(0.1936)	(0.3274)	(0.2519)	(0.3370)
ρ_{T10Y3M}	-0.1114	-0.1377	-0.1566	-0.1611
	(0.1218)	(0.2022)	(0.1613)	(0.1991)
ρ_{T10YIE}	-0.1126	-0.2001	-0.0624	-0.2299
	(0.2196)	(0.3058)	(0.2828)	(0.4041)
LogLik	-5815.7229	-5533.6659	-5774.8598	-5514.1492
AIC	11645.4459	11083.3319	11567.7196	11048.2985
BIC	11684.8250	11128.3366	11618.3500	11104.5544
Panel B: (XRP, VIX)				
ν	-	4.0397 * * *	-	4.0469 * * *
	-	(0.1560)	-	(0.1561)
α_1	-	-	1.1395 * * *	0.1052
	-	-	(0.0800)	(0.0885)
α_2	-	-	-0.0408	-0.5458 * * *
	-	-	(0.0901)	(0.1118)
ω	0.0267	0.0255	0.0149	0.0024
	(0.0235)	(0.0249)	(0.0469)	(0.0360)
a	-0.0209	-0.0235	-0.0317	-0.0263
	(0.0145)	(0.0225)	(0.0234)	(0.0317)
b	0.9192 * * *	0.7008 * *	0.9210 * * *	0.6912 * *
	(0.0586)	(0.3214)	(0.0589)	(0.3474)
rho:GOLD	2.0366 *	1.9300	2.5373 *	1.9822
	(1.1788)	(2.6423)	(1.5365)	(2.6303)
rho:DGS10	0.3247 *	0.3191	0.3994	0.3327
	(0.1953)	(0.3366)	(0.2500)	(0.4283)
rho:T10Y3M	-0.0682	0.1109	-0.0888	0.1343
	(0.1363)	(0.3654)	(0.1656)	(0.4438)
rho:T10YIE	-0.4345 *	-0.5552	-0.5295 *	-0.6097
	(0.2619)	(0.4582)	(0.3146)	(0.4537)
LogLik	-5810.6921	-5417.3202	-5777.0781	-5401.9663
AIC	11635.3843	10850.6403	11572.1561	10823.9326
BIC	11674.7634	10895.6451	11622.7865	10880.1885

Note: The significance of each explanatory variable (Gold, DGS10, T10Y3M and T10YIE) coefficient is indicated with stars. * 10%, ** 5%, and *** 1% le

models without explanatory variables performed better for all pairs except for BTC-VIX and XRP-VIX, where the asymmetric Student$-t$ model with explanatory variables is the preferred choice. For BIC, the asymmetric Student$-t$ model without explanatory variables performs better for all pairs except for BTC-S&P 500 and XRP-S&P 500. We summarize these results in Table 5.11.

Our findings offer market participants and practitioners valuable insights into how various market variables may impact the performance of their portfolios comprising these asset pairs.

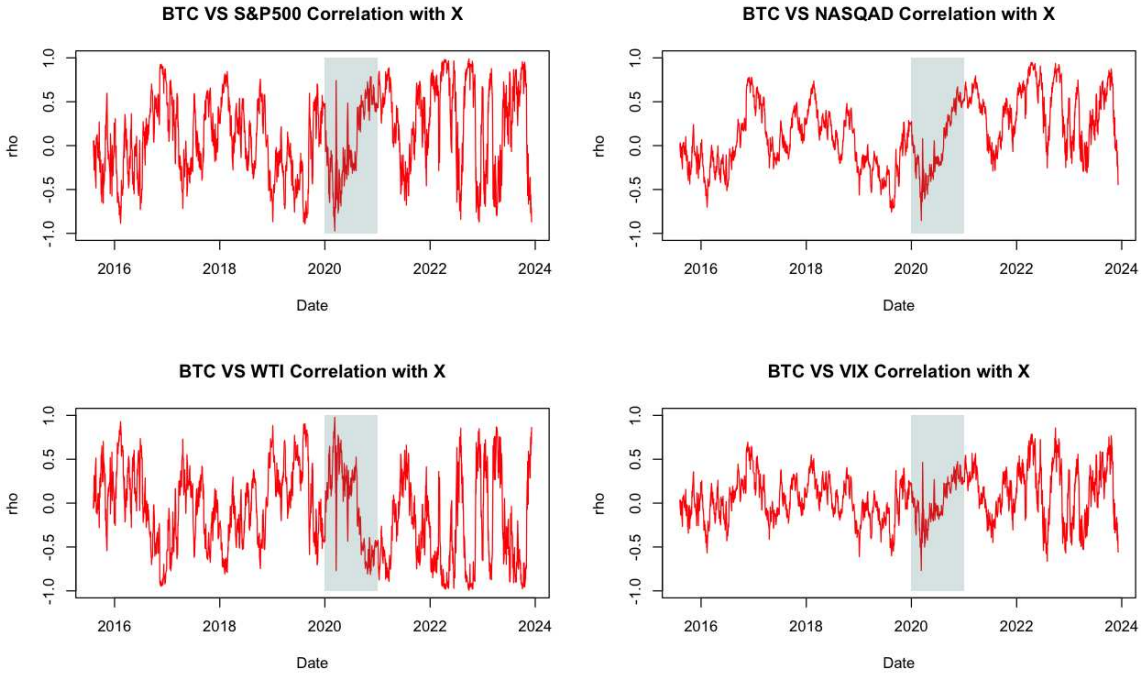

Figure 5.7: Time Varying correlations Plots without Explanatory Variables for BTC-S&P 500, BTC-NASDAQ, BTC-WTI and BTC-VIX.
Note: Explanatory Variables (X) are Gold, DGS10, T10Y3M, and T10YIE

5.4.3 Minimum Variance Portfolios

We investigate our models' capabilities in portfolio construction using the minimum variance portfolio approach. In particular, we compare our four proposals and the DCC model. We first compute the time-varying weights w_t of a two-component minimum variance portfolio consisting of a cryptocurrency and an asset. We optimize the weights

Table 5.11: Best Model for Each Pair Vs DCC Model

	AIC	BIC
(BTC, S&P 500)	Asymmetric Student-t	Student-t
(XRP, S&P 500	Asymmetric Student-t	Student-t
(BTC, NASDAQ)	Asymmetric Student-t	Asymmetric Student-t
(XRP, NASDAQ)	Asymmetric Student-t	Asymmetric Student-t
(BTC, VIX)	Asymmetric Student-t X	Asymmetric Student-t
(XRP, VIX)	Asymmetric Student-t X	Asymmetric Student-t
(BTC, WTI)	Asymmetric Student-t	Asymmetric Student-t
(XRP, WTI)	Asymmetric Student-t	Asymmetric Student-t

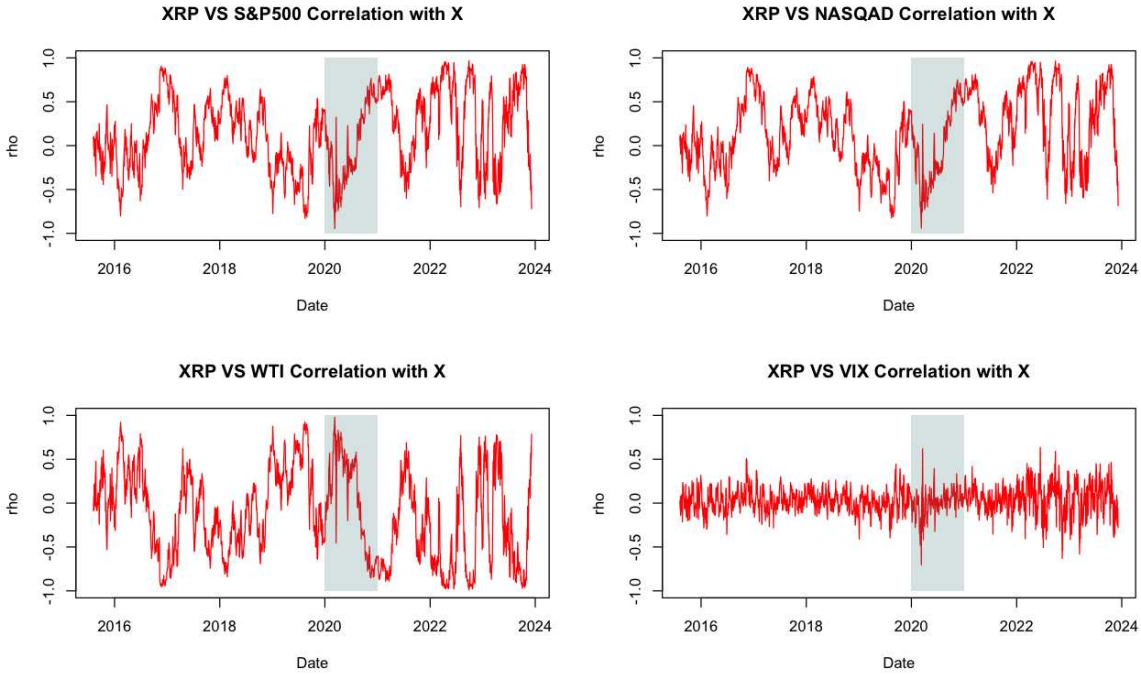

Figure 5.8: Time Varying correlations Plots without Explanatory Variables for XRP-S&P 500, XRP-NASDAQ, XRP-WTI and XRP-VIX.
Note: Explanatory Variables (X) are Gold, DGS10, T10Y3M, and T10YIE

for each point in time of our sample by solving the optimization problem:

$$\begin{aligned} \min_{w_t} \quad & w_t' \mathbf{H_t} w_t \\ \text{s.t.} \quad & w_t' \mathbf{1} = 1 \end{aligned}$$

where $\mathbf{H_t}$ is the covariance matrix and $\mathbf{1}$ is the unit vector. We utilize the global minimum variance portfolio (GMVP) technique, ignoring the expected return and focusing only on volatility. We obtain the weights of the minimum variance portfolio as:

$$w_t = \frac{\mathbf{H_t}^{-1}\mathbf{1}}{\mathbf{1}'\mathbf{H_t}^{-1}\mathbf{1}}.$$

The covariance matrix $\mathbf{H_t}$ has the form:

$$\begin{pmatrix} \sigma_{1,t}^2 & \sigma_{12,t} \\ \sigma_{12,t} & \sigma_{2,t}^2 \end{pmatrix}$$

where $\sigma_{1,t}^2$ and $\sigma_{2,t}^2$ are the variances of the assets 1 and 2 at time t, and $\sigma_{12,t}$ is the covariance, where $\sigma_{12,t} = \rho_t \sigma_{1,t} \sigma_{2,t}$. We extract the conditional variances from the GARCH

model fitted on univariate time-series data. We then use the time-varying correlations, ρ_t, from each fitted model (Normal, asymmetric Normal, Student-t, asymmetric Student-t, and the DCC models) to construct the covariances. The comparisons of the models portfolio performance are based on the Sharpe Ratio (Sharpe, 1966), which measures the investment risk-adjusted performance relative to its volatility. A portfolio with higher Sharpe ratios indicates better risk-adjusted performance.

Table 5.12: Portfolio metrics for pairs BTC-S&P 500, BTC-NASDAQ, BTC-VIX, and BTC-WTI comparing Normal, Student-t, Asymmetric Normal, Asymmetric Student-t and DCC model performance base on Sharpe ratio

	Normal	Student$-t$	Asymmetric Normal	Asymmetric Student$-t$	DCC Model
Panel A: (BTC, S&P 500)					
Annualized Return	0.0525	0.0656	0.0603	0.0648	0.0565
Annualized Volatility	0.2141	0.2130	0.2132	0.2130	0.2141
Sharpe Ratio	0.0224	**0.0261**	0.0246	0.0259	0.0235
Panel B: (BTC, NASDAQ)					
Annualized Return	0.0710	0.0855	0.0782	0.0842	0.0762
Annualized Volatility	0.2439	0.2430	0.2434	0.2430	0.2437
Sharpe Ratio	0.0258	**0.0294**	0.0276	0.0290	0.0271
Panel C: (BTC, VIX)					
Annualized Return	0.3054	0.3189	0.3061	0.3151	0.3091
Annualized Volatility	0.5378	0.5370	0.5379	0.5368	0.5379
Sharpe Ratio	0.0485	**0.0498**	0.0486	0.0495	0.0489
Panel D: (BTC, WTI)					
Annualized Return	0.0547	0.0539	0.0554	0.0537	0.0543
Annualized Volatility	0.3817	0.3821	0.3815	0.3822	0.3819
Sharpe Ratio	0.0217	0.0216	**0.0218**	0.0216	0.0217

In Table 5.12, we present the performance results for portfolios consisting of BTC and the selected asset (S&P 500, NASDAQ, VIX, and WTI). Panel A, B, and C show that the Sharpe Ratio of the Student-t model is the highest and has the highest annualized expected return and lowest volatility. The Sharpe ratio of 0.0261 for BTC and the S&P 500 index reported in Panel A is the highest. This result suggests that, under this model, the portfolio provides the best risk-adjusted return among the models considered. In other words, for each unit of risk (volatility) taken, the GAS (1, 1) Student-t model offers the highest risk-adjusted return. In Panel D, we show that for the portfolio consisting of BTC and WTI, the asymmetric Normal model has the highest Sharpe Ratio. The Student-t and asymmetric Student-t, perform better than the DCC model for the majority of the constructed portfolio, with the only exception of BTC and WTI, where the asymmetric Normal model performs best.

Table 5.13 displays the results for portfolios consisting of XRP and the same assets. The asymmetric Student-t model has the highest Sharpe Ratio (0.0276, see Panel A). The Student-t has the lowest variance and the same expected return as the asymmetric Student-t. For XRP and NASDAQ (Panel B), the asymmetric Student-t and the

Table 5.13: Portfolio metrics for pairs XRP-S&P 500, XRP-NASDAQ, XRP-VIX, and XRP-WTI comparing Normal, Student-t, Asymmetric Normal, Asymmetric Student-t and DCC model performance base on Sharpe ratio

	Normal	Student$-t$	Asymmetric Normal	Asymmetric Student$-t$	DCC Model
Panel A: (XRP, S&P 500)					
Annualized Return	0.0649	0.0695	0.0649	0.0695	0.0669
Annualized Volatility	0.2021	0.2017	0.2021	0.2018	0.2021
Sharpe Ratio	0.0262	0.0276	0.0262	**0.0276**	0.0268
Panel B: (XRP, NASDAQ)					
Annualized Return	0.0824	0.0871	0.0825	0.0871	0.0862
Annualized Volatility	0.2335	0.2333	0.2335	0.2334	0.2334
Sharpe Ratio	0.0289	0.0301	0.0289	**0.0301**	0.0299
Panel C: (XRP, VIX)					
Annualized Return	-0.0491	-0.0386	-0.0482	-0.0388	-0.0471
Annualized Volatility	0.7290	0.7298	0.7293	0.7296	0.7284
Sharpe Ratio	0.0182	**0.0192**	0.0183	0.0191	0.0183
Panel D: (XRP, WTI)					
Annualized Return	-0.0416	-0.0401	-0.0416	-0.0398	-0.0408
Annualized Volatility	0.3950	0.3945	0.3951	0.3945	0.3948
Sharpe Ratio	0.0062	0.0064	0.0062	**0.0064**	0.0063

Student-t models perform better than the DCC, providing a Sharpe ratio of 0.0301. Both models provide the same expected return, but the Student-t has a slightly lower volatility. The portfolio comparisons for XRP-VIX and XRP-WTI are shown in Panel C and D, respectively. Although the negative annualized returns were observed in both cases, the asymmetric Student-t and the Student-t models outperform the DCC model in terms of the Sharpe ratio, expected return, and volatility.

Our result reveals that accounting for heavy tails and asymmetries when dealing with a portfolio containing cryptocurrencies significantly improves the portfolio risk-adjusted returns. Investors seeking better risk-adjusted returns might prefer models that account for the heavy tails and asymmetry in the return distribution, such as the asymmetric Student-t Distribution.

5.5 Conclusions

In this study, we model time-varying correlation between Bitcoin, Ripple and some traditional financial assets. Traditional correlation models often fail to capture the dynamic and non-linear relationships between financial assets, ignoring factors like volatility clustering and tail dependence. For this reason, we proposed a novel framework that leverages an asymmetric Student-t distribution for asset return correlations, enhanced with parameters governed by generalized autoregressive score dynamics. This advanced approach overcomes the limitations of traditional models by offering a more flexible and accurate representation of financial return correlations. Our framework al-

lows to easily incorporate explanatory variables into the model formulation to account for their impact on correlations.

We propose a novel approach considering four possible model specifications: Normal, Student-t, asymmetric Normal, and asymmetric Student-t. We model time-varying correlation between cryptocurrencies (Bitcoin and Ripple) and traditional financial market data (S&P 500 index, NASDAQ index, VIX index, and WTI).

Results show that the asymmetric Student-t model consistently outperforms the alternatives for all the pairs considered. Our proposal effectively captures the asymmetry and heavy tails in the data, making it the most suitable choice for modeling the time-varying correlation between these cryptocurrencies and the financial market.

We also assess the impact of some explanatory variables on the time-varying correlation between pairs of cryptocurrency and financial market data. Results show that Gold positively impacts the correlation between Bitcoin and S&P 500, Ripple and S&P 500, Ripple and NASDAQ, and Ripple VIX, while it negatively impacts Ripple and WTI correlations. The Market Yield on US Treasury Securities positively affects the correlations between Ripple and S&P 500, Ripple and NASDAQ, and Ripple and VIX and negatively impact Bitcoin and WTI. We additionally found that the 10-year Breakeven Inflation Rate positively impacts the correlations between Ripple and WTI and Ripple and VIX.

Our approach enhances portfolio performance, risk management, and loss hedging. Our portfolio analysis shows that accounting for heavy tails and asymmetries when dealing with a portfolio containing cryptocurrencies significantly improves the portfolio risk-adjusted returns.

In addition, our study emphasizes the importance of incorporating explanatory variables into the modelling correlation process across assets for a more comprehensive understanding of their returns and market dynamics. This would also support policymakers in understanding risks more accurately and institute closer surveillance of those risks by financial institutions. Detecting and monitoring correlations could thus enhance regulatory frameworks, strengthen market infrastructure and lessen market manipulation.

Bibliography

Adcock, R. and N. Gradojevic (2019). Non-fundamental, non-parametric bitcoin forecasting. *Physica A: Statistical Mechanics and its Applications 531*, 121727.

Aharon, D. Y. and M. Qadan (2019). Bitcoin and the day-of-the-week effect. *Finance Research Letters 31*.

Ahmad, M. F., O. Kowalewski, and P. Pisany (2023). What determines initial coin offering success: a cross-country study. *Economics of Innovation and New Technology 32*(5), 622–645.

Akaike, H. (1974). A new look at the statistical model identification. *IEEE Transactions on Automatic Control 19*, 716–723.

Algieri, B. (2014). Drivers of export demand: A focus on the giips countries. *The World Economy 37*(10), 1454–1482.

Algieri, B., L. Iania, and A. Leccadito (2023). Looking ahead: Forecasting total energy carbon dioxide emissions. *Cleaner Environmental Systems 9*, 100112.

Algieri, B., M. Kalkuhl, and N. Koch (2017). A tale of two tails: Explaining extreme events in financialized agricultural markets. *Food Policy 69*(C), 256–269.

Algieri, B. and A. Leccadito (2017). Assessing contagion risk from energy and non-energy commodity markets. *Energy Economics 62*(C), 312–322.

Algieri, B. and A. Leccadito (2019). Ask CARL: Forecasting tail probabilities for energy commodities. *Energy Economics 84*(C), 104497.

Algieri, B. and A. Leccadito (2021). Extreme price moves: an INGARCH approach to model coexceedances in commodity markets. *European Review of Agricultural Economics 48*(4), 878–914.

Algieri, B., A. Leccadito, and P. Toscano (2021a). A time-varying Gerber statistic: Application of a novel correlation metric to commodity price co-movements. *Forecasting 3*(2), 339–354.

Algieri, B., A. Leccadito, and P. Toscano (2021b). A time-varying gerber statistic: Application of a novel correlation metric to commodity price co-movements. *Forecasting 3*(2), 1–16.

Almeida, J. and T. C. Gonçalves (2022, May). A systematic literature review of volatility and risk management on cryptocurrency investment: A methodological point of view. *Risks 10*(5), 107.

Aloui, R., M. S. B. Aïssa, and D. K. Nguyen (2011, January). Global financial crisis, extreme interdependences, and contagion effects: The role of economic structure? *Journal of Banking & Finance 35*(1), 130–141.

Amalia, F. F., Suhartono, S. P. Rahayu, and N. Suhermi (2018). Quantile regression neural network for forecasting inflow and outflow in yogyakarta. *Journal of Physics: Conference Series 1028*, 12232.

Ameur, H. B., Z. Ftiti, and W. Louhichi (2022). Revisiting the relationship between spot and futures markets: evidence from commodity markets and nardl framework. *Annals of operations research 313*(1), 171—189.

Ang, A. and G. Bekaert (2002). International asset allocation with regime shifts. *The Review of Financial Studies 15*, 1137–1187.

Ang, A., G. Bekaert, and M. Wei (2008). The term structure of real rates and expected inflation. *The Journal of Finance 63*(2), 797–849.

Ang, A., M. Piazzesi, and M. Wei (2006). What does the yield curve tell us about gdp growth? *Journal of econometrics 131*(1-2), 359–403.

Ante, L. (2023). Non-fungible token (nft) markets on the ethereum blockchain: temporal development, cointegration and interrelations. *Economics of Innovation and New Technology 32*(8), 1216–1234.

Ardia, D., K. Bluteau, and M. Rüede (2019). Regime changes in bitcoin GARCH volatility dynamics. *Finance Research Letters 29*, 266–271.

Arendas, P. (2017). The Halloween effect on the agricultural commodities markets. *Agricultural Economics 63*(10), 441–448.

Azzalini, A. (2005). The skew-normal distribution and related multivariate families. *Scandinavian Journal of Statistics 32*(2), 159–188.

Baek, C. and M. Elbeck (2015). Bitcoins as an investment or speculative vehicle? a first look. *Applied Economics Letters 22*(1), 30–34.

Bakas, D., G. Magkonis, and E. Y. Oh (2022). What drives volatility in Bitcoin market? *Finance Research Letters 50*, 103237.

Basher, S. A. and P. Sadorsky (2022). Forecasting Bitcoin price direction with random forests: How important are interest rates, inflation, and market volatility? *Machine Learning with Applications 9*, 100355.

Baur, D. G., D. Cahill, K. Godfrey, and Z. F. Liu (2019). Bitcoin time-of-day, day-of-week and month-of-year effects in returns and trading volume. *Finance Research Letters 31*, 78–92.

Baur, D. G., T. Dimpfl, and K. Kuck (2018). Bitcoin, gold and the us dollar – a replication and extension. *Finance Research Letters 25*, 103–110.

Baur, D. G. and L. Hoang (2021). The bitcoin gold correlation puzzle. *Journal of Behavioral and Experimental Finance 32*, 100561.

Baur, D. G. and B. M. Lucey (2010). Is gold a hedge or a safe haven? an analysis of stocks, bonds and gold. *Financial review 45*(2), 217–229.

Bauwens, L., S. Laurent, and J. V. Rombouts (2006). Multivariate GARCH models: A survey. *Journal of applied econometrics 21*(1), 79–109.

Bech, M. L. and R. Garratt (2017). Central bank cryptocurrencies. Technical report.

Beckmann, J. and R. Czudaj (2013). Gold as an inflation hedge in a time-varying coefficient framework. *The North American Journal of Economics and Finance 24*, 208–222.

Bedowska-Sójka, B. and A. Kliber (2021). Is there one safe-haven for various turbulences? the evidence from gold, bitcoin and ether. *The North American Journal of Economics and Finance 56*, 101390.

Bekaert, G. and E. Engstrom (2010). Inflation and the stock market: Understanding the "fed model". *Journal of Monetary Economics 57*(3), 278–294.

Bernanke, B. S. (1990). The federal funds rate and the channels of monetary transnission.

Bernardi, M. and L. Catania (2016, Jun). Comparison of value-at-risk models using the mcs approach. *Computational Statistics 31*(2), 579–608.

Birru, J. (2018). Day of the week and the cross-section of returns. *Journal of Financial Economics 130*(1), 182–214.

Bollerslev, T. (1986). Generalized autoregressive conditional heteroskedasticity. *Journal of Econometrics 31*(3), 307–327.

Bollerslev, T. (1987). A conditionally heteroskedastic time series model for speculative prices and rates of return. *The Review of Economics and Statistics 69*(3), 542–547.

Borri, N. (2019). Conditional tail-risk in cryptocurrency markets. *Journal of Empirical Finance 50*, 1–19.

Boudreaux, D. O. (1995). The monthly effect in international stock markets: evidence and implications. *Journal of Financial and Strategic Decisions 8*(1), 15–20.

Bouman, S. and B. Jacobsen (2002). The Halloween indicator, "sell in may and go away": Another puzzle. *American Economic Review 92*(5), 1618–1635.

Bouri, E., R. Gupta, A. Lahiani, and M. Shahbaz (2018). Testing for asymmetric nonlinear short- and long-run relationships between bitcoin, aggregate commodity and gold prices. *Resources Policy 57*(C), 224–235.

Bouri, E., R. Gupta, A. K. Tiwari, and D. Roubaud (2017). Does Bitcoin hedge global uncertainty? Evidence from wavelet-based quantile-in-quantile regressions. *Finance Research Letters 23*, 87–95.

Bouri, E., P. Molnár, G. Azzi, D. Roubaud, and L. I. Hagfors (2017). On the hedge and safe haven properties of Bitcoin: Is it really more than a diversifier? *Finance Research Letters 20*, 192–198.

Brooks, C. and O. Henry (2002). The impact of news on measures of undiversifiable risk: Evidence from the UK stock market. *Oxford Bulletin of Economics and Statistics 64*(5), 487–507.

Bush, P. J., J. Stephens, and S. Mehdian (2020). An investigation of the presence of anomalies in digital asset market: The case of Bitcoin. *Applied Finance Letters 9*, 73–80.

Cannon, A. J. (2011). Quantile regression neural networks: Implementation in R and application to precipitation downscaling. *Computers & Geosciences 37*(9), 1277–1284.

Cannon, A. J. (2018). Non-crossing nonlinear regression quantiles by monotone composite quantile regression neural network, with application to rainfall extremes. *Stochastic Environmental Research and Risk Assessment 32*, 3207–3225.

Caporale, G. M. and A. Plastun (2019). The day of the week effect in the cryptocurrency market. *Finance Research Letters 31*.

Caporale, G. M. and T. Zekokh (2019). Modelling volatility of cryptocurrencies using markov-switching garch models. *Research in International Business and Finance 48*, 143–155.

Chen, C. (2007). A finite smoothing algorithm for quantile regression. *Journal of Computational and Graphical Statistics 16*(1), 136–164.

Cherubini, U., E. Luciano, and W. Vecchiato (2004). *Copula methods in finance*. John Wiley & Sons.

Chhabra, D. and M. Gupta (2022). Calendar anomalies in commodity markets for natural resources: Evidence from India. *Resources Policy 79*, 103019.

Chia, R. C.-J. and V. K.-S. Liew (2012). Month-of-the-year and symmetrical effects in the Nikkei 225. *Journal of Business and Management 3*(2), 68–72.

Chu, J., S. Chan, S. Nadarajah, and J. Osterrieder (2017). GARCH modelling of cryptocurrencies. *Journal of Risk and Financial Management 10*(4), 1–15.

Chung, Y. P., H. Johnson, and M. J. Schill (2006). Asset pricing when returns are nonnormal: Fama-French factors versus higher-order systematic comoments. *The Journal of Business 79*(2), 923–940.

Colon, F., C. Kim, H. Kim, and W. Kim (2021). The effect of political and economic uncertainty on the cryptocurrency market. *Finance Research Letters 39*, 101621.

Conlon, T. and R. McGee (2020). Safe haven or risky hazard? Bitcoin during the COVID-19 bear market. *Finance Research Letters 35*, 101607.

Conrad, C., A. Custovic, and E. Ghysels (2018). Long- and short-term cryptocurrency volatility components: A garch-midas analysis. *Journal of Risk and Financial Management 11*(2).

Cont, R. (2001). Empirical properties of asset returns: Stylized facts and statistical issues. *Quantitative Finance 1*, 223.

Corbet, S., B. Lucey, A. Urquhart, and L. Yarovaya (2019). Cryptocurrencies as a financial asset: A systematic analysis. *International Review of Financial Analysis 62*, 182–199.

Corbet, S., B. Lucey, and L. Yarovaya (2018). Datestamping the Bitcoin and Ethereum bubbles. *Finance Research Letters 26*, 81–88.

Cortese, F. P., P. N. Kolm, and E. Lindström (2023). What drives cryptocurrency returns? A sparse statistical jump model approach. *Digital Finance 5*(3), 483–518.

Cortese, F. P., F. Pennoni, and F. Bartolucci (2024). Maximum likelihood estimation of multivariate regime switching Student-t copula models. *International Statistical Review*, 1–28.

Creal, D., S. J. Koopman, and A. Lucas (2013). Generalized Autoregressive Score models with applications. *Journal of Applied Econometrics 28*(5), 777–795.

Dai, M., M. Qamruzzaman, and A. Hamadelneel Adow (2022). An assessment of the impact of natural resource price and global economic policy uncertainty on financial asset performance: Evidence from bitcoin. *Frontiers in Environmental Science 10*, 897496.

Das, S. R. and R. Uppal (2004). Systemic risk and international portfolio choice. *The Journal of Finance 59*, 2809–2834.

Demir, E., G. Gozgor, C. K. M. Lau, and S. A. Vigne (2018). Does economic policy uncertainty predict the Bitcoin returns? An empirical investigation. *Finance Research Letters 26*, 145–149.

Dickey, D. A. and W. A. Fuller (1981). Likelihood ratio statistics for autoregressive time series with a unit root. *Econometrica: journal of the Econometric Society*, 1057–1072.

Diebold, F. X. and R. S. Mariano (2002). Comparing predictive accuracy. *Journal of Business & Economic Statistics 20*(1), 134–144.

Diebold, F. X. and K. Yilmaz (2009). Measuring financial asset return and volatility spillovers, with application to global equity markets. *The Economic Journal 119*(534), 158–171.

Dufour, J.-M., L. Khalaf, and M.-C. Beaulieu (2003). Exact skewness–kurtosis tests for multivariate normality and goodness-of-fit in multivariate regressions with application to Asset Pricing Models. *Oxford Bulletin of Economics and Statistics 65*(s1), 891–906.

Dyhrberg, A. H. (2016). Bitcoin, Gold and the dollar–a garch volatility analysis. *Finance research letters 16*, 85–92.

D'Innocenzo, E. and A. Lucas (2024). Dynamic partial correlation models. *Journal of Econometrics 241*(2), 105747.

D'Innocenzo, E., A. Lucas, B. Schwaab, and X. Zhang (2024). Modeling extreme events: time-varying extreme tail shape. *Journal of Business & Economic Statistics 42*(3), 903–917.

Elsayed, A. H., G. Gozgor, and L. Yarovaya (2022). Volatility and return connectedness of cryptocurrency, gold, and uncertainty: Evidence from the cryptocurrency uncertainty indices. *Finance Research Letters 47*, 102732.

Engle, R. (2002). Dynamic Conditional Correlation: A simple class of multivariate generalized autoregressive conditional heteroskedasticity models. *Journal of Business & Economic Statistics 20*(3), 339–350.

Engle, R. F. (1982). Autoregressive conditional heteroscedasticity with estimates of the variance of united kingdom inflation. *Econometrica 50*(4), 987–1007.

Engle, R. F. and T. Bollerslev (1986). Modelling the persistence of conditional variances. *Econometric Reviews 5*, 1–50.

Estrella, A. and G. Hardouvelis (1991). The term structure as a predictor of real economic activity. *Journal of Finance 46*(2), 555–76.

Estrella, A. and F. Mishkin (1998). Predicting u.s. recessions: Financial variables as leading indicators. *The Review of Economics and Statistics 80*(1), 45–61.

Estrella, A. and F. S. Mishkin (1996). The yield curve as a predictor of us recessions. *Current issues in economics and finance 2*(7).

Fabozzi, F. J., C. K. Ma, and J. E. Briley (1994). Holiday trading in futures markets. *The Journal of Finance 49*(1), 307–324.

Fama, E. (1981). Stock returns, real activity, inflation, and money. *American Economic Review*.

Fama, E. F. (1965). The behavior of stock-market prices. *The Journal of Business 38*(1), 34–105.

Fama, E. F. and K. R. French (1989). Business conditions and expected returns on stocks and bonds. *Journal of financial economics 25*(1), 23–49.

Feder-Sempach, E., P. Szczepocki, and J. Bogołębska (2024). Global uncertainty and potential shelters: gold, bitcoin, and currencies as weak and strong safe havens for main world stock markets. *Financial Innovation 10*(1), 1–23.

Feng, W., Y. Wang, and Z. Zhang (2018). Can cryptocurrencies be a safe haven: a tail risk perspective analysis. *Applied Economics 50*(44), 4745–4762.

Fissler, T., J. F. Ziegel, and T. Gneiting (2015). Expected shortfall is jointly elicitable with value at risk - implications for backtesting. *arXiv: Risk Management*.

Fleischer, J. P., G. von Laszewski, C. Theran, and Y. J. Parra Bautista (2022). Time series analysis of cryptocurrency prices using long short-term memory. *Algorithms 15*(7).

French, K. R. (1980). Stock returns and the weekend effect. *Journal of Financial Economics 8*(1), 55–69.

Fry, J. and E.-T. Cheah (2016). Negative bubbles and shocks in cryptocurrency markets. *International Review of Financial Analysis 47*, 343–352.

Gerber, S., H. Markowitz, P. A. Ernst, Y. Miao, B. Javid, and P. Sargen (2022). The gerber statistic: A robust co-movement measure for portfolio optimization. *The Journal of Portfolio Management 48*(8), 87–102.

Geuder, J., H. Kinateder, and N. F. Wagner (2019). Cryptocurrencies as financial bubbles: The case of Bitcoin. *Finance Research Letters 31*.

Ghorbel, A. and A. Jeribi (2021). Investigating the relationship between volatilities of cryptocurrencies and other financial assets. *Decisions in Economics and Finance 44*(2), 817–843.

Gibbons, M. R. and P. Hess (1981). Day of the week effects and asset returns. *Journal of business*, 579–596.

Glosten, L. R., R. Jagannathan, and D. E. Runkle (1993, dec). On the relation between the expected value and the volatility of the nominal excess return on stocks. *The Journal of Finance 48*(5), 1779–1801.

Gronwald, M. (2014, December). The Economics of Bitcoins – Market Characteristics and Price Jumps. SSRN Scholarly Paper ID 2548999, Social Science Research Network, Rochester, NY.

Guesmi, K., S. Saadi, I. Abid, and Z. Ftiti (2019). Portfolio diversification with virtual currency: Evidence from Bitcoin. *International Review of Financial Analysis 63*, 431–437.

Hafner, C. M. and L. Wang (2023). A dynamic conditional score model for the log correlation matrix. *Journal of Econometrics 237*(2).

Hansen, B. E. (1994). Autoregressive conditional density estimation. *International Economic Review 35*(3), 705.

Hansen, P. R., A. Lunde, and J. M. Nason (2011). The model confidence set. *Econometrica 79*(2), 453–497.

Haug, M. and M. Hirschey (2006). The January effect. *Financial Analysts Journal 62*(5), 78–88.

Hull, J., A. White, et al. (2004). Valuation of a CDO and an n-th to default CDS without Monte Carlo simulation. *Journal of Derivatives 12*(2), 8–23.

Huynh, T. L. D., M. A. Nasir, X. V. Vo, and T. T. Nguyen (2020). "small things matter most": The spillover effects in the cryptocurrency market and gold as a silver bullet. *The North American Journal of Economics and Finance 54*, 101277.

Jaquart, P., D. Dann, and C. Weinhardt (2021). Short-term bitcoin market prediction via machine learning. *The Journal of Finance and Data Science 7*, 45–66.

Jareño, F., M. de la O. González, R. López, and A. R. Ramos (2021). Cryptocurrencies and oil price shocks: A nardl analysis in the covid-19 pandemic. *Resources Policy 74*, 102281.

Jarque, C. M. and A. K. Bera (1987). A test for normality of observations and regression residuals. *International Statistical Review/Revue Internationale de Statistique*, 163–172.

Johnson, N. L. (1954). Systems of frequency curves derived from the first law of Laplace. *Trabajos de Estadistica 5*, 283–291.

Jondeau, E. and M. Rockinger (2003). Conditional volatility, skewness, and kurtosis: existence, persistence, and comovements. *Journal of Economic Dynamics and Control 27*(10), 1699–1737.

Kaiser, L. (2019). Seasonality in cryptocurrencies. *Finance Research Letters 31*.

Katsiampa, P. (2019). An empirical investigation of volatility dynamics in the cryptocurrency market. *Research in International Business and Finance 50*, 322–335.

Khalaf, L., A. Leccadito, and G. Urga (2021). Multilevel and Tail Risk Management. *Journal of Financial Econometrics*, 1–36.

Kim, C.-W. and J. Park (1994). Holiday effects and stock returns: Further evidence. *Journal of Financial and Quantitative Analysis 29*(1), 145–157.

Kim, J.-M., C. Jun, and J. Lee (2021). Forecasting the volatility of the cryptocurrency market by GARCH and stochastic volatility. *Mathematics 9*(14).

Kim, J.-M., S.-T. Kim, and S. Kim (2020). On the relationship of cryptocurrency price with us stock and gold price using copula models. *Mathematics 8*(11), 1859.

Kinateder, H. and V. G. Papavassiliou (2021). Calendar effects in Bitcoin returns and volatility. *Finance Research Letters 38*, 101420.

Kiymaz, H. and H. Berument (2003). The day of the week effect on stock market volatility and volume: International evidence. *Review of Financial Economics 12*(4), 363–380.

Kjærland, F., A. Khazal, E. A. Krogstad, F. B. G. Nordstrøm, and A. Oust (2018). An analysis of bitcoin's price dynamics. *Journal of Risk and Financial Management 11*(4).

Klein, T., H. Pham Thu, and T. Walther (2018). Bitcoin is not the new gold – a comparison of volatility, correlation, and portfolio performance. *International Review of Financial Analysis 59*(C), 105–116.

Kohli, R. (2014). Day-of-the-week effect and January effect examined in sweet crude oil. *Journal of Finance Issues 13*(1), 43–51.

Kohli, R. K. and T. Kohers (1992). The week-of-the-month effect in stock returns: The evidence from the S&P composite index. *Journal of economics and finance 16*(2), 129–137.

Kristoufek, L. (2015, 04). What are the main drivers of the bitcoin price? evidence from wavelet coherence analysis. *PLOS ONE 10*(4), 1–15.

Kumah, S. P. and J. Odei-Mensah (2022). Do cryptocurrencies and crude oil influence each other? evidence from wavelet-based quantile-in-quantile approach. *Cogent Economics & Finance 10*(1), 2082027.

Kwiatkowski, D., P. C. Phillips, P. Schmidt, and Y. Shin (1992). Testing the null hypothesis of stationarity against the alternative of a unit root: How sure are we that economic time series have a unit root? *Journal of econometrics 54*(1-3), 159–178.

Lahmiri, S. and S. Bekiros (2019). Cryptocurrency forecasting with deep learning chaotic neural networks. *Chaos, Solitons & Fractals 118*, 35–40.

Lawuobahsumo, K. K., B. Algieri, L. Iania, and A. Leccadito (2022). Exploring dependence relationships between bitcoin and commodity returns: An assessment using the Gerber cross-correlation. *Commodities 1*(1), 34–49.

Lawuobahsumo, K. K., B. Algieri, and A. Leccadito (2024). Forecasting cryptocurrencies returns: Do macroeconomic and financial variables improve tail expectation predictions? *Quality & Quantity 58*(3), 2647–2675.

Lee, G. and R. F. Engle (1999). A permanent and transitory component model of stock return volatility. In R. F. Engle and H. White (Eds.), *Cointegration, Causality, and Forecasting: A Festschrift in Honor of Clive W.J. Granger*, pp. 475–497. Oxford University Press.

Liu, Y., A. Tsyvinski, and X. Wu (2022). Common risk factors in cryptocurrency. *The Journal of Finance 77*(2), 1133–1177.

Ljung, G. M. and G. E. Box (1978). On a measure of lack of fit in time series models. *Biometrika 65*(2), 297–303.

Longin, F. and B. Solnik (2001). Extreme correlation of international equity markets. *The journal of finance 56*(2), 649–676.

Ma, D. and H. Tanizaki (2019). The day-of-the-week effect on Bitcoin return and volatility. *Research in International Business and Finance 49*, 127–136.

MacDonald, R. and M. P. Taylor (1988, February). Testing rational expectations and efficiency in the London metal exchange. *Oxford Bulletin of Economics and Statistics 50*(1), 41–52.

Marrett, G. J. and A. C. Worthington (2009). An empirical note on the holiday effect in the Australian stock market, 1996–2006. *Applied Economics Letters 16*(17), 1769–1772.

Meek, A. C. and S. A. Hoelscher (2023, may). Day-of-the-week effect: Petroleum and petroleum products. *Cogent Economics & Finance 11*(1).

Mikhaylov, A. (2020). Cryptocurrency market analysis from the open innovation perspective. *Journal of Open Innovation: Technology, Market, and Complexity 6*(4), 197.

Mikhaylov, A., H. Dinçer, and S. Yüksel (2023). Analysis of financial development and open innovation oriented fintech potential for emerging economies using an integrated decision-making approach of MF-X-DMA and golden cut bipolar q-ROFSs. *Financial Innovation 9*(4).

Moiseev, N., A. Mikhaylov, H. Dinçer, and S. Yüksel (2023, December). Market capitalization shock effects on open innovation models in e-commerce: golden cut q-rung orthopair fuzzy multicriteria decision-making analysis. *Financial Innovation 9*(1), 1–25.

Morris, C., J. Mirkovic, and J. M. O'Rourke (2018, January). House joint resolution 25: Illinois blockchain and distributed ledger task force final report to the general assembly. Technical report, Illinois Department of Financial and Professional Regulation, Cook County Recorder of Deeds, Illinois Department of Commerce and Economic Opportunity.

Moussa, W., N. Mgadmi, A. Béjaoui, and R. Regaieg (2021). Exploring the dynamic relationship between Bitcoin and commodities: New insights through stecm model. *Resources Policy 74*, 102416.

Nadarajah, S. and J. Chu (2017). On the inefficiency of Bitcoin. *Economics Letters 150*, 6–9.

Nakamoto, S. (2009). Bitcoin: A peer-to-peer electronic cash system.

Naz, F., M. Sayyed, R.-U. Rehman, M. A. Naseem, S. N. Abdullah, and M. I. Ahmad (2023). Calendar anomalies and market volatility in selected cryptocurrencies. *Cogent Business & Management 10*(1), 2171992.

Nelson, D. B. (1991). Conditional heteroskedasticity in asset returns: A new approach. *Econometrica 59*(2), 347–370.

Nystrup, P., P. N. Kolm, and E. Lindström (2021). Feature selection in jump models. *Expert Systems with Applications 184*, 115558.

Oosterlinck, K., A. Reyns, and A. Szafarz (2023). Gold, Bitcoin, and portfolio diversification: Lessons from the ukrainian war. *Resources Policy 83*, 103710.

Orlowski, L. T. and C. Soper (2019). Market risk and market-implied inflation expectations. *International Review of Financial Analysis 66*, 101389.

Pabuçcu, H., S. Ongan, and A. Ongan (2020). Forecasting the movements of bitcoin prices: an application of machine learning algorithms. *Quantitative Finance and Economics 4*(4), 679–692.

Pandey, A. K., P. K. Singh, M. Nawaz, and A. K. Kushwaha (2022, sep). Forecasting of non-renewable and renewable energy production in india using optimized discrete grey model. *30*(3), 8188–8206.

Park, Y.-H. (2022). Spread position as a leading economic indicator. *Journal of Financial Markets 59*, 100681.

Patton, A. (2013). Copula methods for forecasting multivariate time series. *Handbook of economic forecasting 2*, 899–960.

Patton, A., D. N. Politis, and H. White (2009). Correction to "automatic block-length selection for the dependent bootstrap" by d. politis and h. white. *Econometric Reviews 28*(4), 372–375.

Patton, A. J. (2004). On the out-of-sample importance of skewness and asymmetric dependence for asset allocation. *Journal of Financial Econometrics 2*, 130–168.

Peng, Y., P. H. M. Albuquerque, J. M. Camboim de Sá, A. J. A. Padula, and M. R. Montenegro (2018). The best of two worlds: Forecasting high frequency volatility for cryptocurrencies and traditional currencies with support vector regression. *Expert Systems with Applications 97*, 177–192.

Phillips, P. C. and P. Perron (1988). Testing for a unit root in time series regression. *biometrika 75*(2), 335–346.

Politis, D. N. and J. P. Romano (1994). The stationary bootstrap. *Journal of the American Statistical Association 89*(428), 1303–1313.

Polizu, C., N. Oliveros-Rosen, M. de la Mata, T. K. Shubhangi Gupta, L. Guadagnolo, and A. Birry (2023). Are crypto markets correlated with macroeconomic factors? Technical report, S&P Global.

Qadan, M., D. Y. Aharon, and R. Eichel (2019). Seasonal patterns and calendar anomalies in the commodity market for natural resources. *Resources Policy 63*, 101435.

Rathore, R. K., D. Mishra, P. S. Mehra, O. Pal, A. S. Hashim, A. Shapi'i, T. Ciano, and M. Shutaywi (2022). Real-world model for bitcoin price prediction. *Information Processing & Management 59*(4), 102968.

Rigby, R. A. and D. M. Stasinopoulos (2005). Generalized additive models for location, scale and shape. *Journal of the Royal Statistical Society Series C: Applied Statistics 54*(3), 507–554.

Rompotis, G. G. (2009). A comprehensive study on the seasonality of Greek equity funds performance. *South-Eastern Europe Journal of Economics 7*(2), 229–255.

Rozeff, M. S. and W. R. Kinney Jr (1976). Capital market seasonality: The case of stock returns. *Journal of financial economics 3*(4), 379–402.

Rudkin, S., W. Rudkin, and P. Dłotko (2023). On the topology of cryptocurrency markets. *International Review of Financial Analysis 89*, 102759.

Schwarz, G. (1978). Estimating the dimension of a model. *The Annals of Statistics 6*(2), 461–464.

Selgin, G. (2015). Synthetic commodity money. *Journal of Financial Stability 17*, 92–99.

Selmi, R., W. Mensi, S. Hammoudeh, and J. Bouoiyour (2018). Is Bitcoin a hedge, a safe haven or a diversifier for oil price movements? a comparison with gold. *Energy Economics 74*, 787–801.

Shapiro, S. S. and M. B. Wilk (1965). An analysis of variance test for normality (complete samples). *Biometrika 52*(3-4), 591–611.

Sharpe, W. F. (1966). Mutual fund performance. *Journal of Business 39*(1), 119–138.

Shen, W. (2022). GARCH-Class analysis of Bitcoin—A comparison with Gold. In *2022 International Conference on Bigdata Blockchain and Economy Management (ICBBEM 2022)*, pp. 926–935. Atlantis Press.

Shum, W. C. and G. Y. Tang (2005). Common risk factors in returns in asian emerging stock markets. *International Business Review 14*(6), 695–717.

Singh, P. K., A. K. Pandey, S. Ahuja, and R. Kiran (2022). Multiple forecasting approach: a prediction of CO2 emission from the paddy crop in India. *Environmental Science and Pollution Research 29*(1), 25461–25472.

Singh, P. K., A. K. Pandey, and S. C. Bose (2023, Jun). A new grey system approach to forecast closing price of bitcoin, bionic, cardano, dogecoin, ethereum, xrp cryptocurrencies. *Quality & Quantity 57*(3), 2429–2446.

Singh, P. K., A. K. Pandey, A. Chouhan, and G. J. Singh (2023, jan). Prediction of surface temperature and CO2 emission of leading emitters using grey model EGM (1,1, α, θ). *Environmental Science and Pollution Research 30*(14), 39708–39723.

Smales, L. A. (2019). Bitcoin as a safe haven: Is it even worth considering? *Finance Research Letters 30*, 385–393.

Tang, G. Y. (1997). Impact of the day-of-the-week effect on diversification of exchange rate risks. *International Business Review 6*(1), 35–51.

Taylor, J. (2000). A quantile regression neural network approach to estimating the conditional density of multiperiod returns. *Journal of forecasting 19*(4), 299–311.

Telli, Ş. and H. Chen (2020). Structural breaks and trend awareness-based interaction in crypto markets. *Physica A: Statistical Mechanics and its Applications 558*, 124913.

Terraza, V., A. B. İpek, and M. M. Rounaghi (2024). The nexus between the volatility of Bitcoin, gold, and American stock markets during the COVID-19 pandemic: evidence from VAR-DCC-EGARCH and ANN models. *Financial Innovation 10*(1), 1–34.

Tiwari, A. K., E. J. A. Abakah, B. Doğan, O. B. Adekoya, and M. Wohar (2024). Asymmetric spillover effects in energy markets. *International Review of Economics & Finance 92*, 470–502.

Tiwari, A. K., S. Kumar, and R. Pathak (2019). Modelling the dynamics of bitcoin and litecoin: GARCH versus stochastic volatility models. *Applied Economics 51*(37), 4073–4082.

Tiwari, A. K., I. D. Raheem, and S. H. Kang (2019). Time-varying dynamic conditional correlation between stock and cryptocurrency markets using the copula-adcc-egarch model. *Physica A: Statistical Mechanics and Its Applications 535*, 122295.

Urquhart, A. (2016). The inefficiency of Bitcoin. *Economics Letters 148*, 80–82.

Urquhart, A. and H. Zhang (2019). Is Bitcoin a hedge or safe haven for currencies? an intraday analysis. *International Review of Financial Analysis 63*, 49–57.

Vasek, M. (2015). The age of cryptocurrency. *Science 348*(6241), 1308–1309.

Wachtel, S. B. (1942). Certain observations on seasonal movements in stock prices. *The journal of business of the University of Chicago 15*(2), 184–193.

Wang, J., F. Ma, E. Bouri, and Y. Guo (2022). Which factors drive Bitcoin volatility: Macroeconomic, technical, or both? *Journal of Forecasting*, 1–19.

Wang, P., W. Zhang, X. Li, and D. Shen (2019). Is cryptocurrency a hedge or a safe haven for international indices? a comprehensive and dynamic perspective. *Finance Research Letters 31*, 1–18.

Wang, W. (2006). *Stochasticity, nonlinearity and forecasting of streamflow processes*. Ios Press.

Wu, S. (2021, October). Co-movement and return spillover: evidence from Bitcoin and traditional assets. *SN Business & Economics 1*(10), 1–16.

Zakoian, J.-M. (1994). Threshold heteroskedastic models. *Journal of Economic Dynamics and Control 18*(5), 931–955.

Zaremba, A., Z. Umar, and M. Mikutowski (2021). Commodity financialisation and price co-movement: Lessons from two centuries of evidence. *Finance Research Letters 38*, 101492.

Zhang, D., Y. Sun, H. Duan, Y. Hong, and S. Wang (2023). Speculation or currency? multi-scale analysis of cryptocurrencies—the case of bitcoin. *International Review of Financial Analysis 88*, 102700.

Zheng, T. and S. Ye (2024). Cholesky gas models for large time-varying covariance matrices. *Journal of Management Science and Engineering 9*(1), 115–142.

Şarkaya İçellioğlu, C. and S. Öner (2019). An investigation on the volatility of cryptocurrencies by means of heterogeneous panel data analysis. *Procedia Computer Science 158*, 913–920.

Appendix A

Appendix

A.1 The reparameterized Johnson's SU distribution

As in Rigby and Stasinopoulos (2005) we consider a reparameterization of the original Johnson Su distribution (Johnson, 1954). For the location and scale parameters $\mu \in \mathbb{R}$ and $\sigma > 0$, respectively, the density evaluated at $x \in \mathbb{R}$ is

$$f(x|\mu, \sigma\, \xi, \eta) = \frac{\eta \mathrm{e}^{-\frac{1}{2}z^2}}{c\sigma(s^2+1)^{\frac{1}{2}}\sqrt{2\pi}}$$

with

$$z = -\xi + \eta \sinh^{-1}(s),$$

$$s = \frac{x - \mu + c\sigma w^{\frac{1}{2}} \sinh(\xi/\eta)}{c\sigma},$$

$$c = \left\{ \frac{1}{2}(w-1)\left[w\cosh(2\xi/\eta)+1\right] \right\}^{-\frac{1}{2}}$$

and

$$w = \mathrm{e}^{1/\eta^2}.$$

The two remaining parameters $\xi \in \mathbb{R}$ and $\eta > 0$ determine skewness and kurtosis, respectively. A positive (negative) value of ξ indicates positive (negative) skewness.

A.2 Proofs: Derivative of the log-likelihood for the scores

A.2.1 Proof of Result 2: Score for Bivariate Student-t Model

Proof.

$$\begin{aligned}\mathbb{E}_{t-1}[g(\boldsymbol{\eta}_t)^2] &= C(\nu,\rho_t)\int\int_{\mathbb{R}^2}\left[\rho_t(\eta_{1,t}^2+\eta_{2,t}^2)-(1+\rho_t^2)\eta_{1,t}\eta_{2,t}\right]^2 \\ &\quad\times\left(1+\frac{1}{(\nu-2)\left(1-\rho_t^2\right)}\left[\eta_{1,t}^2-2\rho_t\eta_{1,t}\eta_{2,t}+\eta_{2,t}^2\right]\right)^{-\frac{\nu+6}{2}}\mathrm{d}\eta_{1,t}\mathrm{d}\eta_{2,t}\end{aligned}$$

$$C(\nu,\rho_t)=\frac{\nu}{2\pi(\nu-2)\sqrt{1-\rho_t^2}}\left(\frac{\nu+2}{(\nu-2)(1-\rho_t^2)^2}\right)^2$$

The results needed for the calculation of $\mathbb{E}_{t-1}[g(\boldsymbol{\eta}_t)^2]$ are

1.

$$\left[1+\frac{x_1^2-2\rho x_1x_2+x_2^2}{(1-\rho^2)\nu}\right]^{-\frac{\nu+6}{2}}=\left[1+\frac{x_2^2}{\nu}\right]^{-\frac{\nu+6}{2}}\left[1+\frac{(x_1-\rho x_2)^2}{(1-\rho^2)(\nu+x_2^2)}\right]^{-\frac{\nu+6}{2}}$$

2.

$$\begin{aligned}I_0(x_2,\nu,\rho) &= \int_{\mathbb{R}}x_1^4\left[1+\frac{(x_1-\rho x_2)^2}{(1-\rho^2)(\nu+x_2^2)}\right]^{-\frac{\nu+6}{2}}dx_1 \\ &= (1-\rho^2)^{5/2}(\nu+x_2^2)^{5/2}B\left(\frac{\nu+1}{2},\frac{5}{2}\right) \\ &\quad+6\rho^2x_2^2(1-\rho^2)^{3/2}(\nu+x_2^2)^{3/2}B\left(\frac{\nu+3}{2},\frac{3}{2}\right) \\ &\quad+\rho^4x_2^4(1-\rho^2)^{1/2}(\nu+x_2^2)^{1/2}B\left(\frac{\nu+5}{2},\frac{1}{2}\right)\end{aligned}$$

3.

$$\int_{\mathbb{R}}\left[1+\frac{x_2^2}{\nu}\right]^{-\frac{\nu+6}{2}}I_0(x_2,\nu,\rho)\mathrm{d}x_2=\frac{6\pi\nu^2}{(\nu+4)(\nu+2)}\sqrt{1-\rho^2}$$

4.

$$\begin{aligned}
& C(\nu,\rho)\int\int_{\mathbb{R}^2}\rho^2\eta_1^4\left(1+\frac{1}{(\nu-2)\,(1-\rho^2)}\left[\eta_1^2-2\rho\eta_1\eta_2+\eta_2^2\right]\right)^{-\frac{\nu+6}{2}}\mathrm{d}\eta_1\mathrm{d}\eta_2\\
&= C(\nu,\rho)\rho^2\left(\frac{\nu-2}{\nu}\right)^3\int\int_{\mathbb{R}^2}x_1^4\left(1+\frac{1}{\nu\,(1-\rho^2)}\left[x_1^2-2\rho x_1x_2+x_2^2\right]\right)^{-\frac{\nu+6}{2}}\mathrm{d}x_1\mathrm{d}x_2\\
&= C(\nu,\rho)\rho^2\left(\frac{\nu-2}{\nu}\right)^3\frac{6\pi\nu^2}{(\nu+4)(\nu+2)}\sqrt{1-\rho^2}\\
&= 3\frac{\nu+2}{\nu+4}\frac{\rho^2}{(1-\rho^2)^4}
\end{aligned}$$

5.

$$\begin{aligned}
I_1(x_2,\nu,\rho) &= \int_{\mathbb{R}}x_1^2\left[1+\frac{(x_1-\rho x_2)^2}{(1-\rho^2)(\nu+x_2^2)}\right]^{-\frac{\nu+6}{2}}\mathrm{d}x_1\\
&= (1-\rho^2)^{3/2}(\nu+x_2^2)^{3/2}B\left(\frac{\nu+3}{2},\frac{3}{2}\right)\\
&\quad+\rho^2x_2^2(1-\rho^2)^{1/2}(\nu+x_2^2)^{1/2}B\left(\frac{\nu+5}{2},\frac{1}{2}\right)
\end{aligned}$$

6.

$$\int_{\mathbb{R}}x_2^2\left[1+\frac{x_2^2}{\nu}\right]^{-\frac{\nu+6}{2}}I_1(x_2,\nu,\rho)\mathrm{d}x_2=\frac{2\pi\nu^2}{(\nu+4)(\nu+2)}\sqrt{1-\rho^2}(1+2\rho^2)$$

7.

$$\begin{aligned}
& C(\nu,\rho)\int\int_{\mathbb{R}^2}[(1+\rho^2)^2+2\rho^2]\eta_1^2\eta_2^2\\
&\qquad\left(1+\frac{1}{(\nu-2)\,(1-\rho^2)}\left[\eta_1^2-2\rho\eta_1\eta_2+\eta_2^2\right]\right)^{-\frac{\nu+6}{2}}\mathrm{d}\eta_1\mathrm{d}\eta_2\\
&= C(\nu,\rho)[(1+\rho^2)^2+2\rho^2]\left(\frac{\nu-2}{\nu}\right)^3\\
&\quad\int\int_{\mathbb{R}^2}x_2^2x_1^2\left(1+\frac{1}{\nu\,(1-\rho^2)}\left[x_1^2-2\rho x_1x_2+x_2^2\right]\right)^{-\frac{\nu+6}{2}}\mathrm{d}x_1\mathrm{d}x_2\\
&= C(\nu,\rho)[(1+\rho^2)^2+2\rho^2]\frac{2\pi\nu^2}{(\nu+4)(\nu+2)}\sqrt{1-\rho^2}(1+2\rho^2)\\
&= \frac{\nu+2}{\nu+4}\frac{(1+\rho^2)^2+2\rho^2}{(1-\rho^2)^4}(1+2\rho^2)
\end{aligned}$$

8.

$$\begin{aligned} I_2(x_2,\nu,\rho) &= \int_{\mathbb{R}} x_1^3 \left[1+\frac{(x_1-\rho x_2)^2}{(1-\rho^2)(\nu+x_2^2)}\right]^{-\frac{\nu+6}{2}} \mathrm{d}x_1 \\ &= 3\rho x_2(1-\rho^2)^{3/2}(\nu+x_2^2)^{3/2} B\left(\frac{\nu+3}{2},\frac{3}{2}\right) \\ &\quad +\rho^3 x_2^3(1-\rho^2)^{1/2}(\nu+x_2^2)^{1/2} B\left(\frac{\nu+5}{2},\frac{1}{2}\right) \end{aligned}$$

9.

$$\int_{\mathbb{R}} x_2 \left[1+\frac{x_2^2}{\nu}\right]^{-\frac{\nu+6}{2}} I_1(x_2,\nu,\rho)\mathrm{d}x_2 = \frac{6\pi\nu^2}{(\nu+4)(\nu+2)}\sqrt{1-\rho^2}\rho$$

10.

$$\begin{aligned} & -2C(\nu,\rho)\int\int_{\mathbb{R}^2} \rho(1+\rho^2)\eta_1^3\eta_2 \\ & \qquad \left(1+\frac{1}{(\nu-2)\,(1-\rho^2)}\left[\eta_1^2-2\rho\eta_1\eta_2+\eta_2^2\right]\right)^{-\frac{\nu+6}{2}} \mathrm{d}\eta_1\mathrm{d}\eta_2 \\ = \; & -2C(\nu,\rho)\rho(1+\rho^2)\left(\frac{\nu-2}{\nu}\right)^3 \\ & \qquad \int\int_{\mathbb{R}^2} x_2 x_1^3 \left(1+\frac{1}{\nu\,(1-\rho^2)}\left[x_1^2-2\rho x_1x_2+x_2^2\right]\right)^{-\frac{\nu+6}{2}} \mathrm{d}x_1\mathrm{d}x_2 \\ = \; & -2C(\nu,\rho)\rho(1+\rho^2)\frac{6\pi\nu^2}{(\nu+4)(\nu+2)}\sqrt{1-\rho^2}\rho \\ = \; & -6\frac{\nu+2}{\nu+4}\frac{\rho^2(1+\rho^2)}{(1-\rho^2)^4} \end{aligned}$$

Points 4, 7, and 10 above are based on the change of variable $x_1 = \sqrt{\frac{\nu}{\nu-2}}\eta_1$, $x_2 = \sqrt{\frac{\nu}{\nu-2}}\eta_2$, with the Jacobian $|J| = \frac{\nu-2}{\nu}$.

Putting all together

$$\begin{aligned} \mathbb{E}[g(\boldsymbol{\eta})^2] &= \frac{\nu+2}{\nu+4}\frac{6\rho^2+(1+2\rho^2)(1+\rho^2)^2+2\rho^2(1+\rho^2)^2-12\rho^2(1+\rho^2)}{(1-\rho^2)^4} \\ &= \frac{\nu+2}{\nu+4}\frac{(1+2\rho^2)(1-\rho^2)^2}{(1-\rho^2)^4} \\ &= \frac{\nu+2}{\nu+4}\frac{1+2\rho^2}{(1-\rho^2)^2} \end{aligned}$$

□

A.2.2 Proof of Result 4: Score for Bivariate Normal Model

Proof. The proof of (5.13) is based on the following results:

$$\begin{aligned}
\mathbb{E}_{t-1}\left[\eta_{1,t}\right] &= \mathbb{E}_{t-1}\left[\eta_{2,t}\right] = \mathbb{E}_{t-1}\left[\eta_{1,t}^3\right] = \mathbb{E}_{t-1}\left[\eta_{2,t}^2\right] = 0 \\
\mathbb{E}_{t-1}\left[\eta_{1,t}^2\right] &= \mathbb{E}_{t-1}\left[\eta_{2,t}^2\right] = 1 \\
\mathbb{E}_{t-1}\left[\eta_{1,t}^4\right] &= \mathbb{E}_{t-1}\left[\eta_{2,t}^4\right] = 3 \\
\mathbb{E}_{t-1}\left[\eta_{1,t}\eta_{2,t}\right] &= \rho_t \\
\mathbb{E}_{t-1}\left[\eta_{1,t}^2\eta_{2,t}^2\right] &= 1 + 2\rho_t^2 \\
\mathbb{E}_{t-1}\left[\eta_{1,t}^3\eta_{2,t}\right] &= \mathbb{E}_{t-1}\left[\eta_{1,t}\eta_{2,t}^3\right] = 3\rho_t
\end{aligned}$$

□